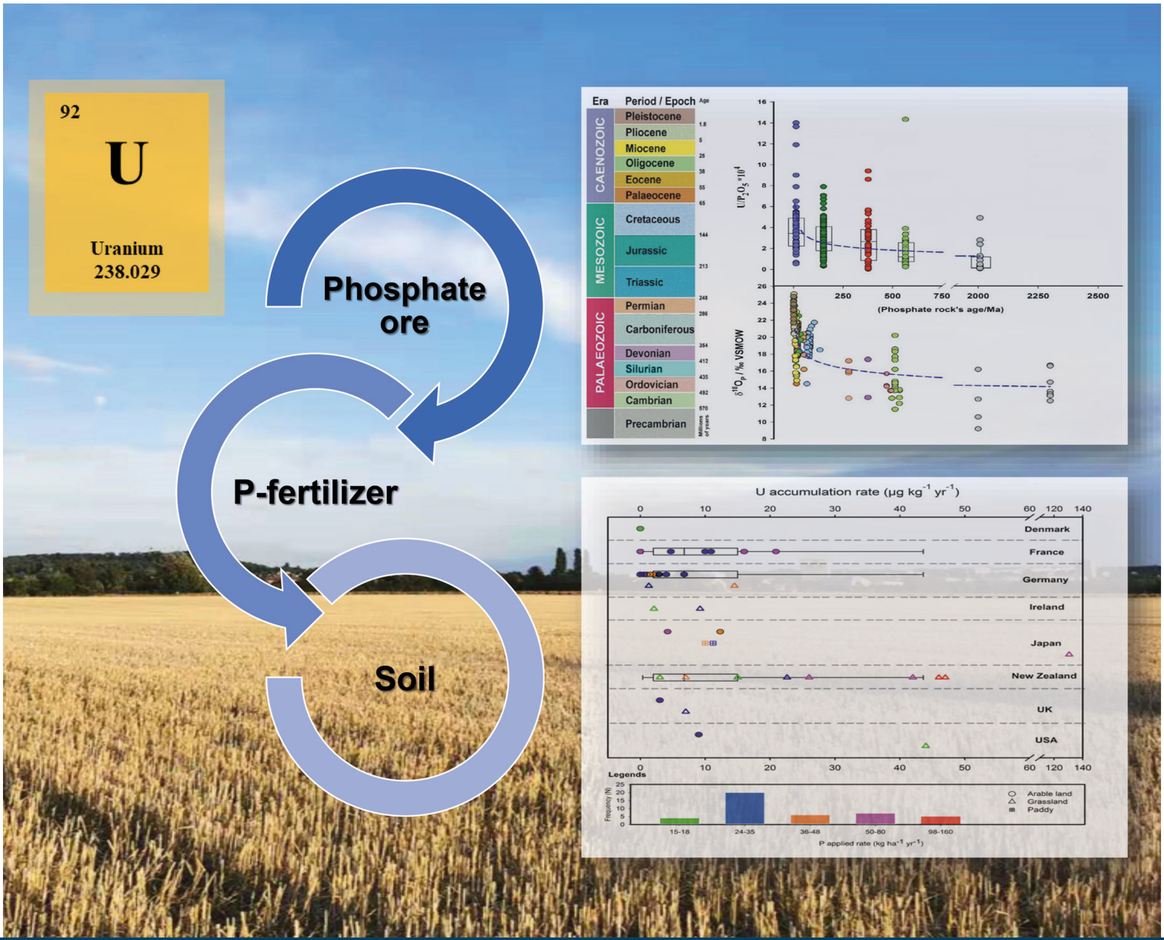

Uranium accumulation in agricultural soils as derived from long-term phosphorus fertilizer applications

Yajie Sun

Energie & Umwelt / Energy & Environment
Band / Volume 527
ISBN 978-3-95806-521-5

Mitglied der Helmholtz-Gemeinschaft

Schriften des Forschungszentrums Jülich
Reihe Energie & Umwelt / Energy & Environment Band / Volume 527

Forschungszentrum Jülich GmbH
Institut für Bio- und Geowissenschaften
Agrosphäre (IBG-3)

Uranium accumulation in agricultural soils as derived from long-term phosphorus fertilizer applications

Yajie Sun

Schriften des Forschungszentrums Jülich
Reihe Energie & Umwelt / Energy & Environment Band / Volume 527

ISSN 1866-1793 ISBN 978-3-95806-521-5

Bibliografische Information der Deutschen Nationalbibliothek.
Die Deutsche Nationalbibliothek verzeichnet diese Publikation in der
Deutschen Nationalbibliografie; detaillierte Bibliografische Daten
sind im Internet über http://dnb.d-nb.de abrufbar.

Herausgeber und Vertrieb: Forschungszentrum Jülich GmbH
Zentralbibliothek, Verlag
52425 Jülich
Tel.: +49 2461 61-5368
Fax: +49 2461 61-6103
zb-publikation@fz-juelich.de
www.fz-juelich.de/zb

Umschlaggestaltung: Grafische Medien, Forschungszentrum Jülich GmbH

Druck: Grafische Medien, Forschungszentrum Jülich GmbH

Schriften des Forschungszentrums Jülich
Reihe Energie & Umwelt / Energy & Environment, Band / Volume 527

D 5 (Diss. Bonn, Univ., 2020)

ISSN 1866-1793
ISBN 978-3-95806-521-5

Summary

It is well known that uranium (U) in mineral phosphorus (P) fertilizers may accumulate in agricultural soils; yet, this U accumulation occurs at different rates, likely depending on the type of fertilizer used. To substantiate this assumption, the aims of my thesis were: i) to quantify the accumulation rates of fertilizer-derived U in different long-term agricultural field experiments with P fertilized soils of central Europe, and ii) to contrast this with data from long-term experimental sites on volcanic soils that require higher amounts of P fertilizers for optimal crop production, and iii) finally to explain the variations of U accumulation rates by an assessment of the formation mechanisms and stocks of U in major phosphate rocks (PRs) deposits of the world.

Soil samples were taken from the surface soils and selected depth profiles of seven long-term experiment sites, i.e. at the grassland fertilization trials in Rengen (Germany), Park Grass (Rothamsted, UK), as well as in Geitasandur and Sámstaðir (Iceland), and the agricultural field experimental sites in Thyrow (Germany), Askov (Denmark), Broadbalk (Rothamsted, UK), Uranium concentrations were analyzed after microwave-assisted acid digestion by nitric acid or/and a complete digestion by lithium meta/tetraborate. In addition, I assessed U concentrations and the natural stable oxygen isotope compositions of phosphate ($\delta^{18}O_P$) in PRs as potential indicators for the genesis of the U in PRs from different deposits all over the world.

My results revealed a wide range of U accumulation rates in soils, ranging from 0-310 μg U kg^{-1} yr^{-1} in the monitored fields. Uranium accumulation was small when the P fertilizers were derived from igneous PRs from Finland and Kola Peninsula, as used for sites in Askov (< 0.4 μg U kg^{-1} yr^{-1}; <1.2 g ha^{-1} yr^{-1} (20 cm)) and Thyrow (0.6 μg U kg^{-1} yr^{-1}; 2.3 g ha^{-1} yr^{-1} (24 cm)), respectively, or when basic slag was applied as used for the Rengen (1.2 μg U kg^{-1} yr^{-1}; 1.3 g ha^{-1} yr^{-1} (10 cm)) site. Higher U accumulation rates (3.4, 7.8 μg U kg^{-1} yr^{-1}; 11.7, 21.9 g ha^{-1} yr^{-1} (23 cm)) were found at Rothemsted experiment stations (Broadbalk; Parkgrass), where P fertilizers used had been predominantly produced from PRs from North Africa. The most serious case of fertilizer-derived U accumulation (up to 310 μg U kg^{-1} yr^{-1}; 33.2 g ha^{-1} yr^{-1} (5 cm)) was found in Icelandic agricultural soil as a consequence of both high U concentrations in the applied P fertilizers (from an unknown PR source) and of large amounts of P fertilizer application. Overall, soil U concentrations will increase by 0.5 μg U kg^{-1} (0-5.1 μg U kg^{-1}) soil for 1 kg P applied per hectare and there will be 2.7-11 g U ha^{-1} yr^{-1} input to the EU's agricultural soil with 21.2 kg P (as P_2O_5) per hectare fertilization.

To explain these variations of U concentrations in the world's PRs, U concentrations in the PRs were discussed corresponding to their $\delta^{18}O_P$ values. I found that there was a 'co-evolutionary' relationship between the U (U/P_2O_5 ratio) and the $\delta^{18}O_P$ value: the lower the $\delta^{18}O_p$ value of the PR was, the lower its U concentration was. In igneous PRs, low U concentration can be explained by the lack of secondary U enrichment processes after rock formation, whereas the low $\delta^{18}O_p$ values was resulted from limited isotope fractionation at high temperatures in the magma. In sedimentary PRs, on the other hand, the variations of U concentrations and $\delta^{18}O_p$ values were related to the geologic age at which PRs were formed. Generally, older sedimentary PRs (formed in Precambrian-Cambrian) exhibited lower U concentrations and lower $\delta^{18}O_p$ values than the younger ones (formed in Ordovician-Neogene), which were influenced by paleoclimate and paleographic features.

In summary, the accumulation rates of fertilizer-derived U in agricultural soils were region-specific, depending on the source and the amount of P fertilizer applied. My data show that when applying P fertilizers with low U content, soil U concentration will remain at a non-critical level even at multi-centennial scale. However, fertilizer-derived U accumulation may pose an environmental issue at the places where large amounts of P fertilizers are needed for maximizing crop production (such as in Andosols). Selecting igneous PRs or ancient sedimentary PRs (formed in Paleozoic and Precambrian) as precursor materials for P fertilizer production is therefore crucial for minimizing potential U contamination risks and thus for sustainable agricultural management.

Zusammenfassung

Es ist bekannt, dass sich Uran (U) in mineralischen Phosphor (P)-Düngern in landwirtschaftlichen Böden anreichern kann; diese U-Anreicherung erfolgt jedoch in unterschiedlichen Raten, wahrscheinlich je nach Art des verwendeten Düngers. Um diese Annahme zu untermauern, waren die Ziele meiner Arbeit: i) die Akkumulationsraten von U aus P-Düngern in verschiedenen landwirtschaftlichen Langzeit-Feldexperimenten mit P-gedüngten Böden in Mitteleuropa zu quantifizieren, und ii) dies mit Daten von Langzeit-Versuchsflächen auf vulkanischen Böden zu vergleichen, die für eine optimale Pflanzenproduktion höhere Mengen an P-Düngern benötigen, und iii) schliesslich die Variationen der U-Akkumulationsraten durch eine Bewertung der Entstehungsmechanismen und U-Vorräte in den wichtigsten Phosphatgesteins- (PR-)Ablagerungen der Welt zu erklären.

Bodenproben wurden von den Oberböden und aus ausgewählten Tiefenprofilen von sieben Langzeitversuchen entnommen, d.h. von den Graslanddüngungsversuchen in Rengen (Deutschland), Park Grass (Rothamsted, UK) und den landwirtschaftlichen Feldversuchen in Thyrow (Deutschland), Askov (Dänemark), Broadbalk (Rothamsted, UK) sowie von Geitasandur und Sámstaðir (Island). Die Urankonzentrationen wurden nach mikrowellenunterstütztem Säureaufschluss durch Salpetersäure oder/und nach einem vollständigen Aufschluss durch Lithiummeta/Tetraborat analysiert. Darüber hinaus bewertete ich die U-Konzentrationen und die natürlichen stabilen Sauerstoffisotopenzusammensetzungen von Phosphat ($\delta^{18}O_P$) in PR als potenzielle Indikatoren für die Entstehung des U in PR aus verschiedenen Lagerstätten auf der ganzen Welt.

Meine Ergebnisse zeigten eine große Bandbreite von U-Akkumulationsraten in Böden, die von 0-304 µg U kg^{-1} Jahr^{-1} in den untersuchten Versuchen reichten. Die Urananreicherung war gering, wenn die P-Dünger aus magmatischem Phosphatgestein aus Finnland und der Kola-Halbinsel gewonnen wurden, wie es für die Standorte in Askov (< 0,4 µg U kg^{-1} Jahr^{-1}; <1,2 g ha^{-1} Jahr^{-1} (20 cm)) bzw. Thyrow (0,6 µg U kg^{-1} Jahr^{-1}; 2,3 g ha^{-1} Jahr^{-1} (24 cm)) verwendet wurde oder bei der Anwendung von basischer Schlacke, wie sie für den Standort Rengen (1,2 µg U kg^{-1} Jahr^{-1}; 1,3 g ha^{-1} Jahr^{-1} (10 cm)) verwendet wurde. Höhere U-Akkumulationsraten (3,4, 7,8 µg U kg^{-1} Jahr^{-1}; 11,7, 21,9 g ha^{-1} Jahr^{-1} (23 cm)) wurden auf der Versuchsstation Rothamsted (Broadbalk; Parkgrass) gefunden, wo die verwendeten P-Dünger überwiegend aus PR aus Nordafrika hergestellt worden waren. Der schwerwiegendste Fall von U-Akkumulation (bis zu 310 µg U kg^{-1} Jahr^{-1}; 33,2 g ha^{-1} Jahr^{-1} (5 cm)) wurde in isländischen landwirtschaftlichen Böden als Folge sowohl hoher U-Konzentrationen in den eingesetzten P-Düngern (aus einer unbekannten PR-Quelle) als auch großer Ausbringungsmengen der P-Dünger gefunden. Insgesamt steigen die U-Konzentrationen im Boden um 0,5 µg U kg^{-1} (0-5,1 µg U kg^{-1}) Boden für 1 kg ausgebrachtes P pro Hektar und es werden 2,7-11 g U ha^{-1} Jahr^{-1} in den landwirtschaftlichen Böden der EU eingebracht bei einer Düngung von 21,2 kg P (als P_2O_5) pro Hektar.

Zur Erklärung dieser Schwankungen der U-Konzentrationen in den weltweiten PRs wurden die U-Konzentrationen in den PRs entsprechend ihrer $\delta^{18}O_P$ Werte diskutiert. Ich stellte fest, dass es eine "ko-evolutionäre" Beziehung zwischen U (U/P_2O_5-Verhältnis) und dem $\delta^{18}O_P$ Wert gab: je niedriger der $\delta^{18}O_p$ Wert des PR war, desto niedriger war die U-Konzentration. Bei magmatischem PRs lässt sich die niedrige U-Konzentration durch das Fehlen von sekundären U-Anreicherungsprozessen nach der Gesteinsbildung erklären, während die niedrigen $\delta^{18}O_p$ Werte auf eine begrenzte Isotopenfraktionierung bei hohen Temperaturen im flüssigen Magma zurückzuführen sind. Bei den sedimentären PRs hingegen standen die Schwankungen der U-Konzentrationen und der $\delta^{18}O_p$ Werte in Zusammenhang mit dem geologischen Alter, in dem die PRs gebildet wurden. Im Allgemeinen wiesen ältere sedimentäre PRs (gebildet im Präkambrium-Kambrium) niedrigere U-Konzentrationen und niedrigere $\delta^{18}O_p$ Werte auf als die jüngeren (gebildet im Ordovizium-Neogen), die durch das Paläoklima und paläographische Merkmale beeinflusst wurden.

Zusammenfassend lässt sich sagen, dass die Akkumulationsraten von U aus Düngemittel in landwirtschaftlichen Böden je nach Quelle und Menge des ausgebrachten P-Düngers regional spezifisch waren. Meine Daten zeigen, dass bei der Ausbringung von P-Düngern mit niedrigem U-Gehalt die U-Konzentration im Boden selbst über mehrere Jahrhunderte auf einem unkritischen Niveau bleibt. Allerdings kann die U-Akkumulation ein Umweltproblem an den Orten darstellen, an denen große Mengen an P-Dünger zur Maximierung der Pflanzenproduktion benötigt werden (wie z.B. bei Andosolen). Die Auswahl magmatischer PRs oder alter sedimentärer PRs (die im Paläozoikum und Präkambrium gebildet wurden) als Vorläufermaterialien für die P-Düngemittelproduktion ist daher entscheidend für die Minimierung potenzieller U-Kontaminationsrisiken und damit für ein nachhaltiges landwirtschaftliches Management.

Acknowledgements

I would like to appreciate the support of all my supervisors, co-authors, technicians, colleagues, family and friends. They provided supports on scientific, technological, financial levels. It is a challenging task to find the right words to express the appreciation.

Here, I would like to keep it simple and start with my sincerely thanks to my supervisors.

Prof. Dr. R. Bol my main supervisor in Forschungzetrum, Juelich, who provided the opportunity to study in Forschungzetrum Juelich, Germany as a PhD student and work on this interesting topic. Thanks for the great company and support during my whole PhD studies. I greatly appreciated his patience, interest and encouragement.

Prof. Dr. W. Amelung, my main supervisor in Bonn University, Germany, who always brings some bright ideas and help to broaden my way of thinking. I have benefited greatly from his constructive reviews and constantly inspiring word. In addition, I would like to extend my thanks to his welcoming group in Bonn, particularly Dr. Bauke and Ye Wang.

Dr. B. Wu, my co-supervisor in Forschungzetrum, who is always nearby and provide great support timely and constantly, in terms of scientific writing, practical assistance and theoretical advice in the laboratory as well as the technological support from ICP-MS. Thanks for your nice advice and helpful discussions.

Apart from my supervisors, I would like to express my special thanks to many experts and colleagues. I would particularly like to thank Prof. Dr. E. Schnug and Prof. Dr. S. Haneklaus who provided precious phosphate rock samples worldwide and they always provide professional and scientific comments on U topic. I would like to thank Dr. M. Miyuki who helped to collect and delivery those phosphate samples. I would like to thank Dr. F. Tamburini and the colleagues in her group at ETH, who helped establish and test the purification method for oxygen isotope analysis. I also want to thank Holger Wissel, our technician for performing the oxygen stable isotope analysis. I would like to thank the supports from all colleagues in our group, as well as the colleagues in IBG-3, especially my officemates. Thanks for providing friendly and welcoming place to work.

I greatly thank Chinese Scholarship Council (CSC201506350148) who provided powerful finance support.

Last but not least, I would like to thank my lovely family and my supportive boyfriend, Shidong. Thanks for your support and understanding. Your kindness and motivation were always with me.

Content

List of figures

LIST OF FIGURES

List of tables

List of abbreviations

As	Arsenic
ANOVA	Analysis of variance
ATSDR	Agency for Toxic Substances and Disease Registry, U.S.,
C	Carbon
Ca	Calcium
$Ca(NO_3)_2$	Calcium nitrate
$CaNH_4NO_3$	Calcium-ammonium nitrate
CCME	Canadian Council of Ministers of the Environment
Cd	Cadmium
EFSA	European Food Safety Authority
EP	European Parliament
EU	European Union
FAO	Food and Agriculture Organization
Fe	Iron
H_2O_2	Hydrogen peroxide
Hexavalent U	U (VI)
HF	Hydrofluoric acid
HNO_3	Nitric acid
IAEA	International Atomic Energy Agency
ICP-MS	Inductively Coupled Plasma Mass Spectrometry
K	Potassium
K_2SO_4	potassium sulfate
KCl	potassium chloride
N	Nitrogen
$NaNO_3$	Chilean nitrate
NCRP	National Council on Radiation Protection and Measurements

LIST OF ABBREVIATIONS

NH_4NO_3	Ammonium nitrate
NIST	National Institute of Standard and Technology, USA
NRC	National Research Council
O	Oxygen
P	Phosphorus
P_2O_5	Pentoxide
PO_4^{3-}	Orthophosphate
PRs	Phosphate rocks
RGE	Rengen grassland experiment
Si	Silicon
Sr	Strontium
Tetravalent U	U (IV)
U	Uranium
USEPA	United States Environmental Protection Agency
USNRC	United States Nuclear Regulatory Commission
VSMOW	Vienna Standard Mean Oceanic water
WHO	World Health Organization
WSRW	Western Sahara Resource Watch
$\delta^{18}O_p$	Natural oxygen isotope compositions of phosphate
$\delta^{18}O_w$	Natural oxygen isotope compositions of water

Chapter 1

General introduction

1. Rationale

Phosphorus (P) is an indispensable and irreplaceable nutrient as well as energy carrier for all forms of life. Population growth and associated increased agriculture production requirements have upped the need and use of mineral P fertilizers, most of which are mainly manufactured from phosphate rocks (PRs).

The presence of heavy metals and other trace elements in PRs has long been known and has caused well-noted concerns (e.g. Altschuler, 1980; Nziguheba and Smolders, 2008; Kratz et al., 2016). Uranium (U), the heaviest naturally occurring radionuclide element, has also been found to be present in significant amounts in PRs. Uranium can potentially cause damage to the health of humans and animals (EFSA 2009; WHO 2011). The U in PRs is during chemical production processes preferentially transferred into mineral P fertilizers (Kratz and Schnug, 2006). Subsequently, over longer decadal timescales U can gradually accumulate in agricultural soils through the repeated mineral P fertilizer application required to optimize plant production. Nevertheless, there is still no consensus on the level of U accumulation in agricultural soils worldwide. One of the first pioneering studies to quantify soil U accumulation in response to P fertilizer was undertaken at Rothamsted Experimental Station (Rothbaum et al., 1979). In the following decades, an increasing number of studies confirmed a worldwide U accumulation in agricultural soils due to P fertilization (e.g. Rogasik et al., 2007; Takeda et al., 2006; Bigalke et al., 2017). These studies concluded that P fertilizer-derived U accumulates predominantly in topsoil of agricultural fields. The average annual U accumulation rates in topsoils varies however considerably, ranging from 7 to 47 $\mu g\ kg^{-1}\ yr^{-1}$ for grassland and from 1 to 18 $\mu g\ kg^{-1}\ yr^{-1}$ for arable land (e.g. Takeda et al., 2006; Wetterlind et al., 2012). It remained unclear to which degree the U accumulation in agricultural soils was directly related to the amounts of P fertilizers applied and to their U contents. The latter is likely determined by the origin of the PRs which are used to produce the P fertilizers. Different deposits of PRs contain various concentrations of U ranging from 0.3 to 247 $mg\ kg^{-1}$ (Altschuler, 1980). **However, a systematic information on PR deposits and their U contents is still lacking, although they could unravel why U is enriched in some PRs but depleted in others.**

Although U poses known risks for environment and health, until now there is still lack of any formal regulations on the limits of U content in fertilizers at both the national or international level. This seems to be related to **the limited systematic research on surface and deeper soil U accumulation at various experiment sites.** Such regulations, however, could be useful when discussing the extent of the future sustainable use of P as fertilizer in agricultural fields. Particularly, using ‘safer phosphates’, i.e. avoiding co-contaminations with heavy metals including U has become an important topic for research, policy making, and technological progress. Hence, it is the overarching goal of this thesis to shed light into the various sources and accumulation rates of fertilizer-derived U in agricultural soils.

2. Background

2.1 Uranium in phosphate rocks and P fertilizers

2.1.1 Basic properties and occurrence

Uranium is the heaviest naturally occurring radionuclide in the environment and consists of 99.284% ^{238}U, 0.711% ^{235}U, and 0.005% ^{234}U by mass (ATSDR, 2013). Uranium is present in the earth’s crust with a concentration of 2.6-2.8 mg kg^{-1} (Hu and Gao, 2008; Herring, 2013). Worldwide U concentrations in soil have been reported to range from 0.3 to 11.7 mg kg^{-1} with the average background concentration of 2 mg kg^{-1} (CCME, 2007, see also Table 1-1).

Uranium is incompatible with many major rock-forming minerals because of its large ionic radius and high charge. Therefore, U in rocks occurs as separated uranium-minerals, in accessory minerals (e.g. zircon), in exchangeable sites, or adsorbed onto the surfaces of zeolites and clays (Fayek et al., 2011). Common U minerals comprise oxides (uraninite and pitchblende), silicates (zircon and coffinite), phosphates (monazite, autunite), and vanadates (carnotite) (Liesch, 2015; Fayek et al., 2011). Various U concentrations (0.003-6 mg kg^{-1}) are observed in different rocks (Table 1-1; Kabata-Pendias and Pendias, 2001; Lamas, 2005). Uranium is more concentrated in organic matter-rich sedimentary rocks and PRs (NRC, 2012; Kabata-Pendias and Pendias, 2001). In the sedimentary rocks, the concentration levels of U are closely related to the former oxidation-reduction conditions. Lower U concentations have usually been found in igneous, felsic rocks, such as granite and rhyolite. And there are still much richer in U than mafic rocks like basalt or gabbro.

2.1.2 U in phosphate rocks

Phosphate rocks are naturally occurring geological materials that contain one or more phosphate minerals suitable for commercial use. PRs are non-renewable resources and found in various places of the world, but the largest deposits are found in Morocco, Western Sahara, China, the US and Russia (e.g. de Ridder et al., 2012).

There are two main types of PR deposits in the world. Sedimentary phosphate deposits, marine deposits mainly, formed during Precambrian to Recent (e.g. Cook, 2005). The more commercially deposits are of Phanerozonic age. The largest economic sedimentary deposits occur in North Africa and the Middle East, which are part of the Late Cretaceous-Eocene South Tethyan phosphogenic province and host to over 85% of the world's P production (USGS, 2018). The important commercial phosphate ore in China formed in Cambrian and Devonian period (He and Zhou, 2015). The Phosphate ores in Florida and North Carolina were formed in the Miocene period which are primary P sources for the United States (Cook, 1984; USGS, 2018).

Another important PRs are igneous phosphate deposits. They are geographically widespread and range in age from Precambrian to Tertiary (e.g. Cook, 2005). They are associated with carbonatites and/or alkali (silica-deficient) intrusions. The largest source of igneous phosphate deposits is the so called Khibina Alkaline Complex in Russia's Kola Peninsula from the Devonian geological period, which produces more than half of world's igneous PRs in 2015 (Pufahl and Groat, 2017). Other important igneous phosphate deposits are present in South Africa and Brazil.

The principal phosphate minerals in PRs are apatites. The group of apatites has a general formula: $[Ca_5(PO_4)_3(OH, F, Cl)]$. Fluor-apatite $[Ca_{10}(PO_4)_6F_2]$ and hydroxy-apatite $[Ca_{10}(PO_4)_6(OH)_2]$ are primarily found in igneous PRs, while francolite $[Ca_{10-x-y}Na_xMg_y(PO_4)_{6-z}(CO_3)_zF_{0.4z}F_2]$ mainly occurs in marine sedimentary PRs (Van Kauwenbergh, 1997; Petr, 2016). Calcium in the apatite structure can be substituted by heavy metals (i.e. Sr, Cd, Fe, U), leading to heavy metal enrichment in PRs. Uranium may exist as UO_2^{2+}/U^{4+} substituting Ca^{2+} or as UO_4^{2-} substituting phosphate (Hendricks and Hill, 1950) when it enters the apatite structure (Baturin and Kochenov, 2001) or chemically adsorbed on the surfaces. The U may also be present as a separate phase as UO_2, UF_4 or $Ca\,(UO_2)_2(PO_4)_2 8H_2O$ (Alschuler, 1958).

Table 1-1. Uranium concentrations in rocks and soils (data from: Kabata-Pendias and Pendias, 2001; Lamas, 2005)

. Type	U content (mg kg^{-1})
Sedimentary Rocks	
Argillaceous sediments	3-4
Shales	3.0-4.1
Sandstones	0.5-0.6
Limestones, Dolomites	2.2-2.5
Magmatic Rocks	
Ultramafic rocks:	
Dunites, Perdotites, Pyroxenites	0.003-0.01
Mafic rocks:	
Basalts, Gabbros	0.3-1.0
Intermediate rocks:	
Diorites, Syenites	1.4-3.0
Felsic rocks	
Granites, Rhyolites, Trachytes, Dacites	2.5-6.0
Soil	
Canada	0.7-2.1
China	0.4-21.1
Great Britain	2.6
Germany	0.4-11.0
India	11
Italy	1.5-8
Poland	0.1-2.3
U.S.	0.3-10.7
U.S. (Alaska)	<0.2-45
Russia	3.8

2.1.3 U in fertilizers

During the last two decades, 80%-90% of world’ s PRs output has been used for fertilizer production (e.g. Dissanayake and Chandrajith, 2009). The PRs are reacted with sulphuric acid to produce phosphoric acid which is then used to produce P fertilizers (IAEA, 2003). During this process, about 70% of U that is present in the PRs is concentrated in phosphoric acid (IAEA, 2003).

Kratz and Schnug (2008) (Table 1-2) found that mineral fertilizers without P (e.g. N, K, NK fertilizer) contained U with concentrations below 2.5 mg kg^{-1}, whereas mineral P fertilizers contain U in a range from 6 to 149 mg kg^{-1}, with a maximum concentration of 362 mg kg^{-1}. The highest U concentrations were found in pure P and in NP fertilizers whose P concentrations were also the highest among all the studied fertilizers. Nevertheless, even a given type of fertilizer can contain variable amounts of U. By contrast, organic fertilizers (e.g. manure and slurries) generally contain low U concentrations with the mean value less than 2.6 mg kg^{-1}.

Table 1-2 Uranium concentrations in different types of P containing fertilizers (modified from Kratz et al., 2008)

Fertilizer type and origin	Min.	Max. (mg kg^{-1})	Mean	n
Supersphosphate				
USA	60.5	172	104	3
Germany			91	1
Brazil	21.4	93.7	65.2	11
Triple superphosphate				
USA	143	208	178	4
Germany	52.3	160	106	2
Brazil	14.7	69.7	50.2	11
NP fertilizers:				
USA	161	165	163	16
Germany	0.6	61	27	3
Brazil	49.6	93.8	71.7	2
PK fertilizers				
USA	69.9	109	89.4	3
Germany	31.2	163	82.1	3
NPK fertilizers				
USA	39.7	113	65.5	5
Germany	<0.05	33.3	9.9	20
Brazil	5.2	54.3	27.1	12
Manure from organic farming:				
Organic cattle manure	0.03	1.4	0.2	197
Organic pig manure	0.05	4.6	1.1	57
Manure from conventional farming				
Conventional cattle manure	0.2	1.4	1.1	28
Conventional pig manure	0.4	11.1	3.5	14

2.2 Uranium accumulation in agricultural soils by P fertilization

A continuous input of U by P fertilization may lead to a significant accumulation of U in agricultural soils (e.g. Kratz and Schnug, 2006; Bigalke et al., 2017), which is of both environmental and health concern. In the meantime, an increasing number of studies reported such a fertilizer-derived U accumulation in agricultural soils, e.g. in France (Wetterlind et al., 2012), in Germany (Kratz et al., 2008; Schnug and Haneklaus, 2015; Utermann and Fuchs, 2008), in Greece (Papastefanou et al., 2006), in Japan (Takeda et al., 2006), in New Zealand (McDowell, 2012; Schipper et al., 2011; Taylor and Kim, 2008), in Switzerland (Bigalke et al., 2018; Bigalke et al., 2017),in United Kingdom (Rothbaum et al., 1979) and in USA (Jones, 1992; Zielinski et al., 2006). Due to the variety of U concentration in different PRs and the different application amount of P fertilizer, the degree of U accumulations in agricultural soils varies regionally. Rogasik et al. (2008) studied the U accumulation in 7 long-term experiment sites in Germany and found a mean accumulation rate of 3.7 µg U kg^{-1} yr^{-1}, with a minimum of 1 µg U kg^{-1} yr^{-1} (e.g., in Halle) and a maximum of 15 µg U kg^{-1} yr^{-1} (e.g., in Schuby). Higher U accumulation rate of 9.3 µg U kg^{-1} yr^{-1} was found in a Japanese long-term experiment (Takeda et al., 2006). In Ireland annual U accumulation even amounted to 14.5 µg U kg^{-1} yr^{-1} (Tunney et al., 2009). Even distinctly higher U accumulation rates of 19-37 µg U kg^{-1} yr^{-1} have been reported for New Zealand and Australia (Imas and Lati, 2005; Lottermoser, 2009; Taylor and Kim, 2008; Schnug and Haneklaus, 2015). Nevertheless, we still lack a comprehensive understanding of the extent of fertilizer-derived U accumulation in different regions of the world, since the lack of a quantitative understanding of U stocks of P fertilizers that were produced from different PRs.

Usually, fertilizer-derived U is found to accumulate in the topsoil (e.g. Takeda et al., 2006; Salmanzadeh et al., 2017) with organic substances and poorly crystalline Fe/Al minerals (Taylor, 2007; Yamaguchi et al., 2009) playing an important role for adsorbing U there. Due to the higher solubility of fertilizer-derived U, this accumulation is more critical than that of geogenic U (Rafsanjani et al., 2008). Especially, in agricultural soils, with the higher redox potentials and pH values (typically 6.5-7.5), U may become mobile due to the formaiton of uranyl-carbonate complexes (Smidt et al., 2011; Schnug and Haneklaus, 2015). To better eludcidate the underlying processes, the subsequent section is devoted to the fate of U in agricultural soils.

A minimal increases of soil U concentration will normally not affect human health, as plants do not actively take up U from soil. The transfer factor from soil to plant is below 1% (Sheppard and Evenden, 1988; Schnug and Haneklaus, 2015). Furthermore, there is also a subsequent low U transfer factor from grasses to animals (EFSA, 2009). The EFSA (2009) thus concluded that U uptake by plants is not a predominant health issue.

However, it has been suggested that drinking water is the main source of human U uptake (Schnug and Lottermoser, 2013). A number of studies indicated a transfer of fertilizer-derived U to water bodies (Bigalke et al., 2018; Azouazi et al., 2001; Huhle et al., 2008; Zielinski et al., 2006). In contrast, it is not possible to unequivocally assign elevated U concentration in freshwater systems to fertilizer-derived U due to various substantial local and regional geogenic background of U concentrations (Roth and FitzGerald, 2015; Liesch et al., 2015). In addition, it is still complicated to specify a direct relationship between fertilizer-derived U and the geologic origin U (Roth and FitzGerald, 2015).

2.3 Behavior of uranium in soil

Uranium in soil is present mainly as hexavalent and tetravalent U species with the former being more soluble than the latter. Soil Eh and pH values as well as the presence of a range of common complexing anions (e.g. SiO_4^{4-}, SO_4^{2-}, CO_3^{2-}) and dissolved organic carbon, may influence U speciation in soil solutions (Cumberland et al., 2016).

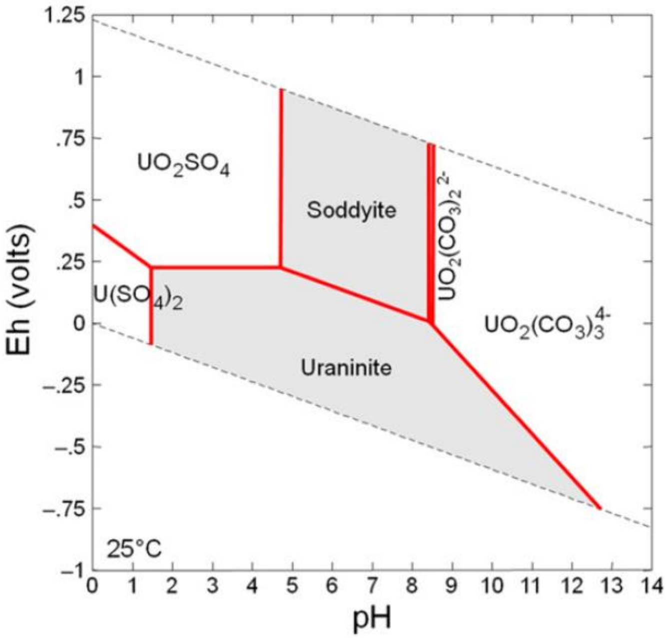

Figure 1-1. Solution chemistry of uranium species as a function of pH and Eh value. Calculations created in Geochemist's Workbench (thermo.dat database) under condition U 10^{-6} M: P_{co2} $10^{-3.5}$ at 1/100 seawater concentration at 25 ℃. Aqueous species included: CO_3^{2-} SO_4^{2-}, PO_4^{3-}, SiO_4^{4+}, UO_2^{2+} (from Cumberland et al., 2016).

Uraninite (UO_2) is the predominant U specie in soil and sparingly soluble over a range of pH values, at low temperatures and under reducing conditions (low Eh value) (Fig. 1-1; Cumberland et al., 2016; Guillaumont et al., 2003). Under oxidizing conditions (high Eh value), U speciation is dominated by UO_2^{2+} cations which may form soluble complexes with other anions such as OH^-, CO_3^{2-} SO_4^{2-} and PO_4^{3-} (Fig. 1-1; Cumberland et al., 2016). When important complexing ligands are lacking, free UO_2^{2+} dominates at acid conditions of pH values of 4-5, whereas a suite UO_2-OH complex dominates at circum-neutral pH, and $(UO_2)_3(OH)_7^-$ becomes the predominant species at a pH value of ≥7 (Figure 1-2) (Guillaumont et al., 2003; Langmuir, 1978). With existence of those anions, UO_2^{2+} -sulfate complexes are stable at pH values below 4, whereas uranyl phosphate complexes become an important species at concentrations of only 0.1 mg kg^{-1} PO_4^{3-} across the whole pH range from 4 to 7.5 (Fig. 1-1). In addition, at higher pH value, uranyl hydroxide or uranyl carbonate complexes predominate

(NRC, 2012; Langmuir, 1978). All the oxidized uranyl ion phosphate, sulphate and carbonate complexes are soluble and thus mobile in environment (Vandenhove et al., 2007).

The mobility of U in soil is influenced by sorption and complexation processes with inorganic soil constituents (clay mineral and oxides) and organic matter (Vandenhove, 2007). A variety of sorption reactions are involved in the dynamics of U in the soils. Uranyl ions and its complexes can adsorb onto soil colloids, such as clay minerals, insoluble organic matter, Fe and Al (hydr)oxides, and micro-organisms (EPA, 1999; Giammar, 2001). The intensity of such reactions depends on soil pH. In well aerated envirionments and ambient pH values of 4-9, sorption of U (VI) onto soil particles is generally higher at lower pH values in soil and decreases strongly with increasing pH value (Giblin et al., 1981; Morrison et al., 1995). Inorganic ligands, such as carbonate and phosphate ions influence largely U (VI) sorption and transport in soil. The presence of carbonate complexes, such as $UO_2(CO_3)_2^{2-}$ or $UO_2(CO_3)_2^{2-}$, though exhibit a lower affinity to soil minerals than uranyl and hydroxy-complexes and thus increase the mobility of U (Echevarria et al., 2001). Free phosphate anions may also compete with U for sorption sites, thus also increasing U mobility. On the other hand, the formation of ternary U-P complexes will increase the sorption of both U and P (Bachmaf et al., 2008). Finally, organic matter, affects retention/mobilization of U in soils, e.g., the mobility of U can be reduced by the formation of complexes with humic acid-alike structures (Dall'Aglio, 1971; Vandenhove, 2007). Therefore, the fertilizer-derived U accumulation in agricultural soils could be different in soils of different pH and carbonate concentrations, especially when estamitate the U accumulation in the trials with liming.

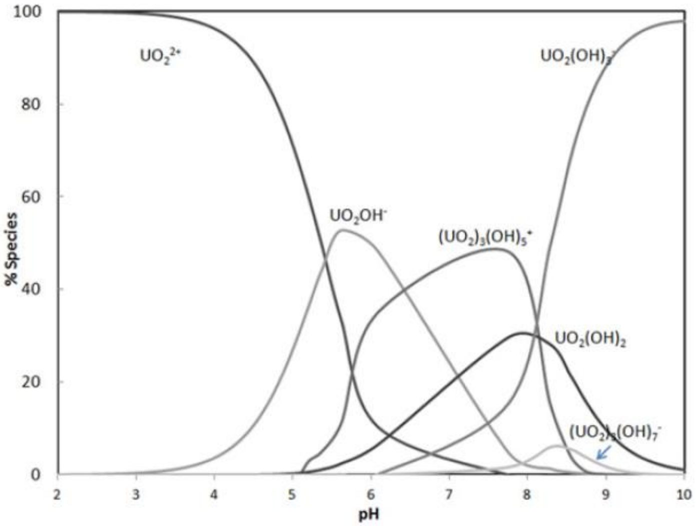

Figure 1-2. Percent of uranium species for the UO_2-H_2O system under the following concentration conditions U 10^{-6} M: P_{co2} 10-3.5; at 1/100 seawater concentration at 25 ℃. Species with an abundance of <5% were not plotted (from Cumberland et al., 2016).

2.4 Isotopes signature of phosphate rocks

Isotope ratio techniques have been used as geochemical indicators to trace the origin of PR deposits. The three most commonly used elements for stable isotope analysis in PRs are O, carbon (C) and sulfur (S), which are the structural components of francolite (main mineral in PRs). Two other relevant radiogenic isotope tracers in PRs, Sr and U, are constituents in the lattice of francolite that replace major elements (Jarvis et al., 1995). Studies on stable C and S isotope ratios showed that they serve as indicators of the depositional and diagenetic history of PRs rather than their geographic origin and therefore not pursued in this section. In contrast, Sr and U isotopes can provide the age information of PRs (Javis, 1995; Kolodny and Luz, 1992), therefore can be useful for identifying the origins of PRs.

The residence time of Sr in seawater is with about 10^6 years, several orders of magnitude longer than oceanic mixing times; thus, it is fair to assume that Sr in ocean water is more or less homogenously mixed (Turner and Whitfield, 1979). The Sr ($^{87}Sr/^{86}Sr$) isotope composition of PRs is in general agreement with the Sr isotope ratio

($^{87}Sr/^{86}Sr$) in contemporary seawater (Kolodny and Luz, 1992). Hence, the Sr isotope-age curve can be applied to date the age of marine sediments (Peterman, 1979), particularly for the Cenozonic (0-20 Ma) time period (Hodell et al., 1991). The procedure is likely less precise when used to date more ancient rocks. Dating phosphogenesis by Sr isotopes has been done by McArthur et al. (1990), for instance. The authors found the age determinations for phosphorites from four different areas agreed well with the geological settings and previous estimates. Sattouf et al. (2008) subsequently used the $^{87}Sr/^{86}Sr$ isotope ratios to classify rock phosphate samples into four different groups: i) igneous rock phosphates from Russia (Kola), sedimentary rock from: 2) Algeria, Israel, Morocco, Tunisia and Syria, 3) the USA ,4) Senegal and Togo.

The U-series isotopes have advantages in dating young phosphorites, because the modern ocean is isotopically uniform with a $^{234}U/^{238}U$ activity ratio of 1.144 ±0.004 (Jarvis et al., 1995). Applying such U-series dating to phosphorites deposits of the Peru-Chile and Namibian margins (e.g. Baturin et al., 1972), of western South Africa (e.g. Birch et al., 1983) and East Australia (e.g. Kress and Veeh, 1980) showed that the $^{234}U/^{238}U$ ratios were similar to those in present seawater, i.e., the formation of these phosphorites must be recent and ongoing. Sattouf (2007) reported that the PRs of the USA did show different $^{234}U/^{238}U$ values from those originating from the Middle East and North Africa, also indicating a younger age of the PRs from the USA.

Oxygen stable isotopes are nowadays popular for better understanding of P cycling in several natural environments including marine environments, soil, sediments and aerosols (Kolodny et al. 1983, Blake et al., 2010; Jaisi and Blake, 2014, Amelung et al., 2015; Bauke et al., 2018). Under Earth's surface conditions, P is always bound to O as orthophosphate (PO_4^{3-} or P_i), providing the possibility of using O isotope signature to differentiate PRs. As O isotope exchange between phosphate and water is extremely slow in inorganic systems (Kolodny et al., 1983), the O isotope composition of the phosphate (express as $\delta^{18}O_p$) can provide information of the paleo-environmental conditions when it was formed. Provided that the O isotope composition of the ancient water ($\delta^{18}O_w$) is known, the paleo-temperature (T) at that time can be calculated using following equation (Longinelli and Nuti, 1973)

$$\mathrm{T} = 111.4 - 4.3\,(\delta^{18}\mathrm{O_p} - \delta^{18}\mathrm{O_w})$$

When comparing PRs of different ages, a temporal trend of decreasing $\delta^{18}O_p$ values (24-9 ‰) was found with increasing rock age (0.01-2000 Ma) (Shemesh et al., 1983 and 1988). This $\delta^{18}O_p$ time trend might be useful to help identify the deposit of PRs. Yet, I am not aware that this system as been applied systematically to the four groups of PRs as identified by Sattouf et al. (2007).

In summary, the analysis of isotopic patterns of U, Sr, O is an analytical tool that may help to identify the age of the PRs rather than true sourcing. Further work is clearly still needed to be able to better and univocally pinpoint the PRs' origins. Here, I will focus on O isotope ratios of phosphates, as they can be detected both in the source PRs and in the fertilizers.

3. Objectives

The current study aims to i) assess the importance of P fertilizer-derived U accumulation in agricultural soils at long-term experiment sites and ii) explore how the fate of U in PRs is related to the origin of PRs by applying the $\delta^{18}O_p$. The results will be used to suggest mitigation opitions for reducing potential U contamination in agricultural systems in the future.

To achieve these aimes, soil samples were taken primarily from long-term agricultural field experiments, such as at Rengen and Thyrow (Germany), Askov (Denmark), Sámstaðir and Geitasandur (Iceland), and Rothamsted (UK). In addition, U concentration and $\delta^{18}O_p$ of worldwide PRs were reviewed and supplemented by own data for a better understanding of the characteristics of U in PRs.

Specifically, following questions were addressed.

i) How fast and to which degree does U accumulate in agricultural soils when using P fertilizers produced from low-U resources?

In chapter 2, I describe the assessment of U accumulations in three long-term P fertilization experimental fields (Rengen and Thyrow in Germany; Askov in Denmark) where historically, P sources with low U content (igneous PRs from Finland and Kola Peninsula for Askov and Thyrow, respectively; and basic slag for Rengen) have been applied.

ii). To what extent does the long-term excessive amount of P fertilizer application lead to an associated unwarranted U accumulation in agricultural soil?

Andosol is important agricultural soil resource for crop production. Due to the low inherent P availability, Andosol require more P fertilizer than many other soils. To elucidate U accumulation in such soils, the levels of U accumulation were therefore examined in two long-term P fertilization grassland (Sámstaðir and Geitasandur, Iceland) after about 50 years' excessive P fertilization (chapter 3).

iii) Why are there different levels of U in various PRs? How do $\delta^{18}O_p$ signatures revel the characteristics of U in PRs related to PRs origins?

In chapter 4, the spatial and temporal U distributions in PRs worldwide were reviewed. In addition, $\delta^{18}O_P$ values in PRs collected worldwide were analyzed to explore the relation of U level and the rock's origin traced by $\delta^{18}O_P$. Such information is helpful as a pre-assessment tool which fertilizers from what PRs have low inherent risks to be contaminated with U.

Chapter 2

Non-critical uranium accumulation in soils of German and Danish long-term fertilizer experiments

Modified on the basis of the manuscript

Sun, Y., Wu, B., Amelung, W., Christensen, B. T., Pätzold, S., Bauke, S. L., Schweitzer, K., Baumecker, M. and Bol, R.

Published in *Geoderma*

1. Introduction

Phosphate rocks (PRs) contain total uranium (U) with an average concentration of 120 µg U g^{-1} (Altschuler, 1980). When processed for fertilizer phosphorus (P) production, the majority (80−90%) of the U is transferred to the final fertilizer products (Kratz and Schnug, 2006). Many studies have shown that repeated application of P fertilizers can lead to elevated U concentrations in agricultural soil (e.g. Rothbaum et al., 1979; McDowell, 2012; Bigalke et al., 2017).

Usually, U accumulates in the topsoil, where it is adsorbed to organic matter and poorly crystalline Fe/Al minerals (Taylor and Kim, 2008; Yamaguchi et al., 2009). Plants do not actively take up U from soil (Sheppard and Evenden, 1988; Schnug and Haneklaus, 2015), but U can be adsorbed on root surfaces and thus enter the food chain through root crops (Keith et al., 2013; Kratz et al., 2008). In addition, fertilizer-derived U can be leached into groundwater, posing a threat to human health (Zielinski et al., 2006; Liesch et al., 2015; Riedel and Kübeck, 2018). Food and water intakes are the major pathways of human exposure to U. In the USA, critical soil contamination has been set at a total U concentration of 30 mg kg^{-1} (USNRC, 1992). Canada has implemented soil quality guidelines for the protection of human and environmental health by setting a threshold value of total U at 23 mg kg^{-1} for agricultural land use (CCME, 2007). At present, there is no regulation of U concentrations in fertilizer products, and the European Union did not include any limits to U content in the recently revised fertilizer regulations (EP and Council of the EU, 2019). To allow for a better risk assessment of U in European agricultural soils, we need a more comprehensive scrutiny of the extent of fertilizer-derived U accumulation in different regions and in soils receiving different sources of P fertilizers. Current estimates for annual total U accumulation vary regionally, ranging from 7 to 47 µg kg^{-1} yr^{-1} for grassland and from 1 to 18 µg kg^{-1} yr^{-1} for arable land (e.g., Takeda et al., 2006; Wetterlind et al., 2012; Bigalke et al., 2017). Differences are related not only to the amounts of P fertilizers applied but also to the actual U concentration in P fertilizers, which in turn depends heavily on the source of raw phosphate rocks used in P fertilizer production (Sun et al., 2019). In this study, we analyze U concentrations in soils from three long-term agricultural field experiments with P fertilizer treatments (Rengen and Thyrow in Germany; Askov in Denmark) to evaluate the accumulation of P fertilizer-derived U in soil, and to link U accumulations in soil and sources of P fertilizers. This may raise awareness regarding the sustainability of P fertilizers that can maintain low levels of U in agricultural soils.

2. Materials and Methods

2.1 Description of study sites

The Rengen grassland experiment

The Rengen grassland experiment (RGE) was established in 1941 in the Eifel mountains (Germany, 50°13´N, 6°51´E) and treatments include continuous applications of basic slag (or Thomas slag) as the P fertilizer (Schellberg et al., 1999). Basic slag is a by-product of steel production, where P in the iron ore is removed to assure the production of the high-quality steel. Basic slag contains significant amounts of P (12-20% is phosphorus pentoxide (P_2O_5)) but is low in U. In addition to basic slag, mineral fertilizers of nitrogen (N) and potassium (K) were applied as ammonium nitrate (NH_4NO_3) and potassium chloride (KCl) or potassium sulfate (K_2SO_4), respectively. The soil is classified as Stagnic Cambisol (IUSS Working Group WRB, 2015). The study site has a mean annual precipitation of 811 mm and a mean annual temperature of 6.9 °C. The RGE is arranged in a completely randomized block design with five fertilized treatments (Ca (lime), Ca/N, Ca/N/P, Ca/N/P/KCl, Ca/N/P/K_2SO_4) and an untreated control, each with five field replications. Annual P fertilizer application has been 35 kg ha^{-1} since 1941 (Table 2-1; see Pätzold et al., 2013, for more details). The permanent grassland vegetation is cut and removed from the fields twice a year in late June or early July and again in mid-October (no grazing since 1941). In the present study, 5 cores of topsoil (0-10 cm depth) were taken from each treatment in 2016 and analyzed for U and P concentrations.

The Thyrow long-term fertilization experiment

The Thyrow long-term "Nutrient Deficiency Experiment" (Thy D41) was established in 1937, about 20 km south of Berlin, Germany (52°15´N, 13°14´E). The soil is Albic Cutanic Luvisol (IUSS Working Group WRB, 2015). The site is characterized by a mean annual precipitation of 510 mm and a mean annual temperature of 9.2 °C. A crop rotation of spring barley, potato and maize is applied at the site. The annual fertilizer applications for the respective treatments are 100 kg K ha^{-1} (as KCl or K_2SO_4) and 24 kg P ha^{-1} (as triple superphosphate), plus 60 kg N ha^{-1} (as NH_4NO_3 and $(NH_4)_2SO_4$)

in years with spring barley and 90 kg N ha^{-1} with potatoes and maize. The limed treatments received calcific or dolomitic lime at about 200 kg CaO ha^{-1} yr^{-1}. Soil cores to 100 cm depth were taken from NK+ lime, NPK and NPK+ lime treatments, with four replications for each treatment. Three soil cores were taken at random places in each plot and separated into five segments at the depth of 24 (soil horizon Ap1), 30 (Ap2), 50 (EBw1), 70 (EBw2) and 100 (E/Bt) cm, respectively. The Ap1 horizon corresponds to the actual soil tillage depth of 22 to 25 cm. The corresponding soil segments of the three cores taken in one plot were well mixed on site and sub-sampled for the present study (see Bauke et al., 2018 for sampling details).

The Askov long-term experiment

The Askov long-term experiment (initiated in 1894) is located on the Lermarken site, Askov Experimental Station, Denmark (55°28´N, 09°07´E). The soil is classified as Luvisol (IUSS Working Group WRB, 2015). The mean annual precipitation and temperature were 862 mm and 7.7 °C (1961-1990), respectively. The experiment tests crop response to different rates of N, P and K applied in animal manure (AM) or mineral fertilizers (NPK). Mean annual P application was 13, 17 and 20 kg P ha^{-1} yr^{-1} in the periods 1894-1922, 1923-1972 and 1973-2016, respectively. In the NPK treatments, P was added as single superphosphate. Mineral N was applied as Chilean nitrate ($NaNO_3$,1894-1939), calcium nitrate ($Ca(NO_3)_2$,1940-1972) and as calcium-ammonium nitrate ($CaNH_4NO_3$) since 1973. Mineral K was applied as KCl. Animal manure was derived from cattle. The experiment grows a four-course rotation of winter cereals, row crops, spring cereals and grass/legumes. Every 4-5 years, 3000-5000 kg ha^{-1} lime is applied to maintain soil pH between 5.5 and 6.5. Soil tillage involves ploughing to 20 cm and seedbed preparation. Since 1923, topsoil (0–20 cm) has been sampled every four years and archived as dried samples. In the present study, we analyzed soils sampled in the B2-field in 1923, 1938, 1945, 1953, 1964, 1976, 1985, 1996 and 2000 from plots with AM and NPK applications. Soils from unfertilized plots were included as references (here termed control treatment). Each soil sample was a pooled sample of the three field replicates. In addition, soils sampled in 2010 and 2016 from each field replicate were analyzed separately. Christensen et al. (2019) provide further details on the Askov long-term experiments.

2.2 Sample preparation and element analysis

Each soil sample was air dried and passed through a 2 mm sieve before analyses. About 0.05 g soil was digested with 3 ml distilled ultrapure concentrated nitric acid (HNO_3, 68 %) and 1 ml hydrogen peroxide (H_2O_2, 30 %) in a pressurized microwave-assisted digestion system (TurboWAVE, Milestone Srl, Italy). Three analytical replicates were processed by the microwave-assisted digestion for each soil sample from all three study sites. The method extracts on average 60% of total U (here termed acid-extractable U), but leaves behind a residual fraction of U in primary and secondary minerals (such as silicate phases) (Tessier et al., 1979; Xing and Yeneman, 1998). After digestion, the soil-acid mixture was centrifuged at 5000 * g for 10 min. The supernatant was diluted with 2 % HNO_3 and its U and P concentrations measured by inductively coupled plasma mass spectrometry (ICP-MS, Agilent 7900, Germany). Soil samples from Askov were also analyzed for total U concentration after digestion of 0.05 g soil with 0.25 g lithium meta/tetraborate at 1050 °C for 3 h (Delijska et al., 1988). Standard reference soil (NIST SRM 2709a) was included for quality control of the analytical procedures.

Statistical analyses were performed separately for each field experiment. Differences among U concentrations in various treatments were analyzed by one-way ANOVA with a significance level $p<0.05$ to detect significant differences among individual treatments for Rengen and Askov (soil sampled in 2010 and 2016). Due to incomplete randomization of the treatments in the Thyrow experiment, we considered the treatments within each block, as well as the five depth intervals within each soil profile, as paired samples. A paired-sample t-test was performed to reveal significant differences in U concentrations among soils from the treatments NK+lime, NPK, and NPK+lime. Differences in vertical soil U concentration among soil horizons were analyzed by repeated measures ANOVA. The relationships between P and U concentrations were examined by linear regression models.

Table 2-1. Summary of the experimental sites

Site	Years	Land use type	Parent materials	Soil type	Clay %	Silt %	Sand %	Treatments	P fertilizer type	Mean P fertilizer application rate (kg ha^{-1} year^{-1})	Total carbon (g kg^{-1})	pH
Rengen, Germany	1941-2016	grassland (meadow)	Lower Devonian sandstones, siltstones, and clay slates	Stagnic Cambisol	23	54	23	Control	-	0	49.0	4.9
								Ca	-	0	41.9	6.5
								Ca N	-	0	43.8	6.5
								Ca N P	Basic slag	35	43.0	6.6
								Ca N P KCl	Basic slag	35	43.9	6.5
								Ca N P K_2SO_4	Basic slag	35	45.2	6.6
Thyrow, Germany	1937-2016	arable land	Periglacial sand overlying a loam and a calcareous glacial till	Cutanic Albic Luvisol	3	14	83	NK+lime	-	0	3.60	6.0
								NPK	Triple Superphosphate	24	-	3.8
								NPK+lime	Triple Superphosphate	24	3.80	6.0
Askov, Denmark	1923-2016	arable land	Morainic deposits from the Weichselian glaciation	Luvisol	12	13	75	No fertilizer	-	0	12.3	6.5
								Animal manure (AM)	Cattle Manure	19	15.0	6.5
								Mineral fertilizer (NPK)	Superphosphate	19	13.7	6.5

Note: total carbon data of Rengen are organic carbon contents from Pätzold et al., 2013.

3. Results

3.1 Uranium concentrations in soil

Rengen (1941-2016)

The U concentration in soil without fertilization (control) at Rengen was 0.80 ±0.08 mg kg^{-1}. Soils receiving lime (Ca) or Ca/N contained similar concentrations of U (0.89 ±0.04 mg kg^{-1}), whereas mean U concentrations were significantly higher in soils fertilized with P in Ca/N/P, Ca/N/P/KCl and Ca/N/P/K_2SO_4, (0.96 ±0.08 mg kg^{-1}) than in soil from control plots (Fig. 2-1). Concentrations of U in soils receiving Ca/N/P, Ca/N/P/KCl, and Ca/N/P/K_2SO_4 did not differ significantly, indicating that the application of K fertilizers did not induce additional U accumulation.

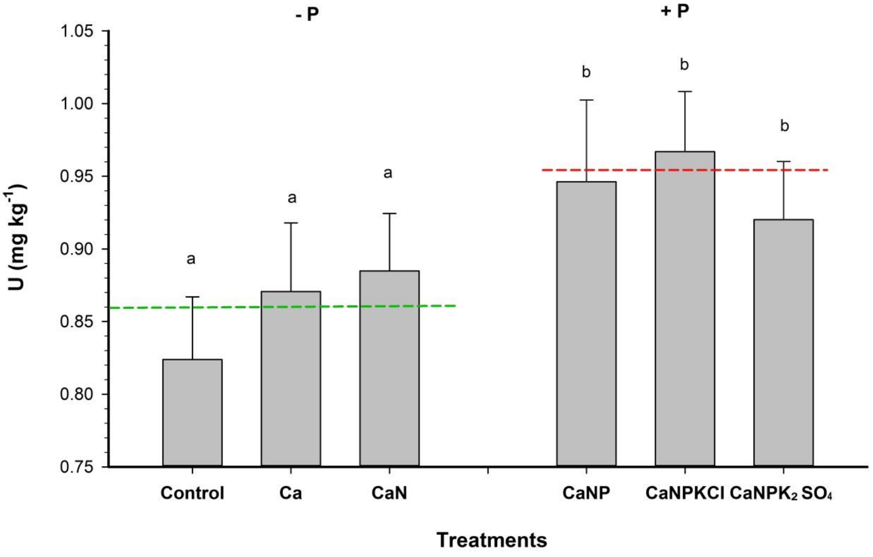

Figure 2-1. Uranium (acid-extractable) concentrations in topsoil of five fertilizer treatments in Rengen grassland. “Control” refers to the unfertilized controls. Different letters indicate significant differences between the treatments at $p < 0.05$ level. The dashe lines represent the average value for the three treatments without and with P fertilization.

Thyrow (1937-2016)

At the experimental site in Thyrow, soil cores down to 100 cm were collected in order to study the depth profile of U concentrations in soil. The vertical patterns of U concentration were similar for all three treatments (NK+lime, NPK+lime, NPK) (Fig. 2-2), with higher U concentrations in the Ap1 horizon (0-24 cm) and in the E/Bt horizon (70-100 cm). Subsoil U concentrations generally increased with depth (30-100 cm). For each treatment, the mean U concentrations at different horizons were significantly different. When comparing different treatments for a given horizon, the U concentrations were significantly higher in the topsoil (Ap1) of the P fertilized plots (NPK+lime, NPK, 0.37 mg kg^{-1}) than in plots without P fertilization (NK+lime, 0.29 mg kg^{-1}) (Fig. 2-2). However, no significant differences in U concentration were observed between the fertilized and unfertilized plots in the deeper soil horizons.

Askov (1894-2016)

The concentration of acid-extractable soil U increased slightly from 1923 to 2016, i.e. from 0.66 to 0.96, 0.61 to 0.84 and 0.79 to 1.08 mg U kg^{-1} for the control, AM and NPK treatments, respectively (Fig. 2-3). The increase in soil U concentration over time can be described by a significant linear regression ($p < 0.05$). The slopes of the linear regression represent annual U accumulation in soils. The highest annual U accumulation was observed for NPK treated soil (5.1 µg kg^{-1} yr^{-1}), followed by the control (4.7 µg kg^{-1} yr^{-1}) and the AM treatment (3.7 µg kg^{-1} yr^{-1}). Differences in soil U concentrations were not significant among the control, AM and NPK treatments in 2010 and 2016. For the entire experimental period of 92 years, no significant differences in acid-extractable U were observed between the control soil and the soils receiving animal manure or mineral fertilizers.

To examine whether fertilizer-derived U in Askov had become un-extractable (by acid digestion) over time, the soils were analyzed for total U concentrations. Mean total soil U concentrations were significantly higher in the NPK treatment for the last 32 years (1985-2016) than for the first 38 years (1938-1976). This trend was not observed for the control and AM treatments (Fig. 2-3 – insert). This suggests that long-term mineral P fertilizer application indeed resulted in U accumulation in the Askov soil, although at a low level. In addition, a significant linear regression was observed for the total U concentrations over time in the Askov soils, but with a steeper slope compared with the acid-extractable U concentration (Fig. 2-3). However, we found no significant difference between the coefficients of regression. Apparently, fertilizer-derived U tend to remain in the acid-extractable fraction.

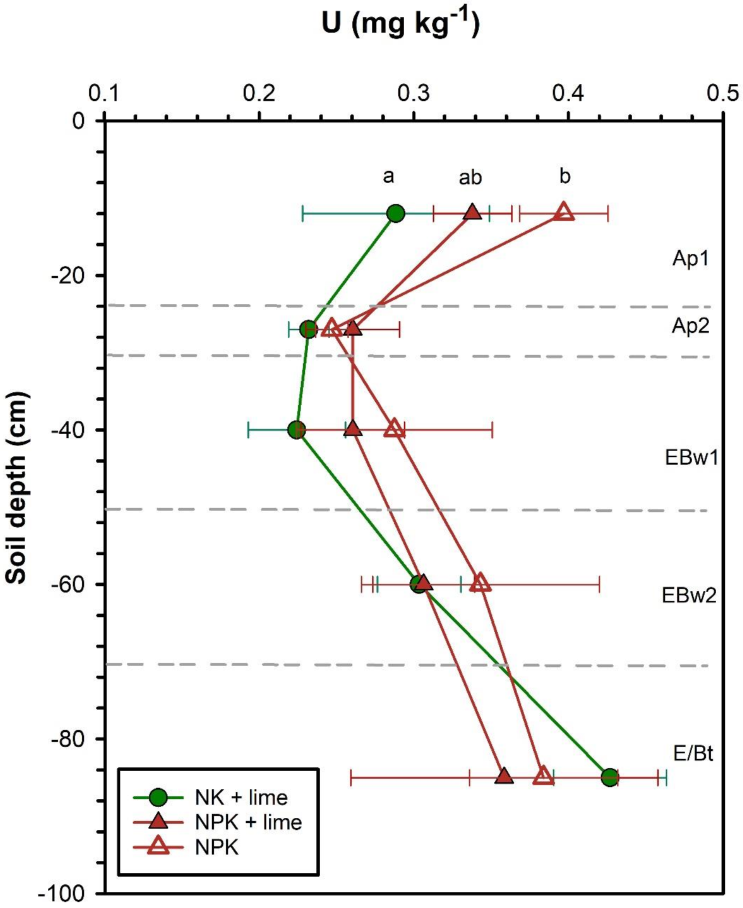

Figure 2-2. Depth profiles of U (acid-extractable) in soils of the long-term experimental field of Thyrow. The error bars present the standard deviations of the four field replicates.

.

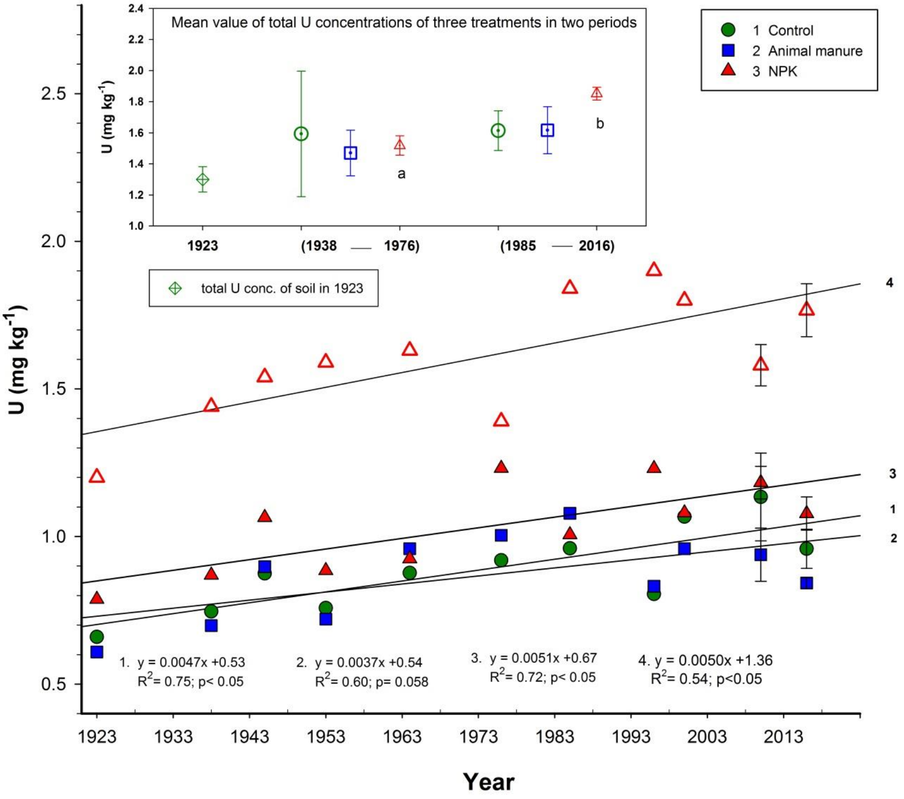

Figure 2-3. Temporal changes of U concentrations (total and acid extractable) in arable topsoil (0-20 cm) of the control, animal manure (AM) and NPK fertilizer treatments at Askov. Different shaped symbols denote samples from three treatments. The filled symbols signify acid extractable U concentrations, whilst empty symbols indicate total U concentrations. Different letters indicated significant differences between the treatments at $p < 0.05$ level.

3.2 The relationship between P and U

At all three experimental sites, elevated concentrations of acid-extractable U in soil correlated with increased P (acid-extractable) concentrations in P fertilized treatments (Fig. 2-4; soil P concentrations are shown in Fig. A1-A3). However, the relation between the U and P concentrations differed for the Rengen, Thyrow and Askov sites. At Rengen, two obvious clusters of treatments were visible for plots with and without P fertilizer addition. The U concentrations were generally lower at Thyrow than at the other two sites, although the range of P concentrations was nearly the same in Askov and Thyrow. There was no significant correlation between the concentrations of U and P at Askov.

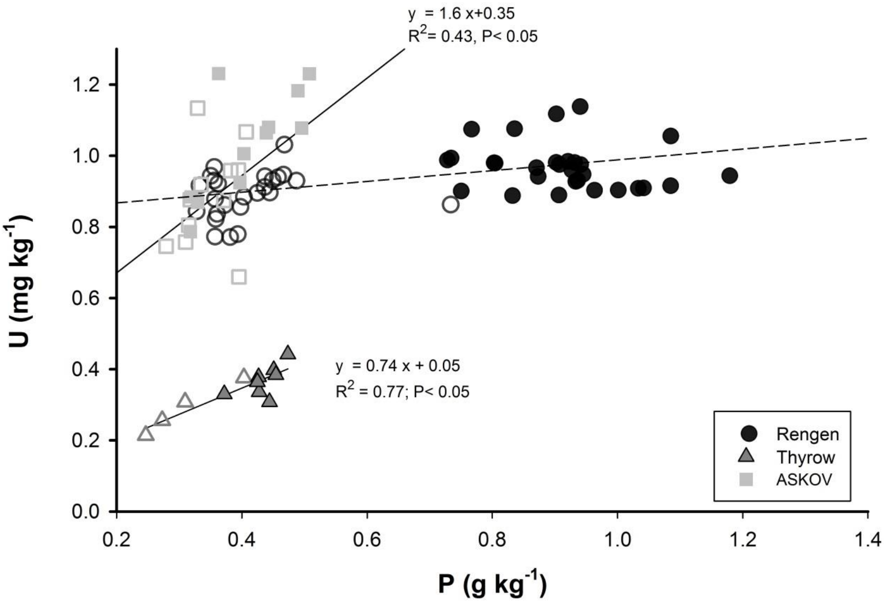

Figure 2-4. Relationships between concentrations of P and U in topsoil of Rengen (Control, Ca, Ca/N, Ca/N/P, Ca/N/P/KCl, Ca/N/P/K_2SO_4), Thyrow (NK+lime, NPK+lime, NPK) and Askov (Control and NPK treatments) long-term experimental sites. The different types of symbols represent different experimental sites. Open symbols indicate treatments without P fertilizer application while filled symbols indicate treatments with P fertilizer application. Significant ($p < 0.05$) linear correlations were found between P and U concentrations of topsoil in Thyrow and Askov.

4. Discussion

4.1 Methods to extract soil uranium

Total U concentrations in soils reflect U derived from parent materials and anthropogenic sources. To obtain total U concentrations, a complete digestion of the sample is mandatory and typically achieved by combinations of highly oxidative acid (such as HNO_3) and hydrofluoric acid (HF), with HF employed to release the element residing in the most recalcitrant fractions (e.g. Bigalke et al., 2017). High-temperature fusion with lithium or sodium borates is also commonly used (e.g. Delijska et al., 1988) but may dissolve substantial amounts of mineral matrix that complicate further analysis (e.g. in stable isotope studies). Other extraction methods attempt to dissolve the samples partially to access different fractions of the element. These sequential extraction schemes are developed to separate U in soil into an exchangeable fraction, a carbonate bound (weakly absorbed) fraction, U associated with Fe and Mn oxides (hydrous-oxide bound), the organically bound or adsorbed fraction, and the fraction of U that resides in components of the mineral matrix (Tessier et al.,1979; Regenspurg et al., 2010). Such fractionations may provide more detailed information on the origin, biological and physicochemical availability and the mobility of the element (Zimmerman and Weidorf, 2010; Filgueiras et al., 2002). Uranium retained in the exchangeable fraction is considered to be bioavailable U. However, differences in pH, temperature, extraction time, and soil texture and mineralogy may lead to large variations in U content in extracted fractions and provide incomparable data.

In the present study, we applied non-HF microwave-assisted digestion using concentrated HNO_3 following a protocol recommend by the United States Environmental Protection Agency (USEPA) (1994). This method has been widely applied to soil for elemental analyses (e.g. Sastre et al., 2002; Eskilsson and Björklund, 2000). The U extracted by this method may reveal the potential of U to enter the biosphere and aqueous systems (Rao et al., 2008) whereas the un-extracted U is considered immobile and sequestered in structural silicate minerals. The concentration of extractable U may provide us information on the fate of anthropogenic U inputs, as these tend to reside in the first four fractions mentioned above, while the natural occurrence of U residing in parent materials is not extracted (Rapin et al., 1986). It has been shown that compared with un-fertilized soil, the fertilizer derived U tends to be adsorbed to organic matter or to poorly crystalline Fe/Al minerals (Yamaguchi et al., 2009; Takeda et al., 2006).

4.2 Uranium accrual in agricultural soil by P fertilizer application

At Rengen and Thyrow, accumulation of U relates significantly to addition of P fertilizers (Fig. 2-2). Accumulation of U also occurred in the Askov arable soil with P fertilization, but intriguingly at a rate similar to the unfertilized control treatment (Fig. 2-3). This suggests that other sources may have contributed to the U accumulation in soil (see section 4.3), while P fertilization was only partially, if at all, responsible for increased U concentrations. The average annual U accumulation was 1.3 µg kg^{-1} yr^{-1} for Rengen grassland and 0.6 µg kg^{-1} yr^{-1} for Thyrow arable land in plots with P additions. The accumulation rates for U in the present study were below 2 µg kg^{-1} yr^{-1} which is small compared with rates reported in previous studies from Germany, France and New Zealand (Table A-1). With similar P fertilizer application rates these studies show annual U accumulation rates up to 47 µg kg^{-1} yr^{-1} (Fig. 2-5). The U accumulation rate in Rengen is almost ten times lower and is ascribed to the type of P fertilizer, (basic slag / Thomas slag / Thomas phosphate) applied during the first half of 20th century. Basic slag is a by-product of steel production but reports on U contents in basic slag used as P fertilizer are scare. According to data published by the former German Federal Agricultural Research Centre (FAL), U concentrations in basic slag (median 0.47 mg kg^{-1}) are far below those of other P sources (Kratz et al., 2004). The U concentration of basic slag applied in Rengen is around 1 mg kg^{-1} and significantly lower than that in typical mineral P fertilizers (with median value of 34 mg kg^{-1} for single superphosphate, 95 mg kg^{-1} for triple superphosphate) (Taylor et al., 2014). Soils from other long-term experiments in Bonn and Freising applying basic slag show no or very low U accumulation rates (2 µg kg^{-1} yr^{-1}; Rogasik et al., 2008).

The low U accumulation rates at Askov and Thyrow also relate to the origin of P fertilizers applied. The two dominating sources of raw phosphate for P fertilizer production are sedimentary deposits and igneous rocks. About 75% of the world's P consumption is from sedimentary phosphate rocks which usually contain substantial U concentrations (27-245 mg U kg^{-1}; Sattouf, 2007) compared with igneous phosphate rocks (0.2-37 mg U kg^{-1}) (Van Kauwenbergh, 1997; Schnug et al., 1996; Sun et al., 2019). The P fertilizers applied in Askov and Thyrow are derived from igneous phosphate rocks mined in Finland and Kola Peninsula of Russia, respectively. Soils from other long-term experimental sites in former East Germany (Halle and Müncheberg) with P fertilizers of igneous origin most likely applied before 1990 show U enrichments (1 and 2 µg kg^{-1} yr^{-1}) comparable to our sites (Rogasik et al., 2008).

Since 1990, most of the P fertilizers used in German agriculture have been of sedimentary origin and inputs of U to soils may therefore have increased over the past 30 years in former East German regions (Rogasik et al., 2008). At Askov, the accumulation of U in soil with cattle manure was similar to that of the control, indicating that the applied manure was low in U contents. In general, organic fertilizers have lower U concentrations than mineral P fertilizers (Kratz et al., 2008). Taylor et al. (2014) reported a median U concentration for cattle manure of 0.17 mg kg^{-1}

The large regional variations of annual U accrual found in other studies (Fig. 2-5) reflect the use of P fertilizers produced from different phosphate sources. The soil U accumulation rates reported for many European long-term experiments are relatively low (< 10 µg kg^{-1}), but higher U accumulation rates (> 10 µg kg^{-1}) have been observed for instance at Schuby (Germany), and Loir-et-Cher and Indre-et-Loire (France) (Wetterlind et al., 2012). This most likely reflects that a large proportion of the phosphate rocks used in Europe is of sedimentary origin with widely different U contents and mainly imported from Morocco (35% of total imported phosphate rocks), Russia (32%), Algeria, Israel, and South Africa (Tulsidas et al., 2019). More dramatic U accrual has been found in Japan and New Zealand with an average U increase of 40.5 and 27.5 µg kg^{-1} yr^{-1}, respectively (Fig. 2-5) (Takeda et al., 2006; Yamaguchi et al., 2009; Taylor and Kim, 2008; Schipper et al., 2011). For Japanese pastures, the annual accural was reported to be above 100 µg U kg^{-1} and partly attributed to application of fertilizers with high U loads (Yamaguchi et al., 2009).

When related to the amounts of P fertilizer applied, U accumulation rates of 0.26-0.77 µg U kg^{-1} P (Table 2-1) were found in Japan, up to 0.84 µg U kg^{-1} P fertilizer in New Zealand, and 0.18-0.74 µg U kg^{-1} P in USA and France (Table A-1). The P fertilizers imported to Japan originate mainly from the USA (Webeck et al., 2015), whereas P fertilizers used in New Zealand originate from Western Sahara (WSRW, 2019). These supply chains are known to have phosphate rocks enriched in U compared with igneous rock sources (Sun et al., 2019).

The average background concentration of U in surface soil is currently about 2 mg kg^{-1} (NCRP, 1984). Considering the low U accumulation rates (< 2 µg kg^{-1} yr^{-1}) found in our study and a continuation of current fertilizer use, it would take ca. 10,000 to 50,000 years before P fertilizer-derived U accumulation exceed the critical soil contamination criteria of 30 mg U kg^{-1} issued by the USNRC (1992).

4.3 Other sources of uranium to agricultural soils

A gain in soil U without P fertilization was observed at Askov. This observation aligns with results from other studies (Rothbaum et al. 1979; Stojanovic et al., 2006). Soil U concentration increased by 0.11 mg kg^{-1} from 1870 to 1976 in unfertilized treatments of the Park Grass (UK) experiment in England (Rothbaum et al. 1979). A study in Serbia found that U concentration increased by 0.66 mg kg^{-1} from 1989 to 1995 without P fertilization (Stojanovic et al., 2006). Possible sources for the additional U in agricultural soils include atmospheric deposition and long-term liming practices. Fly ash and other airborne emissions from coal-fired industry and power plants may historically be a source of U in soil although some studies suggest negligible U input by atmospheric deposition (Bigalke et al., 2017; Kratz et al., 2008).

Another potential source of U accumulation is applications of lime. Jones (1992) suggested that liming accomplish a long-term increase of soil U concentrations while other studies show that lime-derived U is insignificant (e.g. Taylor, 2007) or at least negligible when compared with U applied in mineral P fertilizers. The reported U concentrations in lime range from < 1 to 50 mg kg^{-1} (Bell, 1963), and Taylor et al. (2014) estimated an average U concentration in lime of 0.6 mg kg^{-1}. With an annual application of 1000 kg ha^{-1} lime in the Askov experiment and a concentration in the lime of 0.6 mg U kg^{-1}, the estimated U accumulation induced by liming accounts for 0.3 µg kg^{-1} yr^{-1}. This corresponds to 10% of the U increase in control (4.7 µg kg^{-1} yr^{-1}) and AM (3.7 µg kg^{-1} yr^{-1}) treatments. Since the concentrations of U in lime applied at Askov remain unknown, we cannot assess the importance of lime-derived U at Askov in more detail. However, the concentration of U in lime varies widely and inputs of lime-derived U may be of quantitative significance for soils dressed with P fertilizers low in U contents.

At Thyrow, the vertical distribution of U concentrations was unaffected by P fertilization but probably influenced by soil forming processes. The soil is an Albic Luvisol and illuviation processes may translocate clay, humus and particle-bound U from the eluvial horizon E into the illuvial Bt horizon (Baize et al., 2014) and thereby deplete U in the upper soil horizons. Consequently, the increase in soil U concentration from Ap2 to Bt horizon in Thyrow could be mediated by pedogenic processes. Aubert et al. (2004) found enrichment of U in deeper soil horizons resulting from illuviation, and we surmise the small, but significant U increase in the Ap horizon results from P fertilizer application. In addition, the regression coefficient of the relation between P and U concentrations was statistically significant in the topsoil of Thyrow. However, this was also true for un-fertilized treatments. We attribute this observation to the parent material and local soil formation processes, which warrants further investigation.

5. Conclusions

Soils from P fertilized plots in the Rengen, Thyrow and Askov long-term agricultural field experiments showed very low U accumulation rates (< 2 µg kg^{-1} yr^{-1}). The main reason was the use of P fertilizers derived from sources with low U concentrations (igneous phosphate rocks and basic slag). However, we also found a small but unexplained increase in soil U concentrations in unfertilized plots. We conclude that low and long-term sustainable concentrations of U can be maintained when agricultural production relies on in P fertilizers produced from phosphate ores low in U.

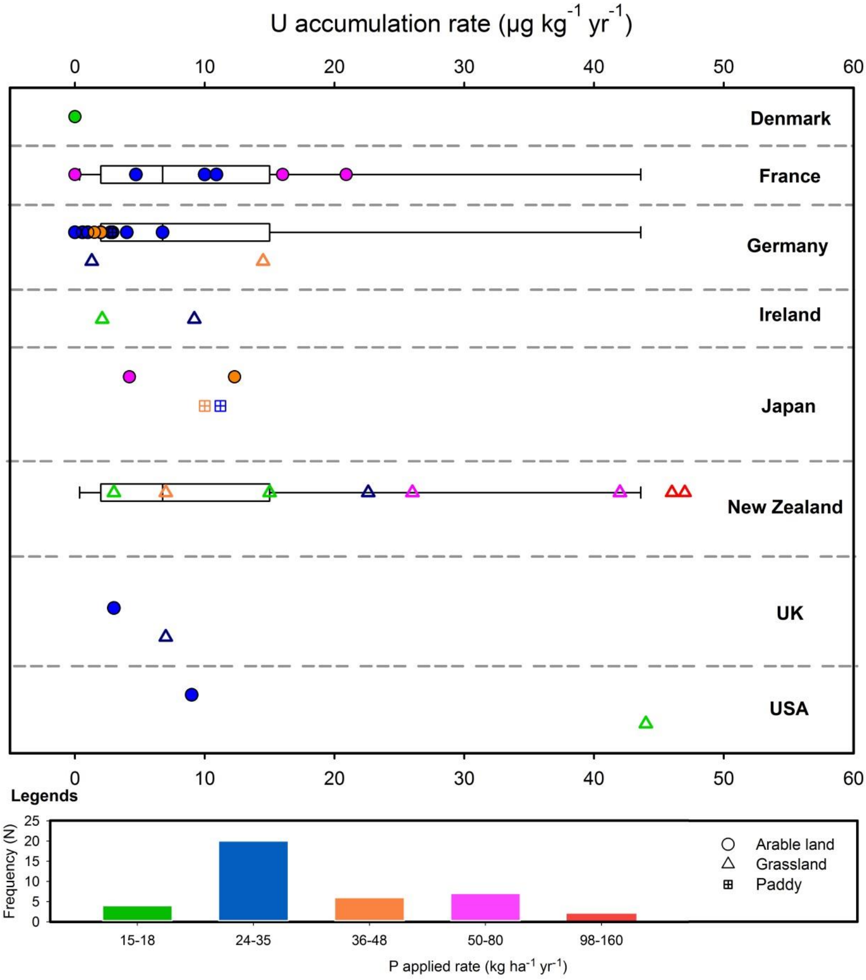

Figure 2-5. Summary of U accumulation rates in topsoil of various related studies (see Table A-1; Supplementary materials, for details). Different colors mean different P applied rate in agricultural soils. Different symbols mean different type of land use.

Chapter 3

Critical accumulation of fertilizer-derived uranium in Icelandic grassland Andosol

Modified on the basis of the manuscript

Sun, Y., Amelung, W., Gudmundsson, T., Wu, B. and Bol, R.

Published in *Environmental Sciences Europe*

1. Introduction

Phosphorus (P) fertilizers are primarily derived from phosphate rocks, which, however, contain various levels of uranium (U) (Van Kauwenbergh, 1997; Schnug et al., 1996; Baturin and Kochenoy, 2001). The majority (80-90%) of U is transferred to the final fertilizer products during mineral processing (Haneklaus et al., 2017). Therefore, U can accumulate in agricultural soil after long-term P fertilizer application (Takeda et al., 2006; Yamaguchi et al., 2009; Taylor and Kim, 2008; Schipper et al., 2011; Schnug and Haneklaus, 2015). After this risk being first mentioned by Rothbaum et al. (1979), the consensus has been reached that P fertilizer-derived U accumulates in the topsoil of agricultural fields (Yamaguchi et al., 2009; McDowell, 2012). Chemical toxicity of U is of greater concern than its radiotoxicity, due to the low intrinsic specific radioactivity of ^{238}U. The most sensitive adverse effect of U on human being is chemically-induced toxicity to the kidney via food and water intake (EFSA, 2009). Since the transfer factor of U from soil to plant is below 1% (Sheppard and Evenden, 1988; Schnug and Haneklaus, 2015), the U uptake by plants and then entering the food chain is not a predominant health issue (EFSA, 2009). However, it has been suggested that drinking water can become a main source of human U intake (Schnug and Lottermoser, 2013). A number of studies indicate the transfers of fertilizer-derived U to water bodies (Bigalke et al., 2018; Azouazi et al., 2001; Huhle et al., 2008; Zielinski et al., 2006).

Despite potential negative impacts of U on human being and the environment, there still is a lack of regulations on the limitation of U in P fertilizers both at the regional or global scales. Worldwide, Canada, rich in U resources and with a long history of U exploration, mining and generation of nuclear power (World Nuclear Association, 2020), is the only country that has implemented a soil quality guideline of 23 mg kg^{-1} U for agricultural land use to protect the human and environmental health (CCME, 2007). However, internationally there still are no limitations for U content in fertilizers (Smolders, 2017). Yet, an increasing number of studies report an accumulation of fertilizer-derived U in agricultural soils or in groundwater (Bigalke et al., 2008; Zielinski et al., 2006; Liesch et al., 2015). The reported accumulation rates of fertilizer-derived U in soil are in the range of 0-130 µg kg^{-1} yr^{-1} with median value of 7.65 µg kg^{-1} yr^{-1} (Sun et al., 2020). Uranium concentrations in soil have been reported to range from 0.3 to 11.7 mg kg^{-1} with an average background concentration of 2 mg kg^{-1}. Therefore, the fertilizer-derived U accumulation can become a cumulative issue after hundreds of mineral P fertilization. Many studies have confirmed that fertilizer-derived U will increase soil U contents, though only marginally and not necessarily to a degree that it significantly increases U exposure to human being via food or beverages (e.g. Sun et al., 2020). As a result, current pressure on governmental legislations is low to set up a guideline value for U in fertilizers.

Volcanic soils (Andosols), covering approximately 124 million hectares of the land surface, are rich in organic matter and mineral nutrients, have high water holding capacity, and thus are considered to be important agricultural soil resources in, e.g., Japan, Iceland, and New Zealand, as well as in several tropical areas (Driessen et al., 2000). However, Andosols are also usually characterized by low inherent P availability, thus requiring higher amounts of P fertilizers than many other soils. Extensive P fertilization on these soils may on the other hand induce high U accumulation that eventually poses risks on the environment and human health. Therefore, in this study, we aimed to evaluate current fertilization strategies on Andosols with respect to fertilizer-induced U accumulation. We thus investigated U accumulation in Andosols at two long-term experimental sites in Iceland, where P fertilizers had been applied for about 50 years on permanent grasslands. Our results will provide useful information on future fertilization strategies on Andosols.

2. Materials and methods

2.1 Studied sites and soil sampling

Soil samples were taken from two long-term permanent grasslands in Sámstaðir and Geitasandur, Iceland, respectively (Table 3-1). The Sámstaðir experimental site was established in 1950 and lasted until 2004. The site is located on drained Histic Andosols, overlying a 3 m thick Histosol, with numerous volcanic ash layers and a high input of aeolian material. For this study we used soil samples were taken from the plots that received mineral P fertilizers at an annual rate of 39.3 kg ha^{-1} (39P/e treatment) and plots without P fertilization. In addition, soil samples were taken outside the experimental field where no fertilization had been applied, serving as the control (0P/a treatment). soil cores (15 to 20) were collected from each plot and mixed to a representative sample and each treatment had 4 replicates.

The Geitasandur experiment started in 1958 and lasted until 2007, which was run on freely drained Vitric Andosols. The site was poorly vegetated at the start of the experiment, but a 10 cm thick fibrous root mat was formed towards the end of the experimental period. From 1958 to 1972, a part of the site received P fertilizers at an annual rate of 39.3 (= 39P/d treatment) kg ha^{-1}, while the other part received no P fertilizers (= 0P/a treatment). Each treatment had three field replicates. In 1973, the original 5x10 m^{2} plots were split into two 5x5 m^{2} sup-plots, with one sub-plot continuing with the same P application (a1 = 0 or d1 = 39.3 kg ha^{-1} yr^{-1}), and the other sub-plot receiving 79.6 kg P ha^{-1} yr-1 (a2 or d2 = 80P treatment). Therefore, there were three field replicates for each treatment (i.e., a1, a2, d1, d2) after 1973 (Table 3-1). that we used in this study. Three soil cores were collected from each plot and sub-plot.

Soil samples were taken from each of these plots at the two sites with a 20 cm long cylindrical auger, with an inner diameter of 3.1 cm. Each soil core was further cut into 0-5, 5-10, and 10-20 cm depth intervals. This study used the soils from the depth intervals of 0-5 and 5-10 cm. More detailed information on these sites and the sampling procedures can be found in Table 1 and the studies of Gudmundsson et al. (2011, 2014). A sample of superphosphate fertilizer applied at the Iceland experiment sites was collected and analyzed for its U concentration.

2.2 Analytical method

The methods for U and P concentrations determination were expressed in section 2.2 Chapter 2. The differences of U concentration in various treatments were analyzed by one-way ANOVA with a significance level p< 0.05) to detect significant differences between individual treatments. The relationships between P and U concentrations were examined by fitting linear regression models. Annual U accumulation rates were calculated as:

$$U\ accumulation\ rate\ (\mu g\ kg^{-1}\ soil\ yr^{-1}) = \frac{(U_{P-fertilized} - U_{Control})}{N_{P-fertilized}}$$

where $N_{P\text{-fertilized}}$ was the number of years when P fertilizers were applied to the soil, and $U_{P\text{-fertilized}}$ and $U_{Control}$ were U concentrations in the soils with and without P fertilizers, respectively.

Table 3-1. Information of soil properties, fertilizer applied annually, sampling depth in in Sámstaðir and Geitasandur long term experiment sites.

Treatment	Annually fertilizer applied (kg ha^{-1})			Soil depth	Total C	Total N	Bulk density
	N	P	K	(cm)	% DM	% DM	g cm^{-3}
Sámstaðir (1950-2004)		**Histic Andosol**					
a (0P)	70	0	75	0-5	15.9	1.19	0.34
				5-10	9.7	0.8	0.45
e (39P)	70	39.3	75	0-5	14.6	1.11	0.34
				5-10	8.8	0.74	0.45
Geitasandur (1958-2007)		**Silandic Andosol**					
0P (a1)	120	0	80	0-5	9.5	0.62	0.49
				5-10	2.2	0.17	1
39P (d1)	120	39.3	80	0-5	16.7	0.98	0.27
				5-10	2.5	0.18	0.94
79P (a2)	120	78.9[a] (55.7)	80	0-5	22.5	1.22	0.2
				5-10	3.5	0.23	0.84
79P (d2)	120	78.9[b] (67.5)	80	0-5	22.1	1.16	0.23
				5-10	3	0.2	0.89

a: 0 kg ha^{-1} year^{-1} was applied from 1958-1972; 79.6 kg ha^{-1} year^{-1} was applied from 1973-2007. 55.7 kg ha^{-1} year^{-1} was the average P application rate in 1958-2007.

b: 39.3 kg ha^{-1} year^{-1} was applied from 1958-1972; 79.6 kg ha^{-1} year^{-1} was applied from 1973-2007. 67.5 kg ha^{-1} year^{-1} was the average P application rate in 1958-2007.

3. Results

Fertilizer-derived U accumulations in Icelandic soil

The U concentration in the fertilizers applied at the two sites was 95 mg U kg^{-1}. After application for about 50 years of such a fertilizer at a rate of 39.3 kg ha^{-1}, soil U concentrations in the surface soil (0-5 cm) increased by 7.3 mg kg^{-1} and 6.1 mg kg^{-1} at Sámstaðir and Geitasandur, respectively. Moreover, the U concentrations in the surface soil of the 80P treatments exceeded 15 mg kg^{-1} and were almost twice that of the 39P treatments in Geitasandur (Fig.3-1A).

No significant difference was found in U concentrations between 0-5 cm and 5-10 cm soil depth in the controls at both sites. However, in the 39P and 80P treatments, U concentrations increased not only in the 0-5 cm but also in the 5-10 cm soil depth, increasing by 1 and 2 mg kg^{-1} for 39P and 80P treatments, respectively (Fig. 3-1A).

The U stocks in the top 0-5 cm soil were significantly smaller in the control than in the P fertilizer treatments, so were the U stocks in the 5-10 cm layer (Fig. 3-1B). In the control, there was no significant difference in U stock between 0-5 cm and 5-10 cm soil, whereas this difference was significant in the P fertilizer treatments both at Sámstaðir and Geitasandur (Fig.3-1B). Compared with the control, 1.04 kg U ha^{-1} had been added at Sámstaðir (0-5 cm) under a P application rate of 39.3 kg ha^{-1}, while 0.92 and 1.55 kg U ha^{-1} had been added at Geitasandur (0-5 cm) in the 39P and 80P treatments, respectively, over a period of about 50 years (Fig. 3-1B). In the soil layer of 0-5 cm, the final fertilizer-derived U input were about ten times those in the control. In the course of the experiments at both sites, over 60% of fertilizer-derived U had accumulated in the top 0-5 cm soil.

The annual U accumulation rates (0-5 cm) were 113, 149, 310 µg kg^{-1} yr^{-1} for the 39P (e), 39P (a1) and 80P (a2, d2) treatments, respectively. In addition, the amounts of annual U input to one hectare were 19, 19 and 32 g ha^{-1} yr^{-1} (Table 3-2).

The concentrations of P and U correlated significantly in both soils ($R^2 > 0.7$, $P < 0.05$; Fig. 3-2), confirming that the U accumulation in the grassland most likely coincided with P accumulation under the P fertilizer applications.

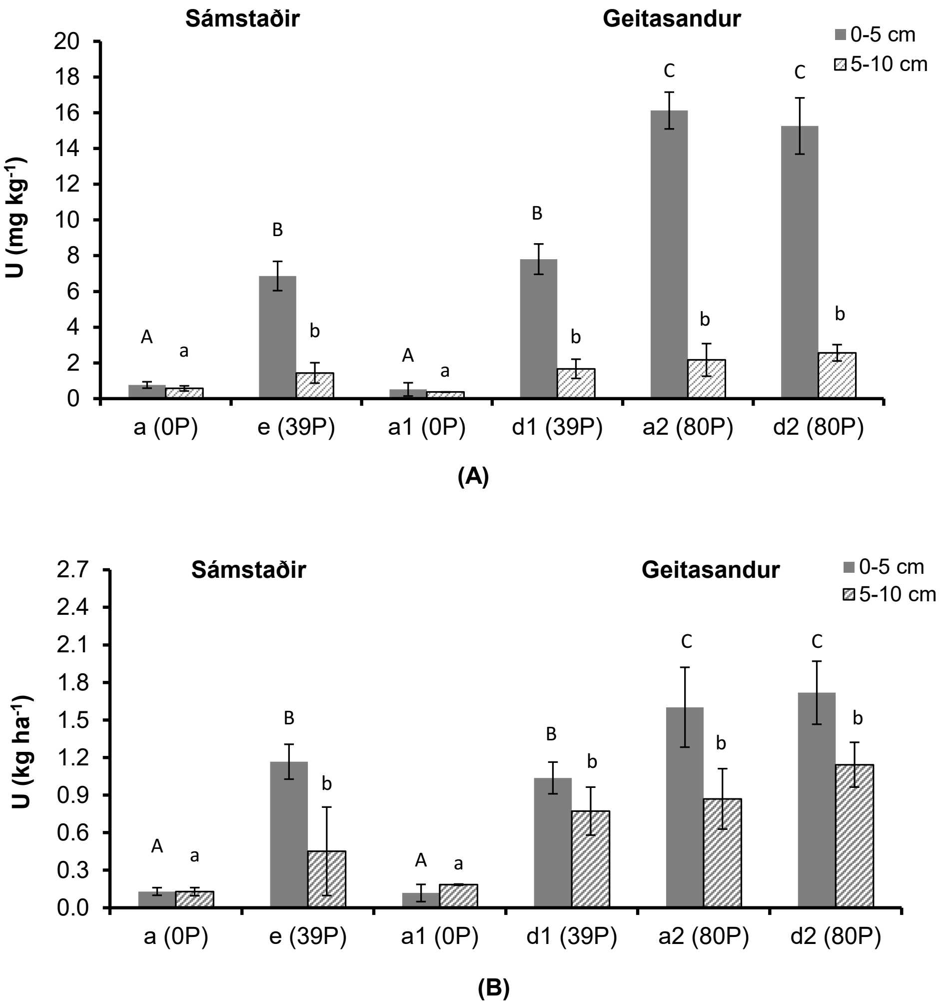

Figure 3-1. Soil U concentrations (A) and U stock (B) in treatments under different phosphorus application rates in Sámstaðir and Geitasandur long-term experiment sites of Iceland. Error bars= ± standard deviation. Different letters indicate significant difference between the treatments, $p < 0.05$.

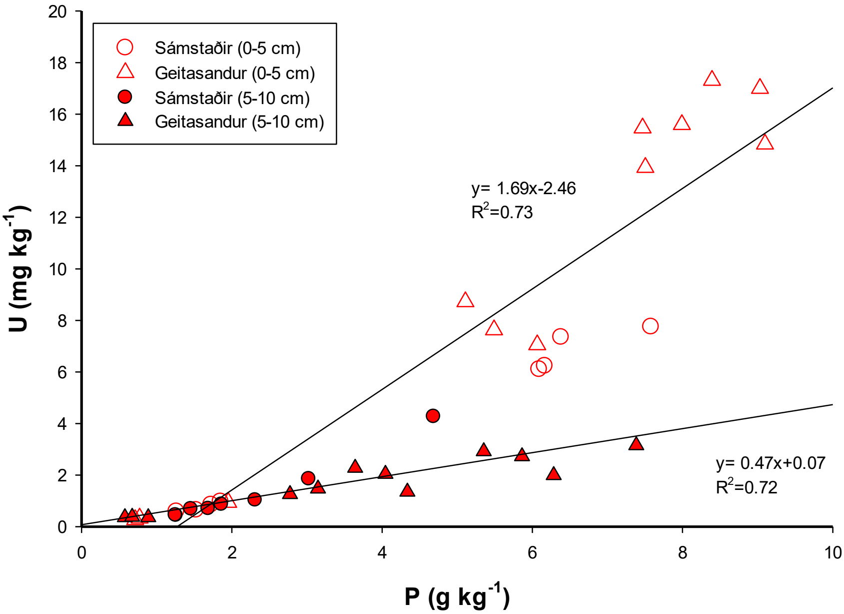

Figure 3-2. Relationships between P and U concentrations in soil depth of 0-5 cm and 5-10 cm in Sámstaðir and Geitasandur.

4. Discussion

Our results support the earlier findings that U accumulates in agricultural soils due to P fertilization (Takeda et al., 2006; Yamaguchi et al., 2009; Taylor and Kim, 2008; Schipper et al., 2011). However, the annual U accumulation rates found in this study exceeded those reported for other ecosystems so far. The U accumulation rates reported in this study (113, 149 µg kg^{-1} yr^{-1}) were far above the high end of the to-date reported U accumulation rates (2-29 µg kg^{-1} yr^{-1}) for other soils with similar P application rates (30-45 kg ha^{-1} yr^{-1}) (Schipper et al., 2011; McDowell, 2012; Wetterlind et al., 2012). Even though a broad range of U accumulation rates (0-130.6 µg kg^{-1} yr^{-1}) were found in previous studies (Takeda et al., 2006; Yamaguchi et al., 2009; Taylor and Kim, 2008; Schipper et al., 2011; Rothbaum et al., 1979; Wetterlind et al., 2012; Tunney et al., 2009; Rogasik et al., 2008), none of them reached the values found in the present study (Table 3-3).

Clearly, the amount of the applied P fertilizers is one of the critical factors for the amount of U that accumulates in soils. In our study, U accumulation rates increased with increasing amounts of P fertilization. The P application rate (79 kg P ha^{-1} yr^{-1}) at Geitasandur was twice or three times that typically applied to non-Andosols, thus leading to the higher U accumulation rates. A high U accumulation rate of 130.6 µg kg^{-1} yr^{-1} was also found in an Andosol in a long-term experiment in Japan with an annual P application of 74.3 kg ha^{-1} yr^{-1} (Yamaguchi et al., 2009). Accumulation rates of U reported in Andosols of New Zealand were 15-67 µg kg^{-1} yr^{-1} with a P application range of 19.7-100 kg ha^{-1} yr^{-1} (Taylor and Kim, 2008; Schipper et al., 2011). Risks of fertilizer-derived U should thus be specifically considered on Andosols.

Uranium concentration in the applied P fertilizer is another factor determining the U accumulation rate (Sun et al., 2020; Takeda et al., 2006). When U concentration in the P fertilizer is small, low U accumulation rate can also occur in Andosols. Takeda et al. (2006) found a relatively low U accumulation rate of 4.2 µg U kg^{-1} yr^{-1} in an Andosol in Japan in spite of a high P application of 65 kg ha^{-1} yr^{-1}. This was attributed to the small U concentration (31 mg U kg^{-1} fertilizer) in the applied superphosphate (Takeda et al., 2006). The differences in U concentration of P fertilizers are attributed to the variability of U concentrations in different phosphate rocks used for P fertilizer production. In general, igneous phosphate rocks (e.g. from Russia) usually contain less U (2.5-40 mg kg^{-1}, mean value 14.4 mg kg^{-1}) than sedimentary rocks (e.g. from Morocco) (57-245 mg kg^{-1}) (Van Kauwenbergh, 1997; Sun et al., 2020). In addition, U concentrations in sedimentary phosphate rocks differ in various deposition environments (Van Kauwenbergh, 1997; Baturin and Kochenov, 2001). The phosphate rocks imported to Europe are predominately from Morocco (35.1%), Russia (31.6%), Algeria (12.3%) and Israel (7.5%) (Tulsidas et al., 2019). As these phosphate rocks are either igneous or sedimentary, their U concentrations would also vary in a wide range. Therefore, for soils like Andosols which require large amounts of P fertilizers, selecting fertilizer products low in U should be a sustainable way to both ensure crop yields and minimize fertilizer-derived U accumulation.

To evaluate the P fertilizer quality regarding U concentration we analyzed a P fertilizer sample applied at the two sites. Its U concentration (95 mg U kg^{-1} fertilizer) was at the middle level in the range of previously reported values (15-208 mg kg^{-1}, Rogasik et al., 2008, Sun et al., 2020). However, as the fertilizers applied during the 50 years also included other superphosphates with unknown U concentrations, we in addition estimated an average U concentration per kg P by using the total increased U stock divided by the total amounts of the applied P, which resulted in 580 and 795 mg U kg^{-1} P for Sámastaðir and Geitasandur, respectively. Since superphosphates contain 8.7% P, the U concentration per kg fertilizer was then 50.5 and 69.2 mg U kg^{-1} fertilizer, respectively. Again, these values were within the range of the reported U concentrations in P fertilizers. Nevertheless, the application of these fertilizers that contained U in a normal range resulted in a remarkable increase of soil U concentration at our study sites.

Table 3-2. Studies of fertilizer-derived uranium in Andosols

Country	Experimental site (Andosols)	P application (kg ha^{-1} yr^{-1})	U accumulation (ug kg^{-1} yr^{-1})	Reference
Japan	Fujisaka Branch	61	4.2	Takeda et al., 2006
	-	74.3	130.6	Yamaguchi et al., 2009
New Zealand	Taupo	19.7	15	Taylor, 2007
	Hinemaiai	98	47	Taylor, 2007
	Whatawhata	30	0	Schipper et al., 2011
		50	42	
		100	67	
Iceland	Sámstaðir	39.3	113	this study
	Geitasandur	39.3	149	this study
		78.6	310	

It is worth noting that the average annual U inputs were19 and 32 g ha^{-1} yr^{-1} when P was applied at a rate of 39.3 and 78.9 kg ha^{-1} yr^{-1}, respectively. These values were within the range of previously reported values (8.6-47 kg ha^{-1} yr^{-1}). Our soils thus exhibited a characteristic U accumulation with high accumulation rates but meanwhile with the moderate annual U inputs. We attribute this observation to the low bulk densities of our Andosols (0.2-0.5 g cm^{-3} in the 0-5 cm soils). Compared with non-Andosols, such low bulk densities resulted in a lower total weight of the soil within a given area and depth, thus increasing the U concentrations and the U accumulation rates. In addition, Andosols usually exhibit elevated contents of organic matter (Arnalds, 2008), which promote the retention of U in the very surface soil (Dall'Aglio, 1971; Roth and FitzGerald, 2015). Besides, no tillage during such long-time fertilization also contributed the high U concentration in those two fields.

Table 3-3. U accumulation rates and U inputs at Sámstaðir and Geitasandur long-term experiment sites.

		Sámstaðir	**Geitasandur**		
Soil depth		39P (e)	39P (a1)	80P (a2)	80P (d2)
0-5 cm	Annual accumulation rate (µg kg^{-1} yr^{-1})	113	149	319	301
	U input (g ha^{-1}yr^{-1})	19	19	30.3	33.2
	U in applied P fertilizers (mg U kg^{-1} P)	489	482	545	492
5-10 cm	Annual accumulation rate (µg kg^{-1} yr^{-1})	16	27	37	45
	U input (g ha^{-1}yr^{-1})	4	12	15	20
0-10 cm	Annual accumulation rate (µg kg^{-1} yr^{-1})	58	52	87	94
	U input (g ha^{-1}yr^{-1})	23	31	45	53
	U in applied P fertilizers (mg U kg^{-1} P)	580	794	811	782

5. Conclusions

In this study, we report two cases of high fertilizer-derived U accumulations at the long-term experiment sites in Iceland (Sámstaðir and Geitasandur). This resulted from a combined effect of two main factors. Firstly, large amounts of P fertilizers were applied to these Icelandic Andosols to maintain grassland productivity of these soils because of their inherent low P availability. Secondly, the low bulk density and high organic matter content in Andosols effectively concentrated U in the upper surface soil. These two factors also play a role in agriculture systems other than Andosols, e.g., on former peatlands, raising the possibility that more unreported areas of agricultural land could contain U with a concentration close to or even higher than the (sole) soil quality guideline of 23 mg U kg^{-1}. Therefore, for these types and other agricultural ecosystems requiring high amounts of P fertilization, proper selection of those P fertilizers low in U content will therefore be particularly important for sustainable land use.

Chapter 4

‘Co-evolution’ of uranium concentration and oxygen stable isotope in phosphate rocks

Modified on the basis of the manuscript

Sun, Y., Amelung, W., Wu, B., Haneklaus, S., Maekawa, M., Luecke, A., Schnug, E. and Bol, R.

Published in *Applied Geochemistry*

1. Introduction

Phosphorus (P) is a vital nutrient and energy carrier for life and it is thus also an indispensable fertilizer in agriculture including animal husbandry. The main route for the P supply relies on the exploitation of geological phosphate deposits, the availability of which is likely limited to the next 40 to 400 years (Obersteiner et al., 2013). However, phosphate rocks (PRs) also contain a significant amount of uranium (U) (0.3 to 247 mg U kg^{-1}), with typical average concentrations of 75 to 120 mg kg^{-1} (Altschuler, 1980). Most recently Windmann (2019) reported an average geometric mean in 128 sedimentary phosphate rock of 56.9 mg U kg^{-1}, compared to only 7.56 mg U kg^{-1} in 22 rocks of igneous origin. Therefore, mineral P fertilizers produced by PRs may also contain various amount of U which can be added to agricultural soils through the application of mineral P fertilizers (Schnug and Haneklaus, 2015). Depending on the source and the amounts of mineral P fertilizers applied, different levels of U accumulation have been observed in agricultural soils in various countries (e.g. Rothbaum et al., 1979; Bigalke et al., 2018).

To avoid potential U contamination and explain the different levels of U accumulation in agricultural soil, it is necessary to reveal the variations of U concentrations in PRs from different deposits. Furthermore, geochemical signatures of PRs are needed to identify the origins of PRs. How and why U concentrations are related to the origin of PRs are the key questions to be understood. Previous studies revealed that, at present, no single element concentration can be used to differentiate PR deposits (Sattouf et al., 2007). An alternative way is to identify the origin of deposits of PRs by using stable isotopes, such as strontium (Sr) isotopes (Sattouf, 2007). For instance, Sattouf et al. (2007) used $^{87}Sr/^{86}Sr$ isotope ratios to classify PRs into four different groups: 1) igneous rock phosphates from Russia (Kola), sedimentary rock from: 2) Algeria, Israel, Morocco, Tunisia and Syria, 3) the USA, and 4) Senegal and Togo. In addition, $^{234}U/^{238}U$ ratios can be used to distinguish PRs and P fertilizers originating from the USA and those of other regions (Sattouf et al., 2008).

Taking advantage of stable isotope discrimination processes to identify the origin of PRs does not apply for P, because this element does not have different stable isotopes. However, we may take advantage of natural oxygen (O) isotope compositions of phosphate ($\delta^{18}O_p$) in the PRs. $\delta^{18}O_p$ is selected as a potential indicator of the origin of the phosphate due to the fact that O stable isotope signatures may provide unique information on the paleo-environmental conditions during PRs formation. Based on pioneering research by Longinelli and Nuti (1973), who constructed an empirical equation between inorganic P-water oxygen isotope fractionations and temperature,

$$T = 111.4 - 4.3\left(\delta^{18}O_p - \delta^{18}O_w\right)$$

where T is the average environmental temperature, $\delta^{18}O_p$ is the natural oxygen isotope composition of phosphate and $\delta^{18}O_w$ is that of water. Oxygen in phosphate is bound tightly to P such that isotope exchange of O between phosphate and surrounding water is essentially negligible by abiotic processes even over geological time scales at low temperatures which relevant to earth surface environments (Jaisi and Blake, 2014; Longinelli and Nuti, 1973; Lecuyer et al., 1999; Blake et al., 2010; Shemesh et al., 1983). This is true even at exterme pH values (10 M nitric acid and 14 M NH_4OH) and at high temperature condition(70 °C), which has been proved on laboratory time scales (Blake et al., 2010). However, using the $\delta^{18}O_p$ value as a tracer for different PR deposits in relation to the occurrence of U is still pending. We therefore aimed to look for possible indicators that can relate the origin of PRs to their U and P content.

This study was performed to contribute to a better background understanding why agricultural soils may show different levels of U contamination through P fertilization. The first part of the paper provides an overview of the spatial and temporal distributions of U in PRs, the second investigates the degree to which the $\delta^{18}O_p$ values of PRs can reflect their deposition, and the third presents the correlation between the U concentration and the natural $\delta^{18}O_p$ for different PR deposits. Details on U geochemistry in PRs and other related isotope studies are not re-reviewed here, since this has already been undertaken by several authors, e.g. Jarvis (1995), or Kolodny and Luz (1992).

2. Materials and Methods

2.1 Data collection

Published U concentrations from overall 18 igneous and 277 sedimentary deposits were retrieved from the literatures. To supplement this data, we collected 74 sedimentary PRs from 11 countries: Algeria, Brazil, China, Israel, Morocco, Russia, Senegal, South Africa, Syria, Togo, USA, and 9 igneous PRs from Brazil, China, South

Africa and Russia. All these PRs samples were analyzed for total U concentration and oxygen isotope composition in phosphate ($\delta^{18}O_p$).

2.2 Uranium analyses

Total concentrations of U in PRs were analyzed by inductively coupled plasma spectrometry (ICP-MS, Thermo Fisher Scientific, Bremen, Germany) after the digestion of 0.05 g soil with 0.25 g lithium meta/tetraborate at 1050 ^{o}C for 3 h. The analytical error for total concentration measurement by ICP-MS was within 2%.

2.3 $\delta^{18}O_p$ analyses

One gram of ground phosphate rock samples was shaken with 50 ml 1M HCl for 16 hours. The soil-acid mixture was then centrifuged for 15 minutes at 1300 g and filtered through Whatman GF/F filters. The supernatant was then used for phosphate purification. The cleaning procedures followed Tamburini et al (2010). This method is based on the preparation of ammonium phosphomolybdate salts (APM), which are precipitated by adding ammonium nitrate solution and ammonium molybdate to the sample solution. Subsequently, the APM is dissolved again in citric acid solution and Mg is added to produce a magnesium ammonium phosphate mineral precipitate (MAP). The precipitation products are then dissolved with 0.5 mol L^{-1} nitric acid and purified via a DOWEX® 50 WX8 (200 -400 mesh) cation resin. By adding Ag nitrate solution, the phosphates to be analyzed are finally precipitated as silver phosphate (Ag_3PO_4). The $\delta^{18}O_p$ values were determined through high temperature reduction of Ag_3PO_4 to CO by a high-temperature conversion isotope ratio mass spectrometry (HTC-IRMS) system, composed of a high temperature oven (HEKA tech GmbH, Germany) and the IRMS Isoprime (Elementar Analysensysteme GmbH, Germany). The measured O isotope ratio was reported relative to that of Vienna Standard Mean Ocean Water (VSMOW).

Details on U content and oxygen isotope signatures of the different PRs can be found in Appendix B (Table B1-3).

3. Results and Discussion

3.1 Spatial and temporal distributions of uranium concentrations in phosphate rocks

3.1.1 Spatial distribution

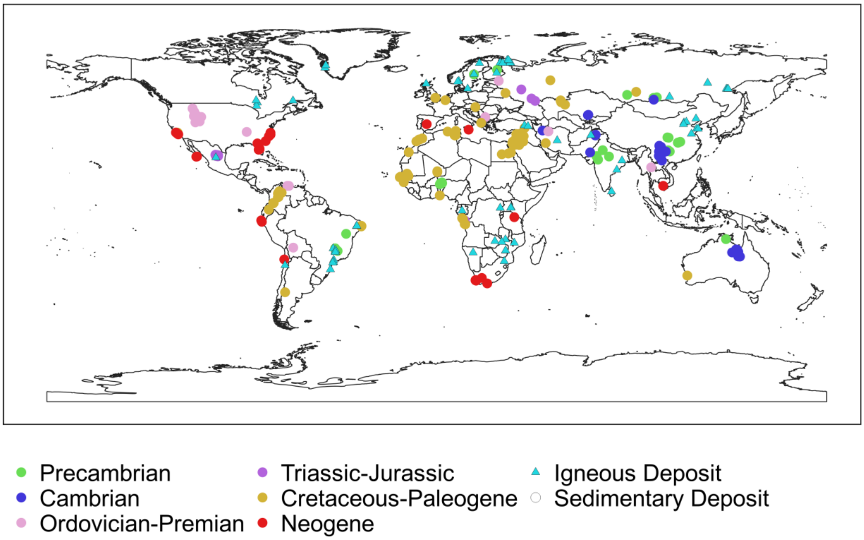

Figure 4-1. Distribution of sedimentary and igneous phosphate deposits with respective ages. (data source for sedimentary and igneous phosphate deposits: Chernoff and Orris, 2002).

Main phosphate ores types include marine sediments, igneous rocks and guano. About 75% of the world’s phosphate resources are obtained from sedimentary PRs, whereas 15-20% are obtained from igneous deposits. Guano, i.e., mainly deposits from birds, penguins, cormorants and bats are enriched in P but not sufficiently available for global use. The majority of sedimentary phosphate deposits have been formed under marine conditions and quantitatively the most important source of the world’s phosphate rocks for fertilizer production. Sedimentary phosphate deposits are found on almost every continent, in the North Africa and the Middle East, China, and the United States and range in age from Precambrian to Recent (Fig. 4-1). The largest P reserves are found in the Late Cretaceous-Eocene South Tethyan phosphgenic province, hosting 85% of the world's PR reservoir (Cook, 1984).

Igneous phosphates are a type of magmatic rock in which the element P was incorporated into the crystal structure of apatite, which took place when the mineral crystallized from the cooling melt (Pufahl and Groat, 2016). In general, the spatial and temporal distributions of igneous apatite deposits are similar to those of alkaline igneous rocks. Igneous phosphate deposits are also geographically fairly widespread and range in age from Precambrian to Tertiary (Cook, 1984). The typical grade of P_2O_5 is 5-15 wt % and most associated phosphate deposits are small and not suitable for commercial exploitation (Pufahl and Groat, 2016). The world's largest source of igneous PRs stems from the Devonian Khibiny Alkaline Complex in Russia's Kola Peninsula, contributing more than 50% of global igneous PRs use (Van Kauwenbergh et al., 2010). The Jacupiranga deposits of Brazil, located at the edges of Paleozoic basins and the Paleoproterozoic Palabora Complex deposit in South Africa, are the two largest reserves of igneous PRs (Van Kauwenbergh et al., 2010; Pufahl and Groat, 2016).

The PRs from different countries generally show various degrees of enrichment with U (Fig. 4-2). The data compilation reveals that igneous PRs, originating, for instance, from Russia, China, South Africa and Finland, generally display U concentrations in the range of 0.3-64 mg kg^{-1}, i.e. much lower than sedimentary PRs (0.6-390 mg kg^{-1}). Among the examined sedimentary PRs, about 60% exhibited U concentrations from 80 to 150 mg kg^{-1}. Sedimentary PRs from Morocco, USA and Israel usually showed relatively high U concentrations, with medians of 94, 116 and 129 mg kg^{-1}, respectively, and also wide content range of 3-250, 57-245 and 8-215 mg kg^{-1}, respectively. However, some sedimentary phosphate rock samples from Australia, Saudi Arabia, and Turkey only contained U in concentrations in the range of 20-50 mg kg^{-1}. In particular, the PRs originating from China show lower U concentrations in the range of 1.4 to 31 mg kg^{-1} with a median of 12 mg kg^{-1}. According to this data base, PRs from selected countries appear to exhibit a lower probability for U contamination than from other countries; yet the range is large and U concentration alone cannot be used to differentiate the origin of the different PRs.

3.1.2 Temporal distribution

In this study, the U content was normalized to the P_2O_5 content (as U/P_2O_5), in order to take into consideration of the fact that U in PRs is generally associated with the phosphoric phase (Brookfield et al., 2009; Föllmi, 1996; Lucas and Abbas, 1989). Overall, the ratios of U/P_2O_5 in sedimentary PRs range from 0.02 to 17.7 in deposits of all different ages, which shows that U deposition is highly variable with respect to phosphorus content (Fig. 4-3). The median values of U/P_2O_5 of the PRs in each age period decline in the deposits with increasing geological age of the deposits, with median values of 0.1 for Precambrian PRs, 1.2 for Cambrian PRs, 2.9 for Ordovician-Permian PRs, 2.6 for Triassic-Paleogene PRs and 3.5 for Neogene PRs, respectively. The distributions of U/P_2O_5 in PRs of Ordovician-Permian, Triassic-Paleogene and Neogene age are rather similar. In contrast, most Precambrian and Cambrian PRs analyzed so far exhibit low U/P_2O_5 ratios below two. Obviously, the very ancient PRs are characterized by low U/P_2O_5 ratios. A few previous studies also noticed the U-depletion in ancient sedimentary PRs (Sokolov, 1996; Volkov, 1994). However, the reasons for U depletion in ancient PRs were seldom investigated. In the following sections the focus in on exploring the mechanisms for U deposit in PRs.

3.2 Mechanisms of various deposition of U in phosphate rocks

3.2.1 U speciation in PRs

Apatite is the most abundant phosphate mineral. It is believed that U is mainly associated with apatite as radioactivity detected in phosphate nodules mostly originates from apatite. In addition, U contents extracted from various PRs samples are essentially the same when only apatite or apatite plus silicates is dissolved (Altschuler, 1958). Igneous apatite rocks consist of three primary mineral forms: chlorapatite [$Ca_5(PO_4)_3Cl$], hydroxylapatite [$Ca_5(PO_4)_3OH$], and fluorapatite [$Ca_5(PO_4)_3F$] (Jarvis, 1995). In sedimentary apatites, the main ore mineral is francolite [$Ca_{10-a-b}Na_aMg_b(PO_4)_{6-x}(CO_3)_{x-y-z}(CO_3{\cdot}F)_{x-y-z}(SO_4)_zF_2$] (Jarvis, 1995; Petr, 2016). Two states of U can be present in these PRs either as UO_2, UF_4 or Ca $(UO_2)_2(PO_4)_28H_2O$ phases, or as isolated U^{4+} ions or UO_2^{2+} radicals adsorbed on mineral surfaces or within internal discontinuities (Hendricks and Hill, 1950). It may also be substituted structurally in apatite, as U^{4+} by replacement of Ca^{2+}, owing to the virtually identical ionic radii of U^{4+} (1.05Å) and Ca^{2+}(1.06Å) (Baturin and Kochenov et al., 2000). Uranium in the structure of apatite dominates as U (IV). The present of U (VI) fixed as a surface-coordinated uranyl pyrophosphate is derived largely from post-depositional oxidation of U(IV) (Altschuler, 1958). In addition, the studies on submarine phosphorite also indicate the observed U(VI) content are not solely the product of surface oxidation and that U is probably incorporated in apatite in both oxidation state (Kolodny and Kaplan, 1970; Burnett and Veeh, 1977).

3.2.2 Variation of U deposition in igneous and sedimentary PRs

Differences in U/P_2O_5 ratios reflect to a large degree the diversities in the formation mechanisms for igneous and sedimentary PRs. Apatite deposits of igneous origin occur as intrusive masses or sheets, as hydrothermal veins or disseminated replacements, or as marginal differentiations along or near the boundaries of intrusions, or as pegmatites (McKelvey, 1967). It has been reported that U concentrations in igneous apatites are in the range of 1-1.2 µg kg^{-1} (Altschuler et al., 1958). The occurrence of U in igneous apatite is governed by the prevailing equilibrium conditions in the magma during the precipitation of the apatite. In contrast to igneous apatite the occurrence of U in marine sedimentary apatite is not governed solely by the equilibrium condition in the ocean but also by the following secondary enrichment processes during marine reworking. This could be the reason why igneous PRs are U/P_2O_5 depleted. The enrichment of U in sedimentary apatite implies that the apatite has acquired additional U by re-exposure to the same or similar solutions by sequestering the U from solid solution or ion exchange for calcium.

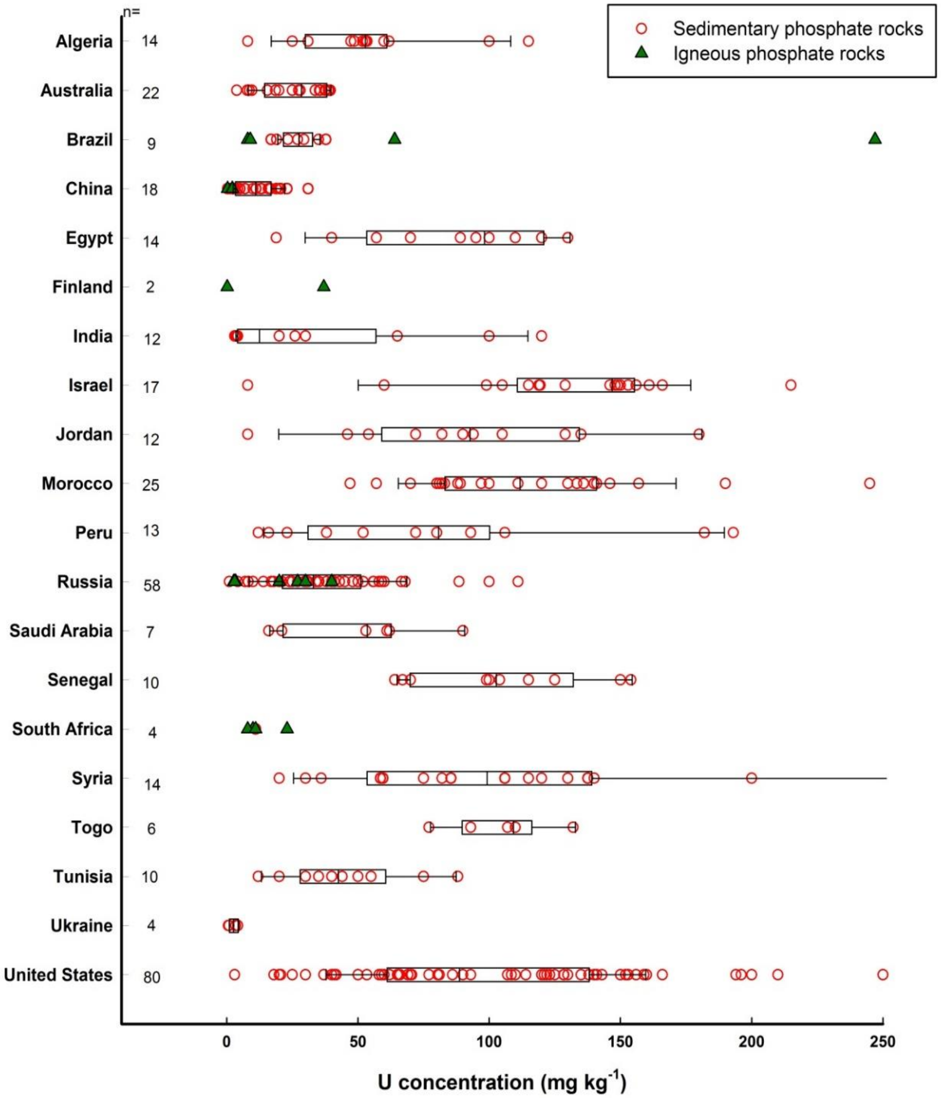

Figure 4-2. Combination plots of scatter and boxplot for U concentrations in phosphate rocks (PRs) from 20 countries (data include 22 igneous and 339 sedimentary samples totally, Appendix B).

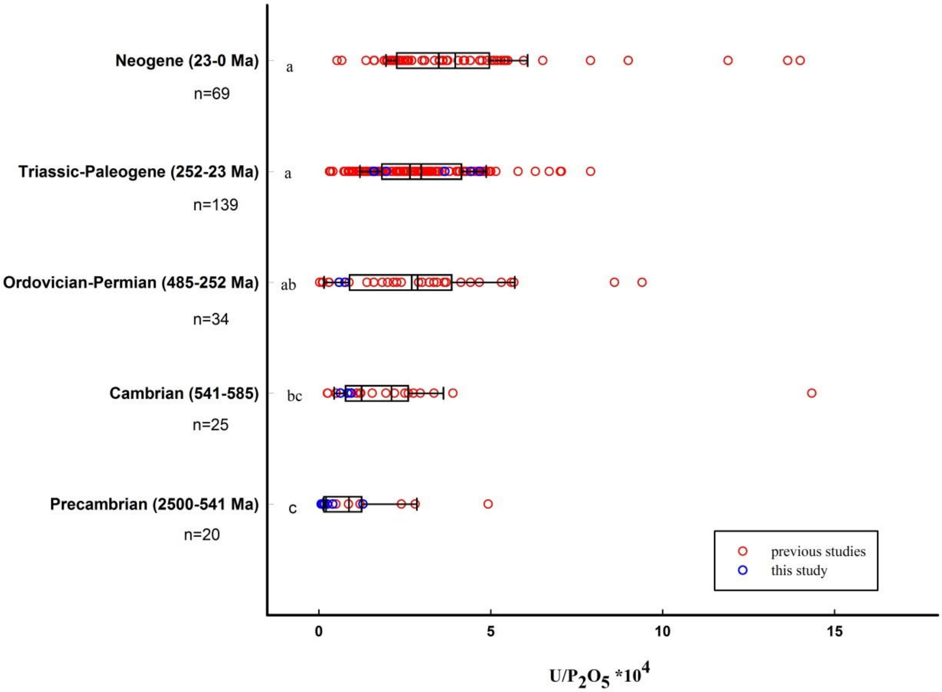

Figure 4-3. The distribution of U/P_2O_5 in phosphate rocks during geologic time from Precambrian to Holocene. The plot is the combination of scatter diagram and boxplot. The green lines are mean values for each geologic time.

3.2.3 Mechanism of U variation in sedimentary PRs

Even if U is enriched in sedimentary PRs, the reasons for considerable low U concentrations in ancient PRs are complex. They may be a comprehensive result of three factors: i) the evolution of U in the earth during geological history, ii) different paleogeographic features, and iii) weathering and catagenesis, which all affect the fate of U in phosphate deposits, as outlined below.

Geochemical evolution of U along the geologic units

The U concentration in sediments reflects the size of the local and perhaps global marine environment U reservoir (Partin et al., 2013). The geochemical evolution of U in marine is affected by two major events: the development of an oxygenated atmosphere about 2.2 billion years ago and the development of land plants at about 0.4 billion years ago (Cuney, 2010). Before oxygenation started, the reduced conditions in the absence of O, resulted in low solubility and low concentration of U in water (Partin et al., 2013). The lack of U enrichment in ancient PRs deposits in this study confirms the low concentration of soluble U in marine waters. In the period of 2.3-0.45 Ga, during and after the Great Oxidation Event (GOE) when oxygen increased near to the present atmospheric level, oxidative processes took place in terrestrial environments and the continental fluxes of dissolved U to the oceans increased dramatically (Holland, 1984). The last period was from 0.45 Ga to the present, when the Earth was colonized by plants. Uraninite and coffinite were precipitated from the U-rich near-surface waters into the oxygenated and organic-rich continental sediments; thus, total U concentrations in the sediments increased significantly (Cuney, 2010). As a consequence, higher U concentrations were found in younger PRs.

Paleogeographic features

The U depletion in ancient phosphorites was additionally caused by the paleogeographic features of relevant basins (such as in Asia and Africa), where U influx was considerably less pronounced during the phosphorus influx into the phosphate accumulation zones (Stephens and Carroll, 1999; Baturin and Kochenov, 2001). In contrast, the U-enrichment in later geologic time units was associated with paleogeographic reconstructions upon upwelling, which promoted both U and P deliveries into the shallow shelves (Baturin and Kochenov, 2001). Additionally, the process of U accumulation is believed to be related to sedimentary reducing conditions (Avital et al., 1983; Altschuler, 1958), where soluble U(VI) was reduced to insoluble U(IV) and deposited in the sediments. Elevated loads of organic matter led to reduced sedimentary conditions (McManus et al., 2005) turning them into a significant sink for U (Altschuler, 1958).

Weathering and catagenesis

Apart from the geochemical conditions during U influx and accumulation, weathering and catagenesis can control the residence time of U within the reservoir (Zanin et al., 2000). The effects of subaerial weathering remove apatite constituents from the apatite structure. Consequently, apatite decomposes, and soluble mineral phases and speciation of trace elements, such as U, are lost during weathering (Howard and Hough 1979; Zanin et al., 1985). In addition, the composition and texture of sedimentary apatite could be essentially modified in catagenesis (Zanin et al., 1985). The catagenesis processes correspond to remove isomorphic impurities from carbonate-apatite, such as carbonate ions, isomorphic trace elements (e.g. Sr, Cd, U), sodium, and H_2O^+ (Zanin et al., 1985). Therefore, the U concentrations in ancient PRs are relatively low, since the ancient phosphate rocks were exposed to catagenesis for a longer period (Baturin and Kochenov, 2001).

3.3 Oxygen isotope signature in phosphate deposits

As all processes mentioned so far interact, with unclear relations to the origins of phosphates in PRs, we included oxygen isotope natural abundances of phosphates ($\delta^{18}O_p$) as an additional indicator for distinguishing PRs from different origin and U concentration.

3.3.1 Oxygen isotope fingerprint of phosphate rocks of various origins

The O isotope compositions of the phosphates in the PRs are variable, fingerprinting their deposits (Fig. 4-4). In general, three different groups of PRs differing in their $\delta^{18}O_p$ natural abundance values can be: 1) igneous PRs from Brazil, China, Russia and South Africa ($\delta^{18}O_p$ ≤8.8‰), 2) sedimentary PRs from China and Brazil ($\delta^{18}O_p$ 12.2 - 18.2‰), and 3) sedimentary PRs from Algeria, Israel, Morocco, Russia, Senegal, South Africa, Syria, Togo and the USA ($\delta^{18}O_p$ ≥ 18.8‰; Fig. 4-4).

.

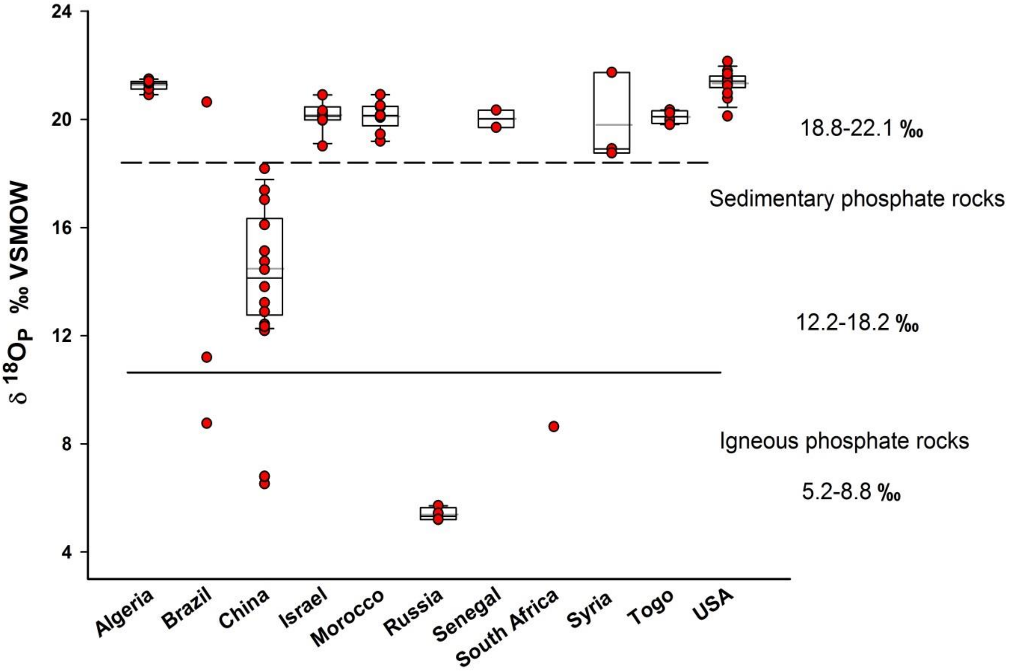

Figure 4-4. Variation of oxygen isotope composition ($\delta^{18}O_p$) in phosphate rocks (PRs) from different countries.

All igneous PRs show relatively low $\delta^{18}O_p$ values (5.2-8.8‰), which are comparable in magnitude with $\delta^{18}O_p$ values of igneous apatite reported previously (Taylor and Epstein, 1962). On the contrary, larger and a wider range of the $\delta^{18}O_p$ values (from 12.2 to 22.1‰) are found in sedimentary PRs. Notably, the $\delta^{18}O_p$ values of sedimentary PRs from China, as well as one sample from Brazil, show an intermediate range of $\delta^{18}O_p$ values (12.2-18.2‰). The other sedimentary PRs of this study exhibit a considerable narrow range of $\delta^{18}O_p$ from 18.8 to 22.1‰.

3.3.2 Mechanisms of various $\delta^{18}O_p$ in phosphate rocks

The final $\delta^{18}O_p$ isotope composition in PRs largely depends on that of the source water and the $\delta^{18}O_p$ values within these rocks may be then regarded as reflections of their crystallization history (Taylor and Epstein, 1962). Potential sources of fluids involved in the formation or alteration of phosphate deposits include magmatic water, meteoric water and ocean water. These three are characterized by specific $\delta^{18}O_w$ values.

Magmatic water which has never been in contact with the hydrosphere has $\delta^{18}O_w$ values from 5 to 8‰ (Shepherd et al., 1985). The relatively low $\delta^{18}O_p$ values of igneous PRs in this study are close to these low $\delta^{18}O_w$ values of magmatic water (Kusakabe and Matsubaya, 1986). In addition, limited fractionation will take place in the high temperature magma during the precipitation of the apatite. Therefore, apatite in igneous rocks may retain the same low $\delta^{18}O$ as the magmatic water. The variation of $\delta^{18}O_p$ values in igneous PRs reflects the range of temperatures at which the fluids were produced.

The $\delta^{18}O_p$ values of sedimentary PRs in this study are in the range of marine sedimentary phosphate (9.2-23.9‰) as reported previously by Shemesh et al. (1988). The ultimate fluid origin of sedimentary materials involves trapped seawater, or evolved meteoric water (Fayek, et al., 2011). The details of $\delta^{18}O$ in seawater will be discussed in the following. Meteoric waters, in turn, are abundant in rivers, lakes, glaciers and groundwater. They usually exhibit elevated $\delta^{18}O$ values due to various degrees of water-rock interactions (Shepherd et al., 1985). In addition, the geographic (such as island effect) (Tang et al., 1998) and climatic parameters (e.g. latitude, elevation, distance from the coast) correlated with the $\delta^{18}O_p$ values (Dutton et al., 2005). These different influences thus explain the large variations in O isotopic compositions, as well as the variations of $\delta^{18}O_p$ values in most of the analyzed sedimentary PRs.

The reasons for the variation of lower $\delta^{18}O_p$ values in sedimentary PRs also deserve to be considered. It can be noted that low $\delta^{18}O_p$ values of the sedimentary PRs were accompanied by older ages of formation. For instance, the sedimentary PRs from China which formed in Ediacaran-Cambrian (485-635 Ma) and Devonian (359-419 Ma) periods (Cook and Shergold, 2005; He and Zhou, 2015), have lower $\delta^{18}O_p$ values. Younger sedimentary PRs from Algeria, Israel, Morocco, Senegal, South Africa, Syria and Togo, formed in Cretaceous-Paleogene (56-145 Ma) times (Notholt, 1986), on the other hand, exhibited relatively higher $\delta^{18}O_p$ values in the range of 18.7-21.4‰. The youngest PRs in this study were from the USA, and also exhibited the highest $\delta^{18}O_p$ values, although within a narrow range (20.1-21.8‰; Fig. 4-4). The findings indicate that there is a clear relation between the $\delta^{18}O_p$ values and the age of the sedimentary PRs. This conclusion is supported by earlier suggestions of, e.g. Longinelli and Nuti (1968), and Shemesh et al. (1988), who found that $\delta^{18}O_p$ values decreased sharply from recent to Cretaceous times (66-145 Ma), and decreased further with a gentle slope to the Precambrian (541 Ma) (Fig. 4-5). The underlying mechanisms, however, are still a matter of debate, particularly because there is no consensus yet to whether it was temperature or the $\delta^{18}O$ value of the ancient ocean water that led to low $\delta^{18}O_p$ values in ancient rocks (Blake et al., 2010; Longinelli and Nuti, 1968; Shemesh et al., 1983, 1988). Three main explanations have been offered: 1) ocean water temperatures must have decreased from ancient to recent times (Knauth and Epstein, 1976; Knauth and Lowe, 2003; Shemesh et al., 1983), 2) the changing $\delta^{18}O$ value of sea water over time (e.g. Chase and Perry, 1972), 3) increasing $\delta^{18}O_p$ values from ancient to recent times caused by post-depositional alterations (Shemesh et al., 1983).

The opinion that ancient PRs were deposited under high temperatures has been put forward by many studies (Shemesh et al., 1983; Piper and Kolodny, 1987; Blake et al., 2010). Such higher temperatures could have been either a reflection of global phenomena, i.e. of warmer oceans in the geological past, or of a shift in the site of phosphate rocks formation in the ocean (Kolodny and Luz, 1992). Assuming that the $\delta^{18}O_w$ of the sea water was about 0‰ and that this value was maintained over geologic timescales in the absence of glacial periods (Muehlenbachs, 1998), the sedimentary PRs should thus have formed at an isotopic equilibrium with $\delta^{18}O_w$= 0‰. The calculated ocean temperatures of the Ediacaran-Cambrian (485-635 Ma), Devonian (359-419 Ma), Cretaceous-Paleogene (56-145 Ma), and Neogene-Quaternary (0.01-23 Ma) in this study would then have been 42.2 ^oC, 36.7 ^oC, 23.9 ^oC and 19.6 ^oC, respectively. This indicates that the temperature of the ocean slowly decreased with time and the evolution of the Earth. An even higher temperature (> 60 ^oC) has been proposed for Archean and early Proterozoic waters (Knauth and Epstein, 1976; Robert and Chaussidon, 2006).

The $\delta^{18}O_w$ values of the ocean can only change very slowly, since the residence time of water in the ocean is very long compared to hydrothermal circulation (Land and Lynch, 1996), and rates of chemical weathering on the continents are also slow. Hence, the seawater $\delta^{18}O_w$ value is assumed to have been fairly constant over time, buffered by hydrothermal and weathering processes at mid-ocean ridges to a $\delta^{18}O_w$ value of about 0‰ (Standard Mean Ocean Water, SMOW) (e.g. Muehlenbachs, 1998; Holland, 1984). Hren et al. (2009) disagreed with this view and considered that, the $\delta^{18}O_w$ value could have been as low as -10 to -13‰ in the Archaean ocean with a subsequent increase to present-day values. However, Blake et al. (2010) argued that based on the equation of Longinelli and Nuti (1973) mentioned above, such a conclusion would imply that the $\delta^{18}O_p$ values of Archaean marine phosphate would have been formed at an unrealistic ocean temperature of -8 °C to -30 °C. This conclusion favored the former interpretation that the increase of δ^{18}O$_p$ with decreasing geological age of the PRs most likely reflects the progressive cooling of sea temperatures during Earth's history. In any case, there was a coincidental 'co-evolution' (but not coupled) of δ^{18}O$_p$ signature in PRs and their U concentration, as a function of sedimentary PRs' age.

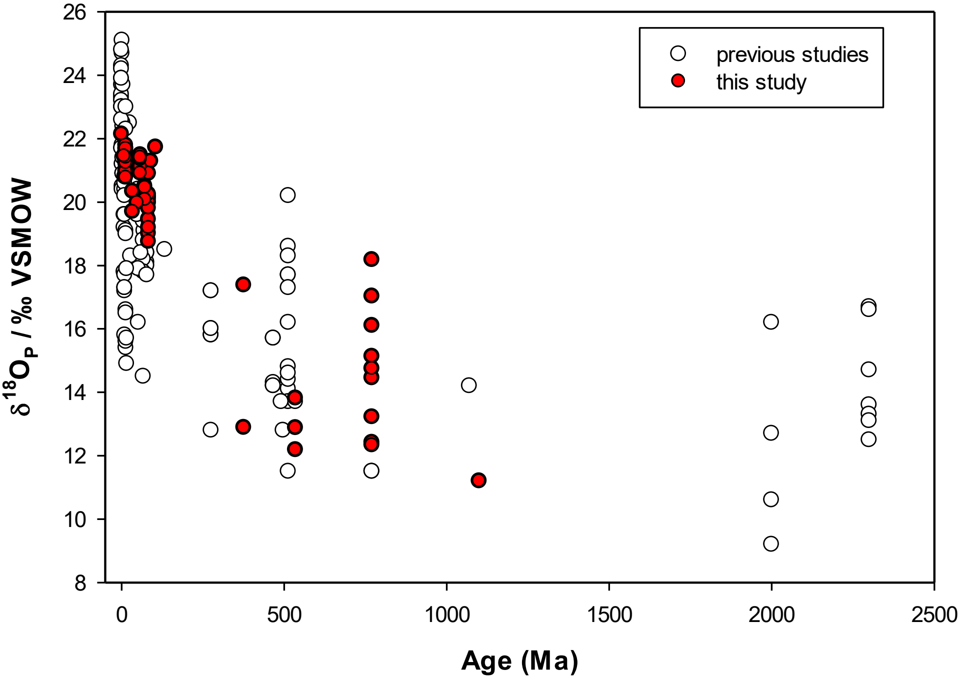

Figure 4-5. Oxygen isotope in phosphates (δ^{18}O$_p$) as related to geological age of the sedimentary phosphate rocks (data for circles are from Shemesh et al., 1983, 1988 and data for red points are from this study).

It should be noted that despite a likely wholescale lowering of δ^{18}O$_p$ values in older marine PRs, the ranges of δ^{18}O$_p$ values found for the PRs in this study are broad, even for those originating from a given geographic region and geologic time unit. It seems therefore likely that additional effects by post-depositional isotopic exchange altered the δ^{18}O$_p$ value between the O in phosphate and that in the surrounding water. Earlier work by Longinelli and Nuti (1968) proposed that post-depositional processes could have shifted the δ^{18}O$_p$ values of sedimentary rocks to lower levels, since alteration commonly occurred in the presence of ^{18}O-depleted meteoric waters or at elevated temperature (Jaffres et al., 2007). Moreover, $\delta^{18}O_p$ studies of fish debris, pointed to considerably larger values than in associated phosphate rocks, indicating the possible existence of a significant post-depositional isotopic exchange in the latter (Kastner et al., 1990).

3.4. Relationship between the U/P_2O_5 and $\delta^{18}O_p$ in phosphate rocks

The U/P_2O_5 and $\delta^{18}O_p$ values showed a clearly positive correlation (Fig. 4-6), pointing to some kind of 'co-evolution' of U history and oxygen isotope exchange in PRs. The igneous rocks clustered at the lower end of the curve, thus clearly distinguishing these PRs from the sedimentary ones. Old sedimentary PRs (Precambrian-Cambrian) with low $\delta^{18}O_p$ values also displayed lower U/P_2O_5 ratios. The younger sedimentary PRs (Cretaceous-Neogene), in turn, exhibited a wide range of U/P_2O_5 ratios with relatively high $\delta^{18}O_p$ values.

In igneous PRs, the low U concentration can be attributed to the lack of secondary U enrichment processes (Alschuler, 1958), whereas the low $\delta^{18}O_p$ values in PRs are likely due to a low concentration of ^{18}O in magmatic water and the limited oxygen isotopic fractionations in high temperature magmatic water (Taylor, 1968). In contrast, in sedimentary PRs, the time trend for U/P_2O_5 ratios and $\delta^{18}O_p$ values reflects a coincidence of paleoclimate and paleogeographic features. A low ratio in PRs indicates either that little U was further precipitated into francolite or that the U was released from the apatite lattices as a result of intensive post-depositional diagenetic processes. The latter process may also lower the $\delta^{18}O_p$ values (Shemesh et al., 1983). It is hard to find direct coupling of processes involved in U deposition and oxygen exchange, but findings rather indicate a time-dependent coincidence of processes altering U content and $\delta^{18}O_p$ signatures in a similar direction.

In summary, the results reported in this paper support the hypothesis that there is a co-evolution of $\delta^{18}O_p$ and U/P_2O_5 ratios in PRs across different geologic time units. Plotting both parameters against each other may provide a novel tool for PR dating, potentially supplementing existing dating tools, which are frequently valid for selected time windows only, in the case of Sr and U isotopes, for instance, precisely only for the 0-20 Ma and 0-1.2 Ma age range, respectively. On the other hand, the data clearly show that selecting mineral P fertilizers on the basis of the geological origin (igneous versus sedimentary) and age (Precambrian-Cambrian versus Cretaceous to Neogene) of their PRs may help to find δ^{18}O$_p$ signatures of fertilizer P that differ from that of soil and plants and could thus be used as a tracer for elucidating the biological cycling of fertilizer P in the terrestrial environment (Tamburini et al., 2012; Amelung et al., 2015; Bauke et al., 2018).

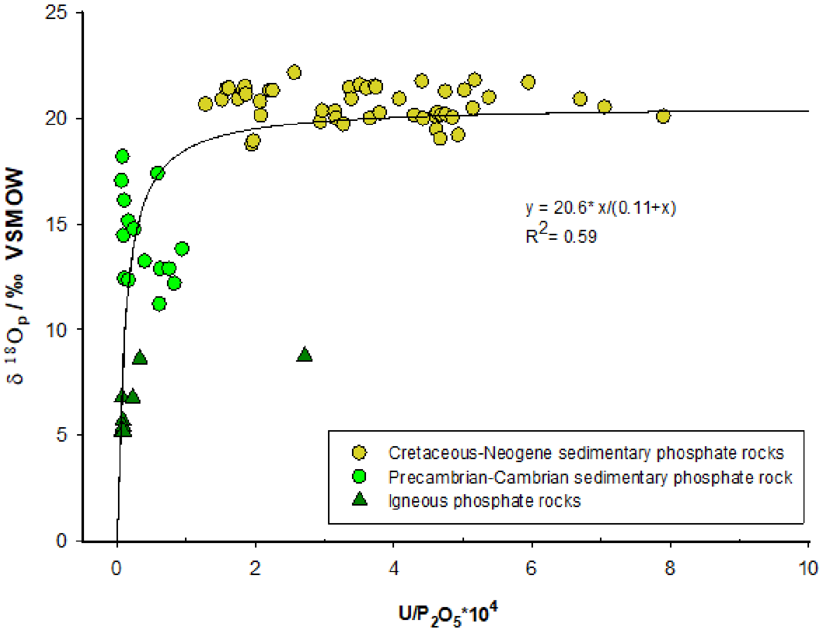

Figure 4-6. Correlation between oxygen isotope composition of phosphate (δ^{18}O$_p$) and U/P_2O_5 in phosphate rocks.

.

4. Conclusion

To prevent and explain different levels of U contamination in agricultural soils, this work provides a comprehensive overview of U levels in various PRs worldwide and the underlining mechanisms of U accrual. We linked these data to information on the oxygen isotope composition of PRs, which provides additional information on the related genesis of P in these rocks. In soil, oxygen isotope abundance measurements of phosphates provide additional information on the efficiency of soil P cycling; yet, linking the latter to the origin of P fertilizers is still in its fledging stages (Tamburini et al., 2012; Amelung et al., 2015; Helfenstein et al., 2018).

The comprehensive overview of U levels in various PRs not only confirmed that igneous PRs contained lower levels of U than sedimentary PRs, but also that older sedimentary PRs (Precambrian-Cambrian) have less U than younger ones (Ordovician-Neogene). In addition, $\delta^{18}O_p$ distinguished the PRs deposits of: 1) igneous PRs ($\delta^{18}O_p$ = 5.2 to 8.8‰, e.g. from Russia), 2) old sedimentary PRs ($\delta^{18}O_p$ = 12.2 to 18.2‰, e.g. from China), and 3) younger sedimentary PRs ($\delta^{18}O_p$ = 18.8 to 22.1‰, e.g. from the USA). Finally, the differences of U levels in PRs were mirrored by the $\delta^{18}O_p$ signatures of the PRs, thus highlighting both their ‘co-evolution’, and inter changeability as a tracer of temporal or process changes in global PRs.

Chapter 5

Final discussion

1 Summary of the research objectives

Application of mineral phosphorus (P) may cause uranium (U) accumulation in agricultural soils. It is understandable that the amount of accumulation depends on fertilization rates, P sources and the soil properties (pH value, the amounts of organic matter, redox conditions). However, a disentangling of these factors on the accumulation of U has hardly happened, especially the relationship between U accumulation and the sources of P fertilizers remained unclear.

In the present work, soil U accumulations were evaluated at long-term experimental sites of Europe, including Rengen and Thyrow (Germany), Askov (Denmark), Sámstaðir and Geitasandur (Iceland) and Rothamsted (UK). In addition, spatial and temporal distributions of U in PRs worldwide were reviewed in the study. The oxygen isotope compositions of the phosphate rocks ($\delta^{18}O_P$) were determined as indicators for distinguishing the origin of PRs to explicate the characteristics of U in PRs.

Specifically, following key questions were addressed in the thesis.

i) How fast and to which degree does U accumulate in agricultural soils when using P fertilizers produced from low-U resources?

We examined U concentrations in agricultural soils from three long-term field experiments with different low U containing P fertilizers: i) Rengen (P fertilizer from basic slag, grassland, Germany), ii) Thyrow (P fertilizer from igneous phosphate rocks, arable land, Germany) and iii) Askov (P fertilizer from igneous phosphate rocks, arable land, Denmark). Accumulation rates of U were relatively low for Rengen (1.3 µg kg^{-1} yr^{-1}) and Thyrow (0.6 µg kg^{-1} yr^{-1}) in P treated plots compared with those without P fertilization. These accumulation rates were 10 times smaller than those previously reported (mean 17 µg kg^{-1} yr^{-1}). Intriguingly, the concentrations of acid-extractable U in the Askov topsoil increased during 1923 to 2016, regardless whether P was added (5.1 µg kg^{-1} yr^{-1}) or not (4.7 µg kg^{-1} yr^{-1}). This suggests that at least part of the accumulated U originated from other sources than P fertilizers. Total U concentrations at Askov was significantly larger in 1985-2016 period compared to 1938-1976 in NPK plot but not in control without P fertilization. Hence, long-term P fertilizer application did increase the soil U concentrations at Askov, although at a low level (< 0.4 µg kg^{-1} yr^{-1}).

The small U accumulation rates in soil from these German and Danish long-term P fertilization experiments indicated that for their current management strategy (current P fertilization type and rate), the soil U concentration will remain at a non-critical level even at centennial scale. This ascribes to the historic use of P fertilizers derived from sources with low U content (igneous phosphate rocks and basic slag). Hence, U accumulation due to long-term P fertilization in agricultural soils can be alleviated by specific targeting of the usage PRs with low U sources in P fertilizer production process.

ii) Can, and if so, to what extent the excessive amount of P fertilizer application leads to the U accumulation in agricultural soil?

I tested the risks of U accumulation in two reprehensive long-term grasslands on Icelandic Andosols (Sámstaðir and Geitasandur) after about 50 years of P fertilization. The results showed that P fertilization rates of 39.3 and 78.6 kg ha^{-1} resulted in a U enrichment of 6.7 and 15 mg kg^{-1}, respectively, compared with non-fertilized soil (0.65 mg U kg^{-1}). The annual U accumulation rate in these two trials exceeded any known earlier reported rate by up to a factor of at least ten times. Hence, our data clearly did also show that some soils may suffer from severe U contamination, even exceeding common soil safeguard values, after a semi-centenial P fertilizer application period. Uranium concentrations in applied P fertilizers should thus be duly considered, especially for those agricultural production systems on Andosols.

iii) Why are there different levels of U in various PRs? How can $\delta^{18}O_p$ signatures revel the characteristics of U in PRs related to PRs origins?

To answer this question, I reviewed the spatial and temporal U variations in PRs to obtain a comprehensive overview of U levels in various PRs worldwide, and investigate why U concentrations in igneous PRs are significantly lower compared with sedimentary PRs, and why less U is present in old sedimentary PRs (Precambrian-Cambrian) than in younger PRs (Ordovician-Neogene). In addition, $\delta^{18}O_p$ values in various PRs were determined to identify their origins in relation to their U concentrations. The $\delta^{18}O_p$ values differed among igneous PRs, old sedimentary PRs, and younger sedimentary PRs. Generally, the PRs with low $\delta^{18}O_p$ values had low U concentrations. In igneous PRs, low U concentrations were due to the lack of secondary U enrichment processes after rock formation, while low $\delta^{18}O_p$ values were resulted from limited isotope fractionation at high temperature. Conversely, in sedimentary PRs, both U concentrations and $\delta^{18}O_p$ values were influenced by paleoclimate and paleogeographic features. Overall, there is a time-dependent coincidence of processes altering U concentration and $\delta^{18}O_p$ signatures of sedimentary PRs in a similar direction.

2. Synthesis

2.1 Uranium accumulation in agricultural soil

There is no ubiquiteous U accumulation in soils, instead, wide range of U accumulation rates (from 0 to 47 µg kg^{-1} yr^{-1}) have been reported, including this study. Hence, U accumulation in soil tends to be local and ingredient-specific depending on the source of PRs used for fertilizer production and depending on the final fertilizer application amounts. In this section, I combined the data in the previous chapters to illustrate the issue of P fertilizer-derived U accumulation in soil on a broader and deep focus scale.

Figure 5-1 highlights the frequency distribution of data on U accumulation rates. About 70% of the reported U accumulation rates are in the range of 0-30 µg kg^{-1} yr^{-1}. The proportions at which U accumulates with rates of 0-2 and 10-30 µg kg^{-1} yr^{-1} are equal, accounting for about 20% for each, while the rest 30% sits in the range of 2-10 µg kg^{-1} yr^{-1}. Extreme values of either low (0 µg U kg^{-1} yr^{-1}) and high U accumulation rates (> 78 µg U kg^{-1} yr^{-1}) have also been found in about 20% of the studies. In this study, low U accumulation rates (< 2 µg kg^{-1} yr^{-1}) were found (Askov, Rengen and Thyrow; chapter 2), and elevated U accumulation rates of 3-10 µg kg^{-1} yr^{-1} were found in two classic long-term (> 130 years) Rothamsted (UK) field experiments (Appendix A). The extreme case of a U accumulation rate of 310 µg kg^{-1} yr^{-1} (with P application rate 78.6 kg ha^{-1} yr^{-1}) was also found in this study at Geitasandur, Iceland (Chapter 3). Overall, the fertilizer-derived U accumulation rate was attributed to a combination of types of P fertilizer applied and the amount of P fertilizer inputs.

2.1.1 U accumulations in response to the P sources

The P source is one of the critical factors determining U accumulation in agricultural soil. About 75% of the world's phosphate resources are obtained from sedimentary PRs, whereas 15-20% are obtained from igneous deposits. In chapter 4, I confirmed that igneous PRs contained lower concentrations of U than sedimentary PRs (Figure 5-2) and older sedimentary PRs (Precambrian-Cambrian) have less U than younger ones (Ordovician-Neogene) (Chapter 4). Therefore, soils applied with P fertilizers produced from igneous PRs showed low U accumulation rates, which have been proved in Askov (Denmark) and Thyrow (Germany) (Chapter 2). In contrast, high U accumulation rate (310 µg kg^{-1} yr^{-1}) showed in Geitasandur (Iceland) indicated that fertilizer-derived U was a critical issue when applied P fertilizers with high U concentrations (Chapter 3). Hence, the issues of U accumulation in agricultural soils induced by long-term P fertilizer applications can be reduced or eliminated when phosphate rocks from low U sources are selected for P fertilizer production. Additionally, “P source selections” should be considered when large amounts of P fertilizers applied.

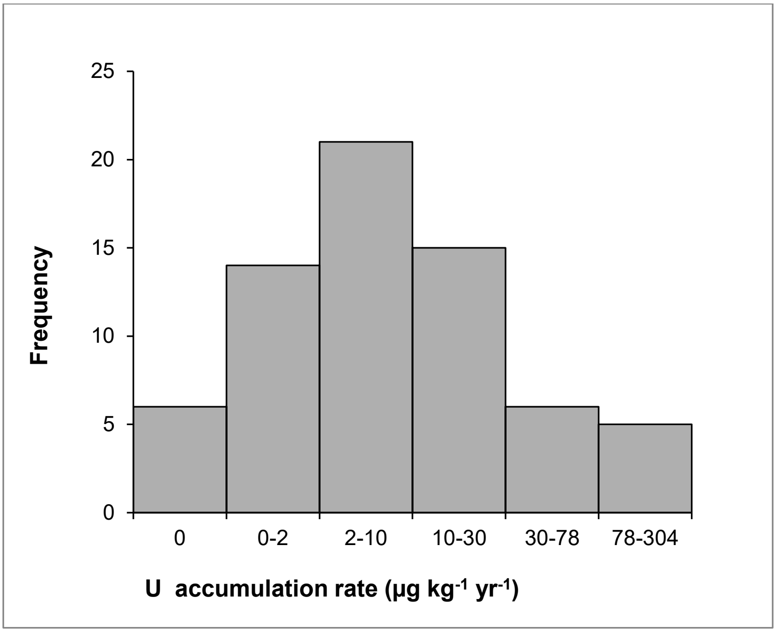

Figure 5-1. The frequency distribution of U accumulation rates (data showed in Table A-1).

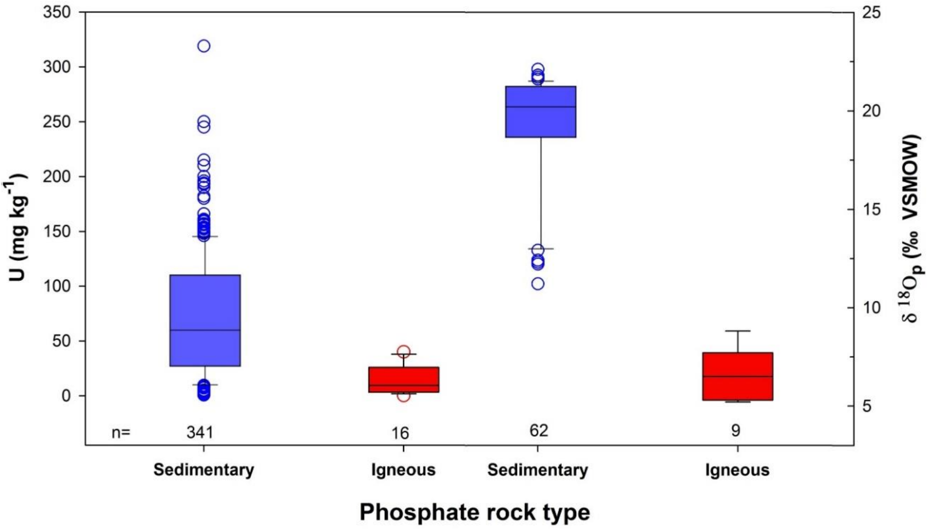

Figure 5-2. Uranium and δ$^{18}O_p$ in sedimentary and igneous phosphate rocks.

The variation of U concentrations in P fertilizers and the opaque of international fertilizer trade make it difficult to identify the origins of P fertilizers, and therefore, to select the fertilizer product on the basis of the P sources. In Chapter 4, the hidden links between the variations of U concentrations in different PRs were expounded. I highlighted that igneous PRs always show low U concentrations and hold relatively low values (Figure 5-2). In addition, PRs which are characterized with low δ$^{18}O_p$ values usually contain low U concentrations due to the simultaneous change of δ$^{18}O_p$ and U in sedimentary PRs in response to geologic time (Figure 5-3). Therefore, the δ$^{18}O_p$ value in phosphate rocks can be an indicator for selecting P sources with low U concentrations.

The δ$^{18}O_p$ value in phosphate rocks is not susceptible to alteration when produced as P-fertilizers, therefore, we can apply this signature for distinguishing the origins of P fertilizers to some extent. Hence, the values of δ$^{18}O_p$ in mineral P fertilizers from four manufacturers were mearsured (Appendix D). I found that the range of δ$^{18}O_p$ in P-fertilizers is comparable to that of PRs. The PR sources for those manufacturers are sedimentary rocks and the sources for Ruhr-stickstoff are 'old sedimentary PRs' with low value of U/P_2O_5 (Table D-1, Figure D-1).

In conclusion, to minimize the environmental risks associated with fertilizer-derived U load to agricultural soils, it can be recommended chossing igneous PRs or old sedimentary PRs (formed in Palaeozoic and Precambrian) as better P fertilizer sources.

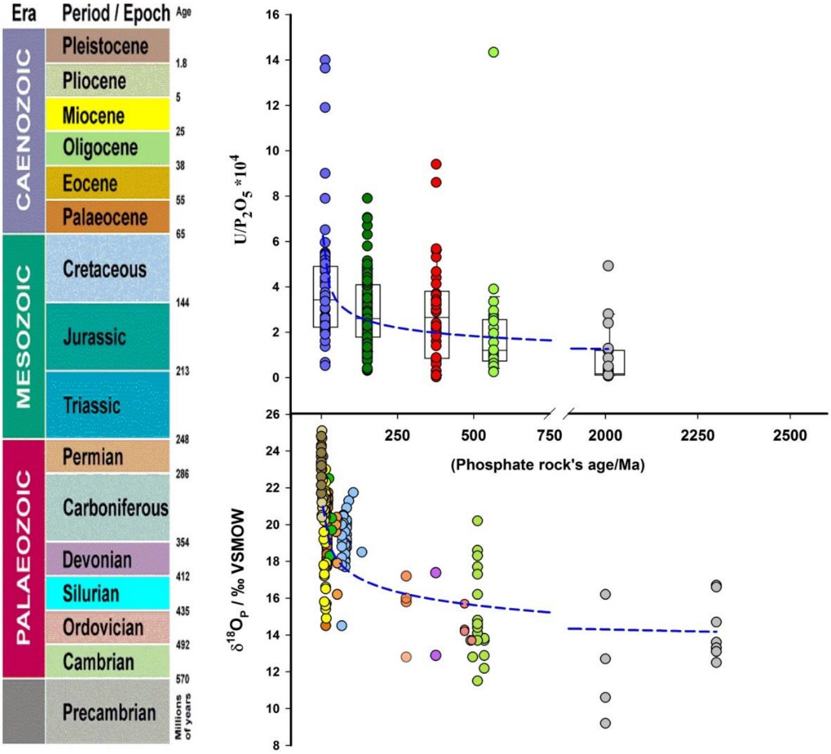

Figure 5-3. The distribution of $\delta^{18}O_p$ and U/P_2O_5 in sedimentary PRs relative to geologic time.

2.1.2 U accumulations respond to the amount of P fertilizers applied

There is no doubt that the amount of P fertilizers applied is critical to evaluate the fertilizer-derived U accumulation. In order to evaluate the correlation between U accumulation rate and P application rate, linear regression models were performed (without outliers) (Figure 5-4). Significance levels were highlighted with * ($p< 0.05$), ** ($p< 0.01$), *** ($p< 0.001$). A highly significant correlation was found between U accumulation rate and P application rate in topsoil for both grassland and arable land

(Fig. 5-4). The coefficient of linear regression equation shows that U concentration would increase 0.52 µg in one hectare by 1 kg P application annually.

Based on the linear regression equation in Figure 5-4, I can estimate the U accumulation rate according to the P application rate. Additionally, the points above the linear regression line indicate that the applied P source contain considerable high U concentration; in contrast, the points below the line indicate that good P sources were applied with low U concentration compared with the average level.

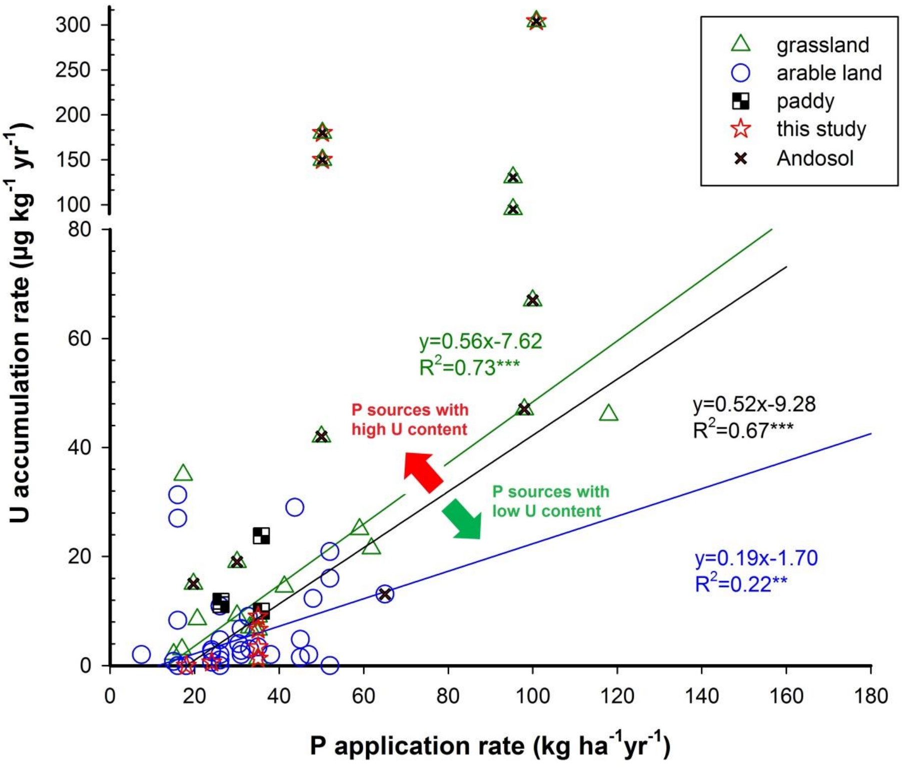

Figure 5-4. Relationship between the P fertilizer application and the U accumulation rate in different land use types.

2.2 Estimates of the amounts of fertilizer-derived U in agricultural soils of the European Union countries

The mineral P fertilizer productions in European countries are almost entirely dependent on the import of PRs from the rest of the world. Therefore, the government and the general public should pay more attention on the quality of the imported PRs, including the ultimate issue of fertilizer-derived U accumulation in agricultural soils. This section aims to provide an estimate on the amount of U inputs to agricultural soils by P application in the European Union (EU) countries, especially for France, Germany, Italy, Spain and the UK, which account for over three-quarters of the EU's imports of P fertilizer products (Marjolein et al., 2012).

Table 5-1. Phosphate rock into the EU-28 by exporting country

Phosphate rock (PR) exporting country	PR exported into EU-28 in 2017		U concentration in PRs		
	million t[a]	% of total	Max	Min (g kg^{-1} P_2O_5)[b]	Mean
Morocco	1.94	35.1	0.58	0.20	0.35
Russia	1.75	31.6	0.43	0.01	0.17
Algeria	0.68	12.3	0.28	0.04	0.16
Israel	0.42	7.5	0.63	0.18	0.41
Egypt	0.23	4.1	0.50	0.14	0.33
Senegal	0.18	3.2	0.48	0.17	0.29
Tunisia	0.02	0.4	0.89	0.04	0.28
Syria	0.01	0.1	0.89	0.11	0.38
Jordan	0	0.1	0.53	0.03	0.34
Others[c]	0.29	5.33	0.25	0.25	0.25
U content in imported PRs of EU countries	-	-	0.47	0.12	0.26

a: The trade date of PRs is from Eurostat Comext (http://epp.eurostat.ec.europa.eu/newxtweb/) (Tulsidas et al., 2019).

b: The range and mean value of U concentrations in PRs of specific import country, which were estimated according to RPs dataset (Chapter 4 and Appendix. B).

According to our dataset showed in Appendix B, the average of U concentrations in PRs worldwide is 252 mg U kg^{-1} P_2O_5 and 260 mg U kg^{-1} P_2O_5 for the PRs imported to the EU countries. This is in good agreement with the previous reported values by

Schung et al., (2013) with average value of 259 mg U kg^{-1} P_2O_5 for PRs worldwide. Thus, the average of annual U load to agricultural soil was calculated by P fertilizer applicate rate and the average U concentrations in P fertilizers. As shown in Table 5-2, the amount of U load to agricultural soil is in a range of 2.1-11 g ha^{-1} with an average of 5.1 g ha^{-1} for those main P fertilizer consuming countries.

Based on average $\triangle$U (0.52 μg kg^{-1}, the U concentration increase in one hector soil by 1 kg P application, see section 2.1.2), the annual U load would then be 10.9 g ha^{-1} (down to 15 cm, with soil density 1.5 g cm^{-3}), which is comparable with the calculation method mentioned in previous paragraph.

Table 5-2. Estimated U load to agricultural soil in European Union countries.

Country	P fertilizer (as P_2O_5) application rate[a] (kg $ha^{-1}yr^{-1}$)	U load to agricultural soil (g $ha^{-1}yr^{-1}$) mean	range
France	21.2	5.6	2.5-10.0
Germany	19.3	5.1	2.2-9.2
Italy	18.2	4.8	2.1-8.6
Spain	24.4	6.4	2.8-11.5
United Kingdom	32.6	8.6	3.8-15.5
European Union	21.2	6.1	2.7-11.0

a: The amounts of applied P (equivalent to P_2O_5) were taken from Food and Agriculture Organization (FAO) database (http://www.fao.org/faostat/en/#data/RFN).

3. Conclusion

In this study, fertilizer-derived U accumulation in agricultural soils has been evaluated at seven long-term experimental sites in Europe. The result shows that the U accumulation in soils is not a universal issue. A wide range of U accumulation rates (0 - 304 μg kg^{-1} yr^{-1}) was observed, with 0, 0.6, 1.3, 3.4 and 8.1 μg kg^{-1} yr^{-1} for Askov (Denmark), Thyrow (Germany), Rengen (Germany), Broadbalk (UK) and Park Grass (UK), respectively, with P fertilizer application rates of 18-35 kg P ha^{-1} yr^{-1}. In addition, extremely high U accumulation rates were found at the long-term experimental sites of Iceland (Geitasandur and Sámstaðir), with 165 and 304 μg kg^{-1} yr^{-1} for 39 and 79 kg P ha^{-1} yr^{-1} application, respectively. The variation of U accumulation rates is related to the differences in P sources and in the amounts of P fertilizers applied. The U accumulation rate is positively correlated with the amount of applied P fertilizers. Small U accumulation rates showed in German and Danish long-term P fertilization experiments were ascribed to the historic use of P fertilizers derived from P sources with low U concentrations (igneous phosphate rocks from Finland and Kola Peninsula for Askov and Thyrow, respectively; and basic slag for Rengen). In contrast, higher U accumulation rates at Rothamsted long-term experiment sites were attributed to P sources from e.g. North Africa (high U content). The current most serious case of fertilizer-derived U accumulation was found in Icelandic agricultural soil as a consequence of high U concentrations in P sources and large amount of P applied, where the awareness of cumulative U contamination should be raised. By reviewing the U accumulation rates in this and previous studies, I expected that soil U concentrations will increase by 0.5 µg U kg^{-1} soil by applying 1 kg P ha^{-1} and there will be 2.7-11 g U ha^{-1} yr^{-1} input to the EU's agricultural soil with 21.2 kg P (as P_2O_5) per hectare fertilization.

The $\delta^{18}O_p$ values were determined in PRs worldwide to help select P sources with low U concentrations. Simultaneous changes of $\delta^{18}O_p$ and U/P_2O_5 values in PRs indicated that the PR with a low $\delta^{18}O_p$ value was generally accompanied by a low U concentration. In igneous PRs, low U concentrations were due to the lack of secondary U enrichment processes after rock formation, with low $\delta^{18}O_p$ values resulting from limited isotope fractionation at high temperature at the same geologic time. In contrast, in sedimentary PRs, U concentrations and $\delta^{18}O_p$ values were found to be influenced by paleoclimate and paleogeographic features. Overall, the characteristics of 'co-evolution' of $\delta^{18}O_p$ and U suggest that good P sources (with low U) are igneous types and old sedimentary PRs (formed in Paleozoic and Precambrian).

In summary, by selecting and applying P fertilizers from better P sources (i.e. igneous type), the issue of U accumulation in soil may be alleviated at centennial scale. Conversely, in agricultural areas where large amounts of mineral P fertilizers are applied P sources should seriously be considered to avoid the potential U contamination by P fertilization. Furthermore, environmental issue with PRs production themselves are an issue, the traceability of PRs from source to fertilizer is opaque and also warrants addreesing.

5. FINAL DISCUSSION

Appendix A

Literature review of fertilizer-derived U increase in different experiment sites

Supporting information to Chapter 2

APPENDIX A

Table A-1. Literature review of fertilizer derived U increase in different experiment sites.

Country	Experiment sites	Years	land use type	Soil depth (cm)	Soil type	Clay %	Silt %	Sand %	Treatments	SOC %	pH	P fertilizer type	P fertilizer application rate (kg ha^{-1} year^{-1})	U accumulation rate (µg kg^{-1} yr^{-1})	Reference
France	Loir-et-Cher	1976-1991	arable	0-25		29	65.9	6	P_0	1.8	6.9	45% P_2O_5 superphosphate	0.0	0.0	Wetterlind et al., 2012
									P_{26}				26.0	0.0	
									P_{52}				52.0	16.0	
	Indre-et-Loire	1976-1997	arable	0-25		18	26.1	56	P_0	2.0	7.9	45% P_2O_5 superphosphate	0.0	0.0	
									P_{26}				26.0	10.9	
									P_{52}				52.0	20.9	
	Vienne	1967-1997	arable	0-25		38	36.9	19	P_0	4.1	7.3	45% P_2O_5 superphosphate	0.0	0.0	
									P_{26}				26.0	4.7	
									P_{52}				52.0	0.0	
Germany	Schuby	1985-2005	grassland	0-10	Haplic Podzol	5--8	15-20	70-80	Control	3.7	5.2		0.0	0.0	Rogasik et al., 2008
									$P_{0.5*uptake}$	3.8	4.9	mineral P fertilizer	20.6	8.5	
									P_{uptake}	4.1	5.0		41.2	14.5	
									$P_{1.5*uptake}$	3.9	5.1		61.8	21.5	
	Thyrow	1937-2005	arable	0-20		3	15-20	70-80	Control	0.3	4.2		0.0	0.0	
									NK+lime	0.4	6.6		0.0	0.0	
									NPK+lime +fym	0.7	6.0	Superphosphate	24.0	2.5	
									NPK+lime	0.34	6		24.0	2.9	
	Muncheberg	1963-1998	arable	0-25		5	15-20	70-80	Control	0.4	5.9	Superphosphate	0.0	0.0	
									NPK + fym	0.5	5.9		26.0	2.0	
									NPK	0.4	5.9		38.0	2.0	

APPENDIX A

									NPK	0.5	5.5		47.0	2.0	
	Braunschweig	1980-2004	arable	0-30		8	50-65	30-45	NP$_{\text{very low}}$K	1.7	6.0		0.0	0.0	
									NP$_{\text{low}}$K	1.6	6.0		7.4	2.0	
									NP$_{\text{moderate}}$K	1.5	5.7		30.4	4.0	
									NP$_{\text{high}}$K	1.5	5.9		45.0	4.8	
	Halle	1949-2002	arable	0-20		12	10-50	40-80	Control	1.2	5.6		0.0	0.0	
									NP$_{\text{low}}$K	1.2	5.8		15.0	0.8	
									NP$_{\text{high}}$K	1.2	5.9		45.0	1.5	
	Bonn	1959-2005	arable	0-30		15	75-90	05--10	Control	0.7	5.6		0.0	0.0	
									Thomas phosphate	0.7	6.2	Thomas phosphate	26.0	0.0	
									Hyperphosphate	0.7	5.7	Hyperphosphate	26.0	1.0	
									Super phosphate	0.7	5.9	Super phosphate	26.0	1.0	
	Freising	1935-1975	arable	0-25		25	50-75	< 25	Control	0.8	6.2				
									Thomas phosphate	0.8	6.5	Thomas phosphate	31.0	2.0	
									Super phosphate	0.9	6.0	Super phosphate	31.0	6.8	
									Hyperphosphate	0.9	6.3	Thomas in first 20 year	31.0	2.8	
Greece	Kalohori		arable											18.0	Papastefanou et al., 2006
Ireland	Johnstown Castle	1968-2006	grassland	0-10	Humic Gleysols	18	10--20	60-70	0	11.0	6.0		0.0	0.0	Tunney et al., 2009
									15P				15.0	2.1	
									30P				30.0	9.2	
Japan	Fujisaka Branch	1940-2001	arable	0-35	Andosol				NPK+compost+lime	7.5	6.2	Superphosphate	65.0	13.1	Takeda et al., 2006
		1933-2000	Paddy	surface soil	Gleysol				Control	0.7		a fused phosphate fertilizer	0.0	0.0	Yamaguchi et al., 2009
									NPK	1.0			26.2	11.2	

APPENDIX A

						NPK+compost 20000	1.6			26.2	11.8	
		1968-2000	Paddy	surface soil	Gleysol	Control	1.7		a fused phosphate fertilizer	0.0	0.0	
						NPK	1.7			35.8	10.0	
						NPK+compost 20000	2.6			35.8	23.8	
		1976-1997	upland	surface soil	Fluvisols	Control	1.3		a fused phosphate fertilizer	0.0	0.0	
						NPK	1.5			48.0	12.3	
						NPK+compost 20000	1.8			43.7	29.0	
		1966-2000	grassland	surface soil	Andosol	Control	7.8		Superphosphate	0.0	0.0	
						NPK	9.3			74.3	130.6	
						NPK+compost 2000-2500	11.0			74.3	95.3	
New Zealand	Mikimiki	43	grassland	0-7.5	Andic Cambisols			5.4	Superphosphate and Triple superphosphate	59.0	25.0	Taylor and Kim, 2008
	Eltham	37	grassland	0-15	Histic Gleysols			5.4		118.0	46.0	
	Taupo	37	grassland	0-7.5	Vitric Andosol			5.4		19.7	15.0	
	Hinemaiai	36	grassland	0-7.5	Vitric Andosol			5.9		98.0	47.0	
	Whatawhata	1983-2006	grassland	0-7.5	Andosol and Acrisols	0	7.6	5.3		0.0	0.0	Schipper et al., 2011
				0-7.5		30	7.0		Triple superphosphate	30.0	19.0	
				0-7.5		50	8.5		Triple superphosphate	50.0	42.0	
				0-7.5		100	8.0		Triple superphosphate	100.0	67.0	
	Winchmore*	1952-1998	grassland	0-7.5	Cambisols	0		5.5-6.0		0.0	0.0	McDowell, 2011
						18P			Superphosphate	17.0	3.0	
						36P			Superphosphate	34.0	7.0	

APPENDIX A

UK	Rothamsted (BK)	95	arable		Luvisol	20-30				0.9-1.1		Superphosphate	33.0	3.0	Rothbaum et al.,1979
	Rothamsted (PG)	100	grassland		Luvisol						5.2	Superphosphate	33.0	7.0	Rothbaum et al.,1979
USA	Morrpw plots	1904-1985	arable	0-17	Histosol	24				1.6		Superphosphate	32.7*	9.0	Jones, 1992
	Florida	30	grassland	0-15								Superphosphate	17.3	35.0	Zielinski et al., 2006
Switzerland	site 65	1985-2009	Arable	0-20	Cambisol	16	67	18		1.5	6.0		16*	8.3	Bigalke et al., 2017
	site 38	1985-2009	Arable	0-20	Gleysol	28	23	49		2.0	5.2		16*	0.0	
	site 48	1985-2009	Arable	0-20	Histosol	-	-	-		16.5	5.2		16*	8.3	
	site 15	1985-2009	Arable	0-20	Gleysol	48	30	22		14.8	6.1		16*	31.3	
	site 25	1985-2009	Arable	0-20	Cambisol	59	30	11		2.4	6.8		16*	0.0	
	site 31	1985-2009	Arable	0-20	Cambisol	21	18	61		2.5	5.9		16*	27.0	
Denmark	Askov	1923-2016	arable	0-20	Luvisol	12	13	75	Unfertilizer	1.2	6.5	-	0.0	0.0	this study
									Mineral P fertilizer	1.4	6.5	Superphosphate	18.0	0.0	
Germany	Rengen	1941-2015	grassland	0-10	Stagnic Cambisol				No Fertilizer	4.9	4.9	-	0.0	0.0	
									Ca N P	4.3	6.6	Thomas slag	35.0	1.3	
									Ca N P KCl	4.4	6.5	Thomas slag	35.0	1.3	
									Ca N P K_2SO_4	4.5	6.6	Thomas slag	35.0	1.3	
	Thyrow	1973-2016	arable	0-24	Cutanic Albic Luvisol				NK+liming	0.4	6.0		0.0	0.0	
									NPK+liming	0.4	6.0	Triple Superphosphate	24.0	0.6	
									NPK		3.8	Triple Superphosphate	24.0	0.6	
Iceland	Geitasandur	1958-2007	grassland	0-5	Vitric Andosol				0	10.5	5.5		0.0	0.0	
		1958-2007							39.2P	15.5	5.5		39.2	149.0	
		1958-2007							78.6P	22.0	5.5		78.6	310.0	

	Sámstaðir	1950-2004	grassland	0-5	Gleyic Andosol	0	15.7	5.3		0.0	0.0
						39.2P	18.9	5.3		39.2	112.9
UK	Broadbalk	1881-2015	arable	0-23	Luvisol	Control	0.9	7.0	Superphosphate	0.0	0.0
						P	0.9	7.0		35.0	3.4
	Parkgrass	1987-2011	grassland	0-23	Chromic Luvisol	Control	3.3	5.2		0.0	0.0
						P	3.3	5.0	Superphosphate	35.0	9.0
						P + liming	3.3	7.0		35.0	6.6

APPENDIX B

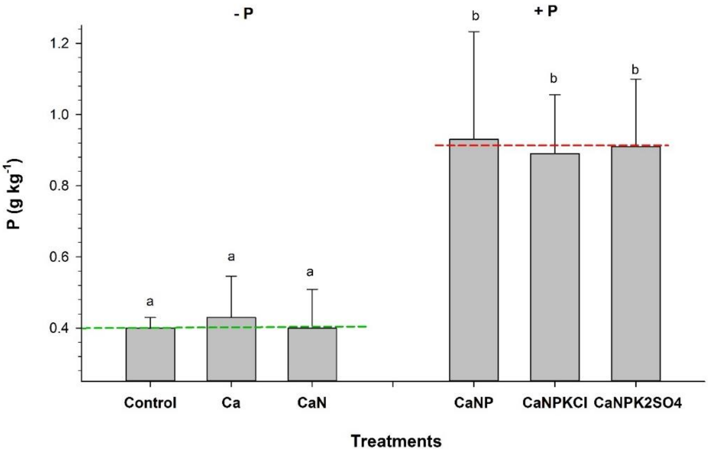

Figure A-1. Concentrations of acid-extractable P in topsoil of five fertilizer treatments in the Rengen Grassland Experiment.

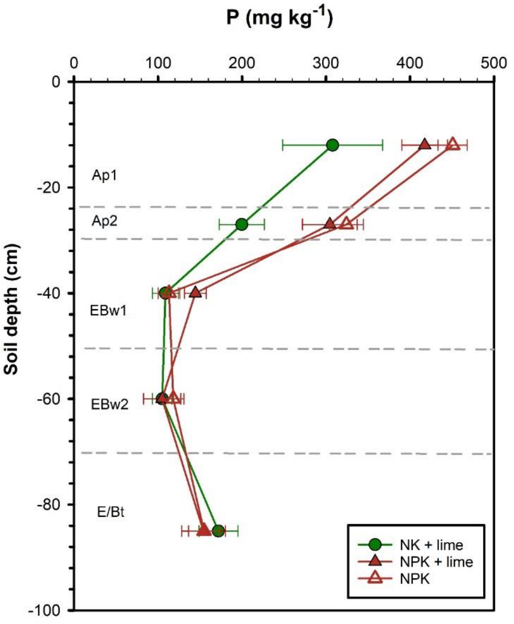

Figure A-2. Depth profiles of acid-extractable P concentration in soils of the long-term experimental field of Thyrow. Error bars represent standard deviations of the four field replicates.

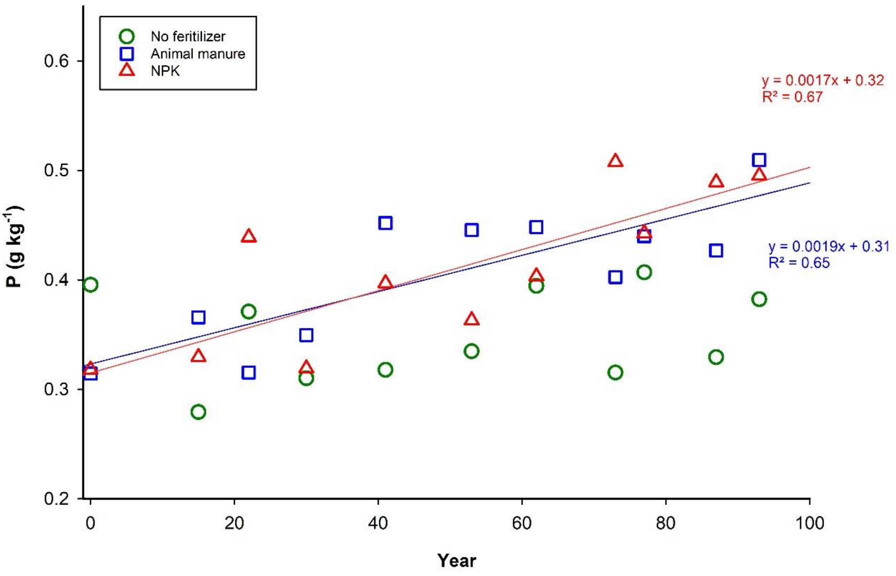

Figure A-3. Temporal changes in concentrations of acid-extractable P in arable topsoil (0-20 cm) of the control, animal manure (AM) and NPK fertilizer treatments at Askov.

Appendix B

Literature review and own data on uranium concentrations and $\delta^{18}O_p$ in phosphate rocks

Supporting information to Chapter 4

APPENDIX B

Table B-1. Literature review and own data on uranium concentrations in phosphate rocks.

Country	Deposit	Type	Age	U (mg kg^{-1})	P_2O_5 %	U/P_2O_5	Reference
Algeria	Djebel Onk	Phosphatic limestone; pelletal; granular;	Late Paleocene	31.0	32.4	1.0	Cevik et al., 2010
Algeria	Djebel Onk	Phosphatic limestone; pelletal; granular;	Late Paleocene	25.0	28.0	0.9	Khater et al., 2016
Algeria	Djebel Kouif	-	-	100.0	27.9	3.6	Parker, 1984
Algeria	Gebel Onk	Granular	Paleocene	8-115, 60	22-30, 21	2.8	Pokryshkin,1981
Algeria	-	Rock phosphate	-	51.8	28.6	1.8	this study
Algeria	-	Rock phosphate	-	52.7	28.8	1.8	this study
Algeria	-	Rock phosphate	-	53.3	28.7	1.9	this study
Algeria	-	Rock phosphate	-	53.5	28.6	1.9	this study
Algeria	-	Calcined phosphate	-	59.9	31.1	1.9	this study
Algeria	-	Rock phosphate	Cretaceous-Eocene	45.0	25.9	1.7	this study
Algeria	-	Rock phosphate	-	47.8	29.7	1.6	this study
Algeria	-	Rock phosphate	-	48.6	30.0	1.6	this study
Algeria	Djebel Onk	Phosphatic limestone; pelletal; granular;	Late Paleocene	25.0	29.3	0.9	Van Kauwenbergh, 1997
Antarctica	Pensacola	Nodules, matrix	Devonian	260.0	30.0	8.6	Altschuler, 1980
Australia	Eastern slope	Nodules	Middle Miocene-Early Pliocene	27-303, 126	11.0	11.9	Cook et al., 1990
Australia	Eastern slope	Nodules	Middle Miocene-Early Pliocene	67.0	9.6	3-13,7.9	Cook et al., 1990
Australia	North Queensland	Argillite-type phosphorites	Early-Middle Cambrian	15-65, 48	7.8-39.1, 18.6	2.6	Cook, 1972
Australia	North Queensland	Replacement phosphorites	Early-Middle Cambrian	10-80, 43	28-39.2, 35.3	1.2	Cook, 1972
Australia	North Queensland	Pelletal phosphorites	Early-Middle Cambrian	45-130, 78	33.7-37.4, 35.6	2.2	Cook, 1972
Australia	Wonarah	Leached phosphorites	Early-Middle Cambrian	2-53, 21.9	17.3-30.9, 24.7	0.1-2.3, 0.9	Howard and Hough, 1979
Australia	D Tree	Leached	Early-Middle Cambrian	8-74, 23	14.4-27.9, 21.7	0.4-3.7,1.1	Howard and Hough, 1979
Australia	D Tree	Replacement phosphorites	Early-Middle Cambrian	18-45, 33	37.6-39.5, 38.7	0.5-1.2, 0.9	Howard and Hough, 1979

APPENDIX B

Australia	Sherrin Creek (Queensland)	Unleached phosphorites	Early-Middle Cambrian	5-42, 25	28-37.8, 25	0.6-4.3, 1.2	Howard and Hough, 1979
Australia	D Tree	Partly leached	Early-Middle Cambrian	19-86, 47	7.8-27.4, 19.9	1-5.2, 2.5	Howard and Hough, 1979
Australia	D Tree	Unleached phosphorites	Early-Middle Cambrian	19-61, 32	3.8-15.5, 8.6	3.1-5.6, 3.9	Howard and Hough, 1979
Australia	Duchess	-	Early Middle Cambrian	80.0	29.1	2.7	Parker, 1984
Australia	Duchess	-	Early Middle Cambrian	80.0	23.9	3.3	Parker, 1984
Australia	Duchess	-	Early Middle Cambrian	92.0	31.2	2.9	Van Kauwenbergh, 1997
Azeri	-	shelly	Ordovician	35-52, 43	5.7-14.4, 10	2.4-9.1, 5.6	Baturin and Kochenov, 2001
Brazil	Bambui	pelletal	Precambrian	30.0	19-35,27	1-1.5,1.2	Altschuler, 1980
Brazil	-	Rock phosphate	Middle-Late Proterozoic	38.1	28.6	1.3	this study
Brazil	-	Rock phosphate		67.5	25.0	2.7	this study
Burkina Faso	Kodjari	-	Middle-Late Proterozoic	125.0	25.4	4.9	Van Kauwenbergh, 1997
China	Wanjhawan	Vaguely granular	Early-Middle Cambrian	12.9	26.0	0.5	Volkov, 1994
China	Kunjan	Granular	Early-Middle Cambrian	15.8	31.0	0.5	Volkov, 1994
China	Undifferentiated	-	-	10.0	31.9	0.3	Parker, 1984
China	Undifferentiated	-	-	20.0	30.3	0.7	Parker, 1984
China	Hubei, Jingzhou	Sedimentary type	Late Proterozoic	2.0	22.2	0.1	this study
China	Hubei, Jingzhou	Sedimentary type	Late Proterozoic	2.6	30.7	0.1	this study
China	Hunan, Shimen	Metamorphic type	Late Proterozoic	3.0	25.0	0.1	this study
China	Hubei, Yichang	Sedimentary type	Late Proterozoic	3.0	22.2	0.2	this study
China	Hubei, Jingmen	Sedimentary type	Late Proterozoic	3.7	29.8	0.2	this study
China	Hubei, Yichang	Sedimentary type	Late Proterozoic	5.0	25.2	0.2	this study
China	Hubei, Yichang	Sedimentary type	Late Proterozoic	5.6	31.4	0.2	this study
China	Hubei, Yichang	Sedimentary type	Late Proterozoic	7.2	30.9	0.4	this study
China	Guizhou, Kaiyang	Sedimentary type	Late Proterozoic	11.4	28.9	0.7	this study
China	Sichuan, Shijiao	Sedimentary type	Middle-Late Devonian	19.5	29.8	0.5	this study
China	Yunnan, Kunming	Sedimentary type	Early Cambrian	14.7	23.8	0.6	this study
China	Sichuan, Hanyuan	Sedimentary type	Middle-Late Devonian	14.3	23.6	1.0	this study

APPENDIX B

China	Yunnan, Kunming	Sedimentary type	Early Cambrian	22.6	27.0	0.8	this study
China	Yunnan, Jinning	Sedimentary type	Early Cambrian	20.4	21.1	1.5	this study
China	Kaiyang	Sedimentary type	Late Proterozoic	31.0	35.9	0.9	Van Kauwenbergh, 1997
Egypt	East Sabaiya	-	Late Cretaceous	57.0	30.6	1.9	Cevik et al., 2010
Egypt	Kosseir	-		40.0	28.3	1.4	Parker, 1984
Egypt	Abu Tartur	Bedded	Late Cretaceous	40.0	26.5	1.5	Parker, 1984
Egypt	Safaga	Granular	Late Cretaceous	100.0	28.9	3.5	Parker, 1984
Egypt	Safaga	Bedded; pelletal;	Late Cretaceous	130.0	32.2	4.0	Parker, 1984
Egypt	Safaga	Bedded; pelletal;	Late Cretaceous	130.0	31.8	4.1	Parker, 1984
Egypt	Safaga	Granular	Late Cretaceous	70-120,95	25.0	3-5, 4	Sokolov, 1996
Egypt	Abu Tartur	Bedded	Late Cretaceous	120.0	31.7	3.8	Van Kauwenbergh, 1997
Egypt	West Makamid	-	-	100.0	26.5	3.8	Van Kauwenbergh, 1997
Egypt	Hamrawen	-	Late Cretaceous	110.0	22.2	5.0	Van Kauwenbergh, 1997
Estonia	Toolse	Shelly	Ordovician	15-45, 30	6.5-8.7,7.6	2.3-5.2, 3.7	Baturin and Kochenov, 2001
Estonia	Narva	Shelly	Ordovician	52-100, 76	6.4-7.1, 6.8	7.3-15.5, 9.4	Baturin and Kochenov, 2001
Estonia	Toolse	Shelly	Ordovician	34.0	11.5	2.9	Levina et al., 1976
Eygpt	El-Sibayia	Bedded	Late Cretaceous	89.0	30.0	3.0	Khater et al., 2016
Eygpt	El-Sibayia	Bedded	Late Cretaceous	89.0	27.0	3.3	Khater et al., 2016
India	Hirapur	stromatolitic	Proterozoic	3-120,			Banerjee et al., 1982
India	Uttar Pradesh	Granular	Proterozoic	1.7-129.7	28.8-31.8	0.05-4.23	Dar et al., 2014
India	Rajasthan	Stromatolitic	Early Proterozoic	20.0	40.1	0.5	Parker, 1984
India	Udaipur	stromatolitic	Proterozoic	30-100, 65	10-37, 23	2.8	Pokryshkin, 1981
India	Mussoorie	-	Early Cambrian	26.0	25.0	1.0	Van Kauwenbergh, 1997
India	Aravalli	Stromatolitic	Proterozoic	3.6-4.2, 4	31.7-33.1, 32.4	0.1	Zanin et al. 2000
India	Aravallian basin	Stromatolitic	Proterozoic	3.6	31.7	0.1	Zanin et al. 2000
India	Aravallian basin	Stromatolitic	Proterozoic	4.2	33.1	0.1	Zanin et al. 2000

APPENDIX B

Israel	Mishash	Granular	Late Cretaceous-Paleocene	105.0	22-33,27.5	3.3	Makarov, 1963
Israel	Arad	granular, pellets	Late Cretaceous	150.0	32.3	4.6	Parker, 1984
Israel	-	-	Paleogene	40-240,140	16-27,22	6.3	Pokryshkin, 1981
Israel	Oron	Granular	Late Cretaceous	8-115, 60	20-32, 26	2.3	Pokryshkin, 1981
Israel	Arad	granular, pellets	Late Cretaceous	153.0	32.1	4.8	Syers et al., 1986
Israel	Arad	Rock phosphate	Late Cretaceous	153.0	33.0	4.6	this study
Israel	Arad	Rock phosphate	Late Cretaceous	148.0	32.9	4.5	this study
Israel	-	Rock phosphate	-	128.0	33.9	3.8	this study
Israel	-	Rock phosphate	-	127.4	33.3	3.8	this study
Israel	-	Rock phosphate	-	125.0	33.1	3.8	this study
Israel	-	Rock phosphate	-	152.0	32.4	4.7	this study
Israel	-	Rock phosphate	-	111.0	26.8	4.1	this study
Israel	Oron	Granular	Late Cretaceous	99.0	33.6	2.9	Van Kauwenbergh, 1997
Israel	Arad	granular, pellets	Late Cretaceous	148.0	32.8	4.5	Van Kauwenbergh, 1997
Israel	Nahal Zin	Rock phosphate	Late Cretaceous	129.0	38.0	3.4	this study
Israel	Oron	Rock phosphate	Late Cretaceous	215.0	33.9	6.3	this study
Japan	submarine rise of the sea of Japan	Granular	Miocene	12-110, 50	10.5-32.3, 21.4	0.4-5,2.7	Baturin and Kochenov, 2001
Jordan	-	Granular	Late Cretaceous-Paleocene	67-155, 111	20-34, 27	4.1	Volkov, 1994
Jordan	El Hasa	Granular	Late Cretaceous Maastrichtian	82.0	32.5	2.5	Jallad et al., 1989
Jordan	El Hasa	Granular	Late Cretaceous Maastrichtian	105.0	33.9	3.1	Jallad et al., 1989
Jordan	-	Granular	Late Cretaceous-Paleocene	90-180,135	20-34,27	5.0	Nabil, 1992
Jordan	Ruseifa	Granular	Late Cretaceous	129.0	30.8	4.2	Parker, 1984
Jordan	El Hasa	Granular	Late Cretaceous Maastrichtian	8-180, 94	23-34,28	3.3	Pokryshkin, 1981
Jordan	El Hasa	Granular	Late Cretaceous Maastrichtian	72.0	30.7	2.3	Syers et al., 1986
Jordan	Shidyia	granular	Late Cretaceous	46.0	30.5	1.5	Van Kauwenbergh, 1997

APPENDIX B

Jordan	El Hasa	Granular	Late Cretaceous	54.0	31.7	1.7	Van Kauwenbergh, 1997
Kazakhstan	Chilisai	Nodules	Eocene	16-53, 29	6.4-13.3, 9.8	2.9	Levina et al., 1976
Kazakhstan	Kara Tau	Bedded (microcrystalline)	Lower Cambrian	22.7	18.6	1.2	Zanin et al. 2000
Kazakhstan	Kara Tau	Bedded (microcrystalline)	Lower Cambrian	25.0	16.1	1.6	Zanin et al. 2000
Mali	Tilemsi	Nodules	Middle Eocene	123.0	28.8	4.3	Van Kauwenbergh, 1997
Mongolia	Hubsugul	Granular and structureless	Early Cambrian	1-31, 11	16-37, 20.7	0.5	Levina et al., 1976
Moricco	Ypussoufia	-	Late Cretaceous-Early Eocene	83.0	30.0	2.8	Cevik et al., 2010
Morocco	-	Granular	Late Cretaceous-Eocene	140.0	33.0	4.2	Altschuler, 1980
Morocco	-	-	-	140.0	33.0	4.2	Altschuler, 1980
Morocco	Khouribge	Bedded	Late Cretaceous-Early Eocene	88.0	33.0	2.7	Khater et al., 2016
Morocco	Youssoufia	Bedded	Late Cretaceous-Early Eocene	97.0	31.0	3.1	Khater et al., 2016
Morocco	Bu Craa	Bedded	Late Cretaceous-Paleocene	70.0	35.3	2.0	Parker, 1984
Morocco	Bu Craa	Bedded	Late Cretaceous-Paleocene	80.0	34.9	2.3	Parker, 1984
Morocco	-	-	-	120.0	31.8	3.8	Parker, 1984
Morocco	-	-	-	130.0	32.2	4.0	Parker, 1984
Morocco	-	Granular	Late Cretaceous-Eocene	57-190, 120	15-33, 24	5.0	Pokryshkin, 1981
Morocco	-	Rock phosphate	-	112.0	31.0	3.6	this study
Morocco	-	Rock phosphate	-	191.0	30.2	6.3	this study
Morocco	-	Rock phosphate	-	127.4	30.8	4.1	this study
Morocco	-	Rock phosphate	-	147.0	34.4	4.3	this study
Morocco	Khouribga	Rock phosphate	Late Cretaceous-Middle Eocene	127.5	31.4	4.1	this study
Morocco	Khouribga	Rock phosphate	Late Cretaceous-Middle Eocene	128.0	31.9	4.0	this study
Morocco	Khouribga	Rock phosphate	Late Cretaceous-Middle Eocene	245.0	34.4	7.1	this study

APPENDIX B

Morocco	Khouribga	Bedded; granular; shell	Late Cretaceous-Middle Eocene	81.0	32.3	2.5	Van Kauwenbergh, 1997
Morocco	Khouribga	Bedded; granular; shell	Late Cretaceous-Middle Eocene	100.0	33.4	3.0	Van Kauwenbergh, 1997
Morocco	Youssoufia	Bedded	Late Cretaceous-Early Eocene	111.0	32.5	3.4	Van Kauwenbergh, 1997
Morocco	Khouribga	Bedded; granular; shell	Late Cretaceous-Middle Eocene	82.0	33.4	2.5	Van Kauwenbergh, 1997
Morocco	Youssoufia	Bedded	Late Cretaceous-Early Eocene	97.0	32.1	3.0	Van Kauwenbergh, 1997
Morocco	Youssoufia	Bedded	Late Cretaceous-Early Eocene	89.0	27.6	3.2	Van Kauwenbergh, 1997
Nauru	-	-	-	40.0	37.1	1.1	Parker, 1984
Nauru	-	-	-	50.0	38.5	1.3	Parker, 1984
Nauru	-	-	-	60.0	38.7	1.6	Parker, 1984
Nauru	-	-	-	64.0	35.7	1.8	Syers et al., 1986
New zealand	submarine bChatham rise	Granular	Miocene	117-524, 230	21.8	5-24,14	Kolodny and Kaplan, 1970
Niger	Tapoa	Granular	Early Cambrian	7.1	27.0	0.3	Volkov, 1994
Niger	Tapoa	Granular	Late Proterozoic	8.2	31.0	0.3	Volkov, 1994
Niger	Parc W	-		65.0	33.5	1.9	Van Kauwenbergh, 1997
Peru	Peru shelf	Curst	Pleistocene-Holocene	12-38, 23	2.1-9.4, 4.4	3-8.3,5	Baturin and Kochenov, 2001
Peru	Peru shelf	Curst	Pleistocene-Holocene	52-193, 106	11.2-25.2, 14.7	4.6-8.3,4.9	Baturin and Kochenov, 2001
Peru	Peru shelf	Nodular	Pleistocene-Holocene	16-182, 93	5.9-28.7, 17.3	2.0-17.7,5.3	Burnett and Veeh,1977
Peru	Sechura	Pelletal	Middle Miocene	72.0	29.5	2.4	Parker, 1984
Peru	Sechura	Pelletal	Middle Miocene	80.0	30.8	2.6	Parker, 1984
Peru	Sechura	Pelletal	Middle Miocene	80.0	29.7	2.7	Parker, 1984
Peru	Sechura	Pelletal	Middle Miocene	47.0	29.3	1.6	Van Kauwenbergh, 1997
Peru	Sechura	Pelletal	Middle Miocene	80.0	31.3	2.6	Van Kauwenbergh, 1997

APPENDIX B

Portugal	Continental slope	Nodular	Miocene	5-158, 80	6.4-21.5, 14	0.5-11.1,5.5	Gaspar, 1981
Russia	Seleuk	Nodules	Late Jurassic-Paleogene	4.2	13.5	0.3	Baturin and Kochenov, 2001
Russia	Egor'ev	Nodular	Late Jurassic-early Cretaceous	17.0	12.6	1.3	Baturin and Kochenov, 2001
Russia	Penze	Nodules	Late Jurassic-Paleogene	31.0	24.1	1.3	Baturin and Kochenov, 2001
Russia	Bessonov	Nodules	Late Jurassic-Paleogene	27.0	19.2	1.4	Baturin and Kochenov, 2001
Russia	Bogdanov	Nodules	Late Jurassic-Paleogene	27.0	18.4	1.5	Baturin and Kochenov, 2001
Russia	Trukhanov	Nodules	Late Jurassic-Paleogene	27.0	17.9	1.5	Baturin and Kochenov, 2001
Russia	Tarkhanov	Nodules	Late Jurassic-Paleogene	31.0	20.1	1.5	Baturin and Kochenov, 2001
Russia	Tambov	Nodules	Late Jurassic-Paleogene	45.0	24.9	1.8	Baturin and Kochenov, 2001
Russia	Kingisepp, Baltic region	Shelly	Ordovician	24.0	12.5	2.0	Baturin and Kochenov, 2001
Russia	Egor'ev	Nodular	Late Jurassic-early Cretaceous	50.0	23.3	2.1	Baturin and Kochenov, 2001
Russia	Podbuga	Nodules	Late Jurassic-Paleogene	45.0	18.3	2.5	Baturin and Kochenov, 2001
Russia	Krolevitskoe	Nodules	Late Jurassic-Paleogene	40.0	16.1	2.5	Baturin and Kochenov, 2001
Russia	Undor	Nodules	Late Jurassic-Paleogene	59.0	23.2	2.5	Baturin and Kochenov, 2001
Russia	Oraush	Nodules	Late Jurassic-Paleogene	68.0	25.3	2.7	Baturin and Kochenov, 2001
Russia	Polpino	Nodules	Late Cretaceous	52.0	16.1	3.2	Baturin and Kochenov, 2001
Russia	Shchigrov	Nodules	Late Jurassic-Paleogene	68.0	16.0	4.3	Baturin and Kochenov, 2001
Russia	Slobodsk-Kostoretsk	Nodules	Late Jurassic-Paleogene	40.0	6.9	5.8	Baturin and Kochenov, 2001
Russia	Trekhostrovsk	Nodules	Late Jurassic-Paleogene	88.5	12.6	7.0	Baturin and Kochenov, 2001

Russia	Vyatka-Kama	Nodules	Late Jurassic-Paleogene	17-59, 38	12.6-23.3, 18.0	0.7-4.6, 2.6	Baturin and Kochenov, 2001
Russia	Maardu, ibidem	Shelly	Ordovician	14-68, 41	10.8-26, 18	1.3-2.6, 2.0	Baturin and Kochenov, 2001
Russia	Maardu, ibidem	Shelly conglomerate	Ordovician	24.0	17.0	1.4	Levina et al., 1976
Russia	Maardu, ibidem	shelly	Ordovician	7-48, 21	3.0-29, 13	1.6	Levina et al., 1976
Russia	Egor'ev	Nodular	Late Jurassic-early Cretaceous	34.0	21.1	1.6	Levina et al., 1976
Russia	Egor'ev	Phosphatized fauna	Late Jurassic-early Cretaceous	40.0	32.1	1.7	Levina et al., 1976
Russia	Vyatka-Kama	Phosphatized fauna	Late Jurassic-Paleogene	40.0	23.1	1.7	Levina et al., 1976
Russia	Gornaya shoria	Brecciated	Late Proterozoic	10-60, 35	5-13.6, 12	2.4	Levina et al., 1976
Russia	Maardu, ibidem	Phosphatized sandstone	Ordovician	20.0	8.2	2.4	Levina et al., 1976
Russia	Lagap(Shantar Island)	Brecciated	Early-Middle Cambrian	7-56, 25	5-32, 20	2.5	Levina et al., 1976
Russia	Vyatka-Kama	Nodules	Late Jurassic-Paleogene	17-58, 34	10.7-19.5, 12.2	2.8	Levina et al., 1976
Russia	Maardu, ibidem	Pebble	Ordovician	25.0	8.6	2.9	Levina et al., 1976
Russia	Polpino	Nodules	Late Cretaceous	1-111, 43	5-8, 7	2-12, 4.8	Levina et al., 1976
Russia	Polpinsk	Nodular	Upper Cretaceous	30.4	27.8	1.1	Zanin et al. 2000
Russia	Egor'ev	Nodular	Upper Jurassic-lower Cretaceous	29.6	25.8	1.1	Zanin et al. 2000
Russia	Egor'ev	Nodular	Upper Jurassic-lower Cretaceous	29.6	25.8	1.1	Zanin et al. 2000
Russia	Egor'ev	Nodular	Upper Jurassic-lower Cretaceous	30.7	25.5	1.2	Zanin et al. 2000
Russia	Polpinsk	phosphatic wood	Upper Cretaceous	55.8	28.5	2.0	Zanin et al. 2000
Russia	Egor'ev	Nodular	Upper Jurassic-lower Cretaceous	35.2	15.8	2.2	Zanin et al. 2000
Russia	Polpinsk	phosphatic wood	Upper Cretaceous	66.5	28.8	2.3	Zanin et al. 2000
Russia	Polpinsk	phosphatic wood	Upper Cretaceous	100.0	20.8	4.8	Zanin et al. 2000
Russia	Sakhalin Island	Nodular	Neogene	8.2	15.5	0.5	Zanin et al. 2000

Russia	Sakhalin Island	Nodular	Neogene	17.9	26.8	0.7	Zanin et al. 2000
Saudi Arabia	Al-Jalamid	bedded; pelletal	Early Paleocene	21.0	21.0	1.0	Khater et al., 2016
Saudi Arabia	Al-Jalamid	bedded; pelletal	Early Paleocene	21.0	21.0	1.0	Khater et al., 2016
Saudi Arabia	Amm Wa ual	bedded; pelletal	Paleocene-Oligocene	61.0	32.0	1.9	Khater et al., 2016
Saudi Arabia	Amm Wa ual	bedded; pelletal	Paleocene-Oligocene	62.0	27.0	2.3	Khater et al., 2016
Saudi arabia	-	Granular	Late Cretaceous-Paleocene	16-90, 53	18.1-31.4, 24.7	2.1	Pokryshkin, 1981
Seamounts of the Pacific Ocean	-	Phosphatized limestones, breccia, and effusives	Late Cretaceous-Quaternary	1.3-9.2	4.8-31.6	0.06-0.7	Baturin et al., 1982
Senegal	Taiba	Bedded	Middle Eocene-Oligocene	67.0	36.0	1.9	Khater et al., 2016
Senegal	Taiba	Rock phosphate	Middle Eocene-Oligocene	96.0	36.7	2.6	this study
Senegal	Taiba	Rock phosphate	Middle Eocene-Oligocene	90.0	36.6	2.5	this study
Senegal	Taiba	Granular	Middle Eocene-Oligocene	70.0	27.2	2.6	Parker, 1984
Senegal	Taiba	Granular	Middle Eocene-Oligocene	100-150,125	25-31, 29	2.6	Pokryshkin, 1981
Senegal	Taiba	Granular	Middle Eocene-Oligocene	64.0	36.9	1.7	Van Kauwenbergh, 1997
Senegal	Taiba	Granular	Middle Eocene-Oligocene	99.0	37.0	2.6	Zanin et al. 2000
Senegal	Taiba	Granular	Middle Eocene-Oligocene	154.0	38.0	4.1	Zanin et al. 2000
Siberia	Siberian platform, Vikhoreva river area, Angara River Basin	Shelly	Middle Ordovician	11.0	38.2	0.3	Zanin et al. 2000
Siberia	Siberian platform, Vikhoreva river area, Angara River Basin	Shelly	Middle Ordovician	11.0	37.2	0.3	Zanin et al. 2000
Siberia	Siberian platform, Kuonamka Formation, Kachelkuan River valley	Nodular	Upper Lower Cambrain	56.6	29.0	2.0	Zanin et al. 2000
Siberia	Siberian platform,	Nodular	Upper Lower Cambrain	374.2	26.1	14.3	Zanin et al. 2000

APPENDIX B

South Africa	Kuonamka Formation, Kachelkuan River valley			11.2	38.0	0.3	this study
Southern of African	Agulhas Bank	Nodular	Miocene-Pliocene	10-166, 79	17.3-24, 21	0.4-9.8, 5.1	Kolodny and Kaplan, 1970
Syria	-	Granular	Late Cretaceous-Paleocene	120-140, 130	25.0	4-6, 5	Volkov, 1994
Syria	-	Granular	Late Cretaceous-Paleocene	30-200,115	25.0	4.6	Baturin and Kochenov, 2001
Syria	Hims-Palmyra (Alsharqia)	-	Late Cretaceous	36.0	26.7	1.4	Cevik et al., 2010
Syria	-	Granular	Late Cretaceous-Paleocene	20-319, 82	18-36, 26.3	3.2	Lucas and Abbas, 1989
Syria	-	Rock phosphate	-	58.6	24.6	2.4	this study
Syria	-	Rock phosphate	-	58.6	24.6	2.4	this study
Syria	Khneifies	bedded	Late Cretaceous	75.0	31.9	2.4	Van Kauwenbergh, 1997
Syria	Khnefies	Ground rock phosphate	Late Cretaceous	59.5	30.4	2.0	this study
Syria	Ain Layloun	Friable phosphate rock	Cretaceous	137.6	31.2	4.4	this study
Tanzania	Minjingu	-	Neogene-Quaternary	390.0	28.6	13.6	Van Kauwenbergh, 1997
Togo	-		Middle Eocene	110.0	36.7	3.0	Parker, 1984
Togo	-	Rock phosphate		107.0	36.4	2.9	this study
Togo	-	Rock phosphate	Early-Middle Eocene	104.0	33.7	3.1	this study
Togo	-	Rock phosphate	-	96.7	36.0	2.7	this study
Togo	-	-	-	77.0	36.5	2.1	Van Kauwenbergh, 1997
Togo	-	-	Early-Middle Eocene	93.0	37.0	2.5	Khater et al., 2016
Tunisia	Gafsa	-	Paleocene-Early Eocene	20.0	26.1	0.8	Cevik et al., 2010
Tunisia	-	-		44.0	29.0	1.5	Khater et al., 2016
Tunisia	-	-	Paleocene-Early Eocene	12.0	29.2	0.4	Parker, 1984
Tunisia	-	-	Paleocene-Early Eocene	30.0	29.5	1.0	Parker, 1984
Tunisia	-	-	Paleocene-Early Eocene	40.0	29.2	1.4	Parker, 1984
Tunisia	-	-	Paleocene-Early Eocene	50.0	28.0	1.8	Parker, 1984
Tunisia	-	-	Paleocene-Early Eocene	88.0	30.7	2.9	Parker, 1984

APPENDIX B

Tunisia	Gafsa	Granular	Paleogene	35-75, 55	25-31, 28	2.3	Pokryshkin, 1981
Turkey	Mardin	Granular	Late Cretaceous-Paleocene	25-57, 40	10-25, 17.5	2.3	Baturin and Kochenov, 2001
Turkey	Mazidagi	bedded; pelletal; nodular; oolitic; fossiliferous (fish remains and bones); limonitic and glauconitic phosphatic limestone	Late Cretaceous	33.0	33.5	1.0	Cevik et al., 2010
Ukraine	Podol region	Concretionary radiated	Vendian	0.6	24.8	0.0	Zanin et al. 2000
Ukraine	Podol region	Concretionary radiated	Vendian	0.9	35.3	0.0	Zanin et al. 2000
Ukraine	Podol region	Concretionary radiated	Vendian	3.4	33.0	0.1	Zanin et al. 2000
Ukraine	Podol region	Concretionary radiated	Vendian	4.2	35.1	0.1	Zanin et al. 2000
USA	Continental slope of Carolina	Nodular	Miocene	40-130, 77	22.4-29.7, 26	1.4-5.8,3.6	Altschuler et al., 1958
USA	Pango River, North Carolina	Granular	Miocene	65.0	30.0	2.0	Altschuler, 1980
USA	Bone Valley, Florida	Granular and nodular	Miocene-Pliocene	140.0	30-35, 33	4.4	Altschuler, 1980
USA	Phosphoria	Microgranular	Permian	20-210, 90	23-37, 30	3.0	Gulbrandsen , 1966
USA	North Florida	-		81.0	31.0	2.6	Khater et al., 2016
USA	Idaho	-	Middle-Late Permian	107.0	32.0	3.3	Khater et al., 2016
USA	Florida	-	Early-Middle Miocene	141.0	32.0	4.4	Khater et al., 2016
USA	submarine blake plateau	Nodular	Miocene	18-70, 37	18-20, 19	1-4,2.5	Kolodny and Kaplan, 1970
USA	North Florida	-	Miocene-Pliocene	50.0	30.9	1.6	Parker, 1984
USA	North Carolina	bedded; granular	Early-Middle Miocene	60.0	30.5	2.0	Parker, 1984
USA	North Florida	-	Miocene-Pliocene	70.0	32.5	2.2	Parker, 1984
USA	Idaho	peloidal	Middle-Late Permian (late paleozoic)	70.0	32.3	2.2	Parker, 1984
USA	North Carolina	bedded; granular	Early-Middle Miocene	70.0	30.0	2.3	Parker, 1984
USA	North Carolina	bedded; granular	Early-Middle Miocene	93.0	30.2	3.1	Parker, 1984
USA	Idaho	peloidal	Middle-Late Permian (late paleozoic)	110.0	32.0	3.4	Parker, 1984
USA	Idaho	peloidal	Middle-Late Permian (late paleozoic)	110.0	30.2	3.6	Parker, 1984
USA	Central Florida	-	Neogene	120.0	32.2	3.7	Parker, 1984

USA	Central Florida	-	Neogene	160.0	32.7	4.9	Parker, 1984
USA	Central Florida	-	Neogene	150.0	27.8	5.4	Parker, 1984
USA	Central Florida	-	Neogene	200.0	30.7	6.5	Parker, 1984
USA	lower Carolina	Nodular	Neogene	3-65, 30	8.5-21, 15	2.0	Pokryshkin, 1981
USA	Hawthorne Formation, Florida	Granular and nodular	Miocene	40-65, 50	10-25, 17	3.0	Pokryshkin, 1981
USA	North Carolina	Granular	Miocene	25-250, 135	11-18, 15	9.0	Pokryshkin, 1981
USA	North Carolina	bedded; granular	Early-Middle Miocene	65.0	29.1	2.2	Syers et al., 1986
USA	North Florida	-	Miocene-Pliocene	143.0	30.5	4.7	Syers et al., 1986
USA	Florida	Rock phosphate	-	74.0	32.1	2.3	this study
USA	North Florida	Pebble phosphate	-	103.0	31.1	3.3	this study
USA	North Florida	Rock phosphate	Early-Middle Miocene; Holocene	104.0	33.5	3.1	this study
USA	South Florida	Pebble phosphate	-	128.0	36.0	3.6	this study
USA	Florida	Pebble phosphate	-	114.0	32.4	3.5	this study
USA	Florida	Pebble phosphate	-	112.0	34.3	3.3	this study
USA	Florida	Rock phosphate	late Miocene	95.3	31.4	3.0	this study
USA	Florida	Rohphosphat normal (Pebble-Phosphat)	Early-Middle Miocene	154.0	32.6	4.7	this study
USA		Pebble phosphate, commercial quality	-	153.0	30.4	5.0	this study
USA		Pebble phosphate	-	104.2	32.4	3.2	this study
USA	Florida	Rohphosphat Pebble	Early-Middle Miocene	147.0	28.4	5.2	this study
USA	Florida	Rock phosphate (as raw material)	Early-Middle Miocene	191.0	33.3	5.7	this study
USA	Central Florida	-	Neogene	128.4	34.6	3.7	Van Kauwenbergh, 1997
USA	Idaho	peloidal	Middle-Late Permian (late paleozoic)	141.0	30.2	4.7	Van Kauwenbergh, 1997
USA	Central Florida	-	Neogene	135.0	33.3	4.0	Van Kauwenbergh, 1997
USA	North Carolina	bedded; granular	Early-Middle Miocene	41.0	29.9	1.4	Van Kauwenbergh, 1997
USA	Idaho	peloidal	Middle-Late Permian (late paleozoic)	60.0	32.6	1.8	Van Kauwenbergh, 1997
USA	Central Florida	-	Neogene	59.0	31.0	1.9	Van Kauwenbergh, 1997

APPENDIX B

USA	North Carolina	bedded; granular	Early-Middle Miocene	70.0	32.2	2.2	Van Kauwenbergh, 1997
USA	Central Florida	-	Neogene	128.5	34.5	3.7	Van Kauwenbergh, 1997
USA	North Carolina	bedded; granular	Early-Middle Miocene	58.0	28.1	2.1	Wakefield, 1980
USA	North Florida	-	Miocene-Pliocene	69.0	32.7	2.1	Wakefield, 1980
USA	North Florida	-	Miocene-Pliocene	66.0	31.1	2.1	Wakefield, 1980
USA	North Carolina	bedded; granular	Early-Middle Miocene	69.0	29.9	2.3	Wakefield, 1980
USA	North Carolina	bedded; granular	Early-Middle Miocene	62.0	26.2	2.4	Wakefield, 1980
USA	North Florida	-	Miocene-Pliocene	86.0	28.1	3.1	Wakefield, 1980
USA	Idaho	peloidal	Middle-Late Permian (late paleozoic)	135.0	32.7	4.1	Wakefield, 1980
USA	Central Florida	-	Neogene	140.0	33.3	4.2	Wakefield, 1980
USA	Central Florida	-	Neogene	140.0	33.0	4.2	Wakefield, 1980
USA	Idaho	peloidal	Middle-Late Permian (late paleozoic)	138.0	31.3	4.4	Wakefield, 1980
USA	Central Florida	-	Neogene	152.0	32.5	4.7	Wakefield, 1980
USA	Central Florida	-	Neogene	156.0	30.1	5.2	Wakefield, 1980
USA	Central Florida	-	Neogene	166.0	30.5	5.4	Wakefield, 1980
USA	Kentucky	Nodular	Upper Devonian-Lower Carboniferous	20.6	23.4	0.9	Zanin et al. 2000
USA	Kentucky	Nodular	Upper Devonian-Lower Carboniferous	53.4	23.6	2.3	Zanin et al. 2000
USA	phosphoria formation	Bedded (microcrystalline)	Upper Permian	41.7	13.0	3.2	Zanin et al. 2000
USA	phosphoria formation	Bedded (microcrystalline)	Upper Permian	108.5	33.8	3.2	Zanin et al. 2000
USA	phosphoria formation	Bedded (microcrystalline)	Upper Permian	123.1	23.2	5.3	Zanin et al. 2000
USA	phosphoria formation	Bedded (microcrystalline)	Upper Permian	194.0	34.2	5.7	Zanin et al. 2000
Venezuela		-	Late Cretaceous-Paleogene	65-80, 72	27.9	3.5	Volkov, 1994
Venezuela	Recieto	-	-	51.0	15-35.6, 25.3	1.8	Van Kauwenbergh, 1997
Western Sahara	Bu Craa	Granular	Paleocene	40-90, 65	37.0	2.6	Pokryshkin, 1981

Russia	Kola	Igneous type	-	6.0			Menzel, 1968
Finland	-	Igneous type	-	0.2			Schnug et al., 1996
Russia	Kola	Igneous type	-	3.0			Schnug et al., 1996
South Africa		Igneous type	-	10.0			Schnug et al., 1996
South Africa		Igneous type	-	23.0			schnug, 2007
Brazil	Araxa	Igneous type	-	117.0	37.0	3.2	Syers et al., 1986
Brazil	-	Igneous type	-	59.2	15.5	3.8	this study
Brazil	-	Igneous type	-	18.7	27.0	0.7	this study
China	Hebei	Igneous type	-	0.3	29.1	0.0	this study
China	Hunan	Igneous type	-	2.7	33.9	0.1	this study
Finland	-	Igneous type	-	0.9	49.1	0.0	this study
Russia	Kola	Igneous type	-	3.2	40.1	0.1	this study
Russia	Kola	Igneous type	-	3.7	40.0	0.1	this study
Russia	Kola	Igneous type	-	3.5	38.6	0.1	this study
Russia	Kola	Igneous type	-	2.5	39.0	0.1	this study
Russia	Kola	Igneous type	-	27.0	36.0	0.8	this study
Brazil	Araxa	Igneous type	-	247.0	37.4	6.7	Van Kauwenbergh, 1997
Brazil	Catalao	Igneous type	-	220.0	33.3	5.9	Van Kauwenbergh, 1997
Finland	Siilinjarvi	Igneous type	-	37.0	39.5	0.9	Van Kauwenbergh, 1997
Russia	Kola	Igneous type	-	20.0	38.1	0.5	Van Kauwenbergh, 1997
Russia	Kola	Igneous type	-	20.0	40.1	0.5	Van Kauwenbergh, 1997
Russia	Kola	Igneous type	-	30.0	22.9	1.3	Van Kauwenbergh, 1997
Russia	Kola	Igneous type	-	40.0	32.4	1.2	Van Kauwenbergh, 1997
South Africa	Phalaborwa	Igneous type	-	8.0	41.5	0.2	Van Kauwenbergh, 1997
South Africa	Phalaborwa	Igneous type	-	37.0	36.4	1.0	Van Kauwenbergh, 1997
Sweden	Kiiruna	Igneous type	-	20.0			Van Kauwenbergh, 1997

Zimbabwe	Dorowa	Igneous type	-	8.0	33.1	0.2	Van Kauwenbergh, 1997

Table B-2. $\delta^{18}O_p$ in sedimentary phosphate rocks of different geological ages in this study.

Country	Deposit	Age	Estimated age (Million years)	$\delta^{18}O_p$ (‰VSMOW)
Algeria	-	Cretaceous-Eocene	58	20.9
Algeria	-	Cretaceous-Eocene	58	21.1
Algeria	-	Cretaceous-Eocene	90	21.3
Algeria	-	Cretaceous-Eocene	58	21.3
Algeria	-	Cretaceous-Eocene	58	21.4
Algeria	-	Cretaceous-Eocene	58	21.4
Algeria	-	Cretaceous-Eocene	58	21.5
Brazil	-	-	-	11.2
Brazil	-	-	-	20.6
China	Yunnan, Kunming	Early Cambrian	535	12.2
China	Hubei, Yichang	Late Proterozoic	770	12.3
China	Hubei, Jingmen	Late Proterozoic	770	12.4
China	Yunnan, Kunming	Early Cambrian	535	12.9
China	Sichuan, Hanyuan	Middle-Late Devonian	376	12.9
China	Guizhou, Kaiyang	Late Proterozoic	770	13.2
China	Yunnan, Jinning	Early Cambrian	535	13.8
China	Hunan, Shimen	Late Proterozoic	770	14.5
China	Hubei, Yichang	Late Proterozoic	770	14.7
China	Hubei, Yichang	Late Proterozoic	770	15.1
China	Hubei, Yichang	Late Proterozoic	770	16.1
China	Hubei, Jingzhou	Late Proterozoic	770	17.0
China	Sichuan, Shijiao	Middle-Late Devonian	376	17.4
China	Hubei, Jingzhou	Late Proterozoic	770	18.2
Israel	-	Late Cretaceous	83	19.0
Israel	Arad	Late Cretaceous	83	20.0
Israel	-	Late Cretaceous	83	20.0
Israel		Late Cretaceous	83	20.0
Israel	Arad	Late Cretaceous	83	20.1
Israel	-	Late Cretaceous	83	20.2
Israel	-	Late Cretaceous	83	20.2
Israel	Nahal Zin	Late Cretaceous	83	20.3
Israel	Oron	Late Cretaceous	83	20.9
Israel	Nahal Zin	Late Cretaceous	83	20.9
Morocco	-	Late Cretaceous	72	19.2
Morocco	-	Late Cretaceous	72	19.5
Morocco	Khouribga	Late Cretaceous-Middle Eocene	72	20.1
Morocco	-	-	-	20.1
Morocco	-	-	-	20.1

Morocco	-	-	-	20.2
Morocco	Khouribga	Late Cretaceous-Middle Eocene	72	20.5
Morocco	Khouribga	Late Cretaceous-Middle Eocene	72	20.5
Senegal	Taiba	Middle Eocene-Oligocene	34	19.7
Senegal	Taiba	Middle Eocene-Oligocene	34	20.3
Syria	Khnefies	Late Cretaceous	83	18.8
Syria	Ain Layloun	Cretaceous	105	21.7
Togo	-	-	-	19.8
Togo	-	-	-	20.0
Togo	-	-	-	20.2
Togo	-	-	-	20.4
USA	-	-	-	20.1
USA	Florida	Miocene-Pliocene	13	20.8
USA	Florida	Miocene-Pliocene	13	21.0
USA	Florida	Miocene-Pliocene	13	21.2
USA	North Florida	-	13	21.3
USA	-	-	-	21.3
USA	Florida	Miocene-Pliocene	13	21.4
USA	South Florida		13	21.4
USA	Florida	Miocene-Pliocene	13	21.5
USA	Florida	Miocene-Pliocene	13	21.6
USA	Florida	Miocene-Pliocene	13	21.7
USA	-	-	-	21.8
USA	North Florida	Early-Middle Miocene; Holocene	0.01	22.1

Table B-3. $\delta^{18}O_p$ in igneous phosphate rocks from different deposits in this study.

Deposit	$\delta^{18}O_p$ (‰VSMOW)
Brazil	8.8
Hebei, China	6.5
Hebei, China	6.8
Liaoning, China	6.8
South Africa	8.6
Kola, Russia	5.2
Kola, Russia	5.7
Kola, Russia	5.4
Kola, Russia	5.2

APPENDIX B

Appendix C

Accumulation of uranium in topsoils of Rothamsted long-term experiments site due to phosphate fertilizer application

Modified on the basis of the manuscript

Sun, Y., Wu, B., Macdonald, A., Amelung, W., Haneklaus, S., Schnug, E. and Bol, R.

Manuscript in preparation

1. Introduction

Phosphorus (P) fertilizers that are produced from processed phosphate rocks contain various amounts of trace elements, such as uranium (U) (e.g. Van Kauwenbergh, 1997; Schnug et al., 1996). Long-term application of mineral P fertilizers to soil in agricultural systems can therefore lead to U accumulation in soil (e.g. Rothbaum et al., 1979; Kratz et al., 2006; McDowell, 2012; Bigalke et al., 2017). Consequently, although needed in many cases to maintain or even improve soil fertility status, this practive may threaten the integrity of agricultural soils and the sustainability of agriculture and drinking water supplies (Liesch et al., 2015; Schnug et al., 2015).

The U content of PRs depend on their origins. The extent of U accumulation in soil depends, therefore, on the U content and the amount of P fertilizer applied. It is therefore necessary to assess and quantify the extent of soil U accumulation under well recorded long-term phosphorus fertilizer applications, and to improve our understanding of the rate of U accumulations and transformations in soil. One of the first pioneering reports on the quantification of U accumulation in soils in response to P fertilizer was undertaken at Rothamsted Experimental Station (Rothbaum et al., 1979). The related researches increased in the last 20 years (e.g. McDowell, 2012; Bigalke et al., 2017). However, since that time there has no further study looking at the rate of U accumulation in the ongoing Rothamsted long-term field P fertilizer trials. The proposed work aims to further corroborate and expand the timespan of the results from crucial key earlier study by Rothbaum et al. (1979), and to assess the current and future potential environmental implications and impacts on these agricultural systems.

2. Materials and methods

Park Grass Experiment

The Park Grass Experiment is the oldest experiment on permanent grassland in the world (started in 1856). It located on the Rothamsted estate, Hertfordshire, UK, 40 km north of London. The soil is Chromic Luvisol (FAO classification) and the topsoil (0-23 cm) is a slightly flinty silty-clay loam. The aim of the Park Grass Experiment was to examine the effects of various types and amounts of fertilizers and lime on the yield and composition of grass cut for hay (Blake and Goulding, 2002). Treatments include different combinations and amounts of nitrogen (N), P, potassium (K), magnesium (Mg) and sodium (Na), as well as an unfertilized control (Nil). Nitrogen is applied either as ammonium sulphate or sodium nitrate. Phosphate fertilizers were applied at 35 kg P $ha^{-1}yr^{-1}$ as superphosphate made from bone ash (1856/8-1888), single superphosphate (1889-1896, and 1903-1986), basic slag (1897-1902) or triple superphosphate (since 1987).

The plots were split into limed (chalk) and non-limed halves in 1903 and further sub-divided into four sub-plots (a, b, c and d) in 1965. The 'a', 'b' and 'c' sub-plots are limed to maintain soil (0-23 cm) pH close to 7, 6 and 5, respectively, while 'd' sub-plot is non-limed (Silvertown et al., 2006). Archived soil samples (0-23 cm), spanning from 1876 to 2011 (1876, 1959, 1976, 1991, 2002 and 2011) were collected for this study, including from both limed (a) and non-limed (d) sub-plots-on plots 3 (Nil), 4/1 (P only) and 9/2 (N2PKNaMg); N was applied at 96 kg N ha^{-1} on plot 9/2.

Broadbalk Experiment

The Broadbalk Experiment (established in 1843) is also at Rothamsted Research. The soil is classified as Chromic Luvisol (FAO classification). The experiment was designed to examine the effects of various combinations of inorganic fertilizer (N, P, K, Na and Mg) and farmyard manure on the yield of wheat, including 20 strips (more details in Watts et al., 2006; Goulding et al., 2000). Chalk was added to maintain a stable soil pH since the 1950s.

Archive soil samples consisting of the ploughed layer (0-23, 23-46 cm), from strips 3 (Nil), 5 (PK(Na)Mg), and 11(N2P), were collected for this study from several years during the period of 1881-2015 (1881, 1944, 1976, 2000 and 2015). Phosphorus was applied as triple superphosphate with rate of 35 kg P ha^{-1} yr^{-1}. On strip 11, 96 kg N ha^{-1} was applied up to 2000; since 2001, 192 kg N ha^{-1} has been applied with Mg. Further details of fertilizer applications are given in Macdonald et al (2018).

The methods for U and P concentrations determination were expressed in section 2.2 Chapter 2.

3. Results

3.1 Uranium concentrations in soil

Park Grass Experiment

In 1876, all plots (control, P, N2PKNaMg) contained 0.90 ± 0.02 mg U kg^{-1} in the soil. Between 1876 and 2011, U concentrations (acid extractable) in the unfertilized control soil were stable; around 0.85 ± 0.04 mg kg^{-1} and 0.92 ± 0.07 mg kg^{-1} for limed and non-limed plots, respectively (Fig. C-1A). In contrast, U concentrations in limed plots (pH= 7) with P fertilizer addition (P, N2PKNaMg) increased by 0.57 mg kg^{-1} (67%) in 1959 compared to 1876 and reached 1.93 mg kg^{-1} in 2011 which was twice the concentration as in 1876 (Fig. C-1A). In non-limed plots (pH= 5), the trends of soil U concentration were similar to the limed plots (Fig. C-1).

Broadbalk

In plots without P fertilizers, U concentration was always around 0.92 ± 0.04 mg kg^{-1} in the topsoil during the period of 1881 to 2015. Plots that received P fertilizers (PK(Na)Mg, NPMg) also showed similar U concentration (0-23 cm) 0.90 mg kg^{-1} in 1880 relative to control plot, but since 1944 substantial increases of soil U concentration were observed. By 2015, the average soil U concentration in P fertilization plots was 1.2 mg kg^{-1}, corresponding to an increase of 33%.

In the soil profile of 23-46 cm, all plots with P fertilization or not (Control, PK(Na)Mg, NPMg) showed similar trend of soil U concentrations with an average of 0.91± 0.06 mg kg^{-1}. This illustrates fertilizer derived U tends to accumulate in topsoil only (0-23 cm).

The trends of total U concentration were similar to the soil acid extractable U in both Park Grass and Broadbalk experiment sites (Fig. C-1B and Fig. C-2B). The total U concentrations were about double those of acid extractable U, which indicated the fertilizer derived U were most likely in the acid extractable fraction and more active compared with the nature origin U.

APPENDIX C

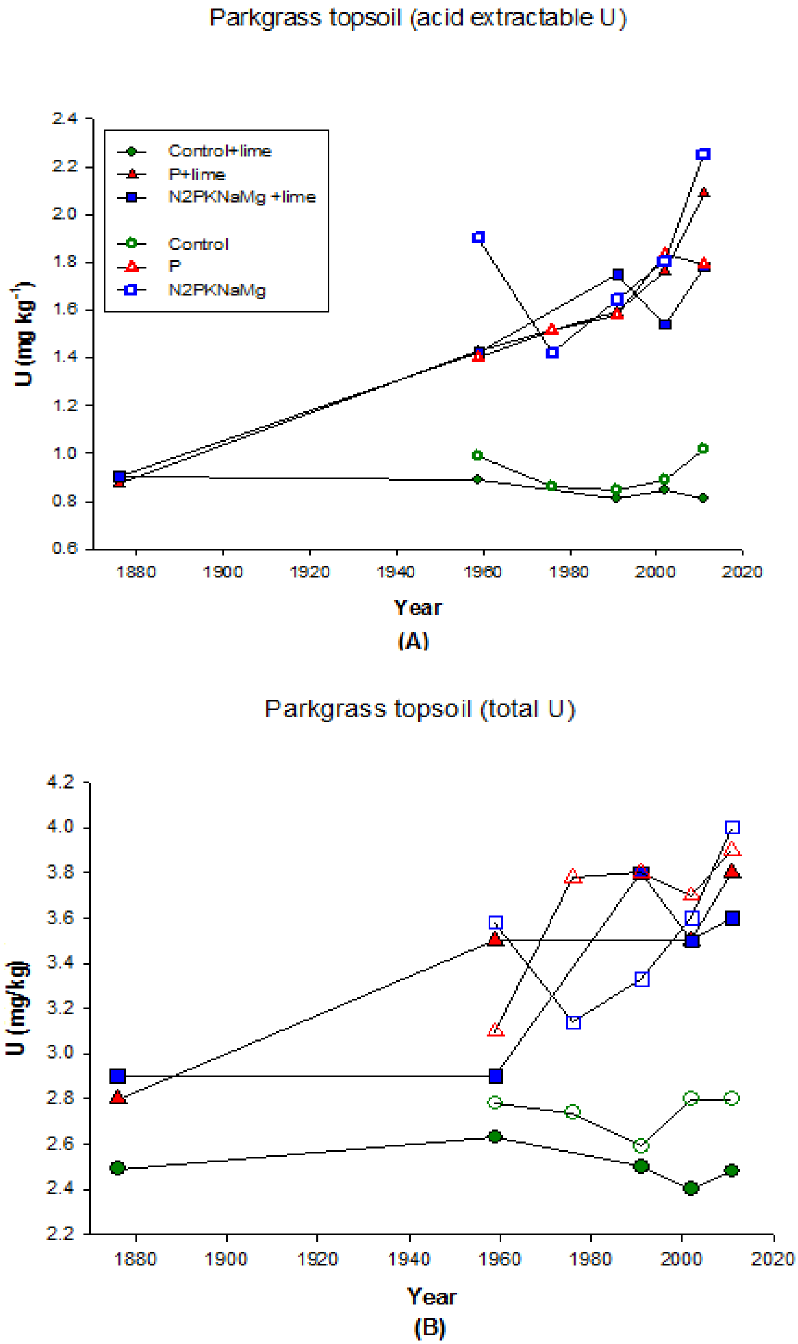
Parkgrass topsoil (acid extractable U)

Parkgrass topsoil (total U)

Figure C-1. Changes in the concentration of acid extractable U (A) and total U (B) in the topsoil (0-23 cm) from different plots of the Park Grass Experiment.

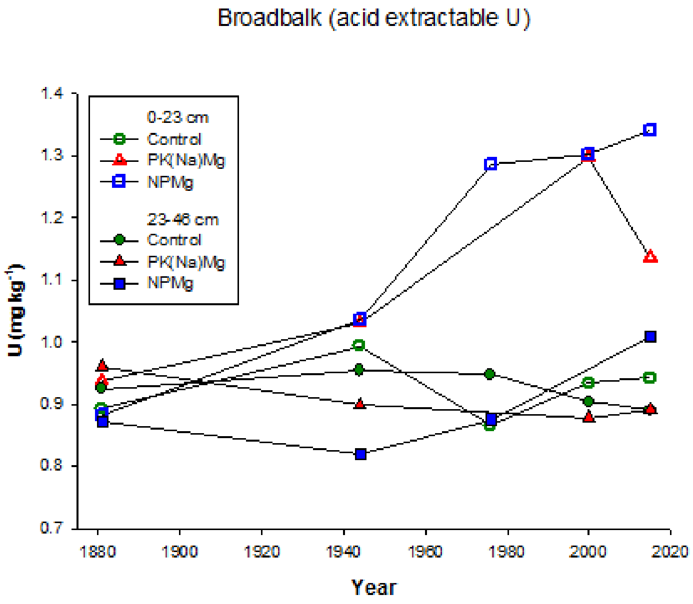

Broadbalk (acid extractable U)

(A)

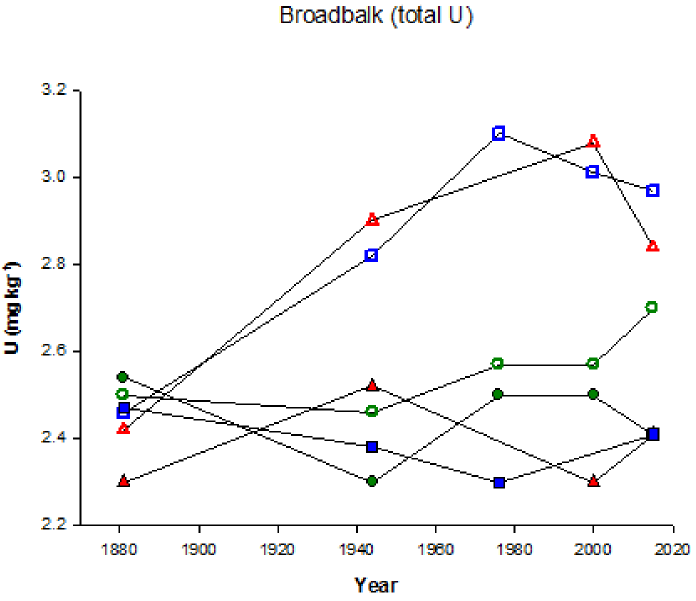

Broadbalk (total U)

(B)

Figure C-2. Changes in the concentration of acid extractable U (A) and total U (B) in the topsoil (0-23 cm) from different plots of the Broadbalk Experiment.

3.2 The correlation of P and U

The relationships between P and U concentrations were examined by linear regression models. The trends of soil P concentration were similar and well correlated with the trend of soil U in all plots both in Park Grass Experiment and Broadbalk Experiment (Fig. C-3). The correlation between soil P and U in Park Grass Experiment and Broadbalk Experiment indicate that the increases of U concentration in soil are due to the P fertilizer application.

4. Discussion

4.1 Enrichment of U in Rothamsted experiments

During 1840s to 1888, superphosphate applied in soil was made from bone ash which contains little or no U (< 1 mg kg^{-1}) (Rothbaum et al., 1979). Therefore, since 1889, the tendency of U to accumulate in soil coincides with the period in which commercial superphosphate was applied, which is consistent with the observed increases in soil U concentrations in plots given P fertilizers in 1959 and 1944 on Park Grass and Broadbalk, respectively. Substantial increases of soil U contents were observed in P fertilization plots in both experimental sites due to superphosphate (applied in 1889-1896 and 1903-1904) and triple superphosphate (since 1987) application. Rothbaum et al. (1979) analyzed the four commercial superphosphates applied in Rothamsted (probably made from North African rocks) and found an average of U content was 34 mg kg^{-1} (range 24-42 mg U kg^{-1}). As superphosphate normally contains 7-9.5% P, therefore, there should be around 14.4 g U ha^{-1} input to soil annually. This number is in the same magnitude with the estimate U load by mineral fertilization (22 kg P ha^{-1} yr^{-1}) in Germany with a mean value of 15 g U ha^{-1} (Kratz et al., 2008).

The slope of linear regression which described soil U concentration over time can be regarded as the U accumulation rate. The average U accumulation rate in the P fertilization plot was 6.6 µg kg^{-1} yr^{-1} for limed plots and 9.0 µg kg^{-1} yr^{-1} for non-limed plots in Park Grass, while it was 3.4 µg kg^{-1} yr^{-1} Broadbalk. The U accumulation rates observed in this study were consist with Rothbaum et al. (1979) who found the U accumulation rates were 7 and 3 µg kg^{-1} yr^{-1} for Park Grass and Broadbalk. In addition, these values are in the range of reported U accumulation rate of 7-14.5 µg kg^{-1} yr^{-1}(in e.g. Germany, New Zealand, Japan) under the similar P application amount (30-45 kg ha^{-1} yr^{-1}) (e.g. McDowell, 2012; Schipper et al., 2011; Wetterlind et al., 2012).

4.2 The long term Rothamsted experience

The U derived from P fertilizer accumulates in agricultural soil is a threat to the sustainability of agricultural system. The Rothamsted experiments are the oldest continuing agricultural field experiments in the world which provides valuable archived and current soil samples. The changes of U concentration in soil indicate precious information in relation to environmental issues surrounding to the sustainability of agriculture.

The first pioneering study related to fertilizer derived U accumulation in soils was reported at Rothamsted Experimental Station (Rothbaum et al., 1979). Forty years later, we found that the increase in soil U concentration is continuing at a similar rate as that reported before (7 and 3 μg kg^{-1} yr^{-1} for Park Grass and Broadbalk). The average U input to topsoil (0-23 cm) by P fertilizer was 20.9 g and 11.7 g for Park Grass and Broadbalk, respectively, with 35 kg P $ha^{-1}yr^{-1}$. Taking Rothamsted as a represented agricultural production system in UK, with the average P applicate rate 15.1 kg P $ha^{-1}yr^{-1}$ (FAO database), inputs to UK agricultural soils should be around 7 g U ha^{-1} yr^{-1}.

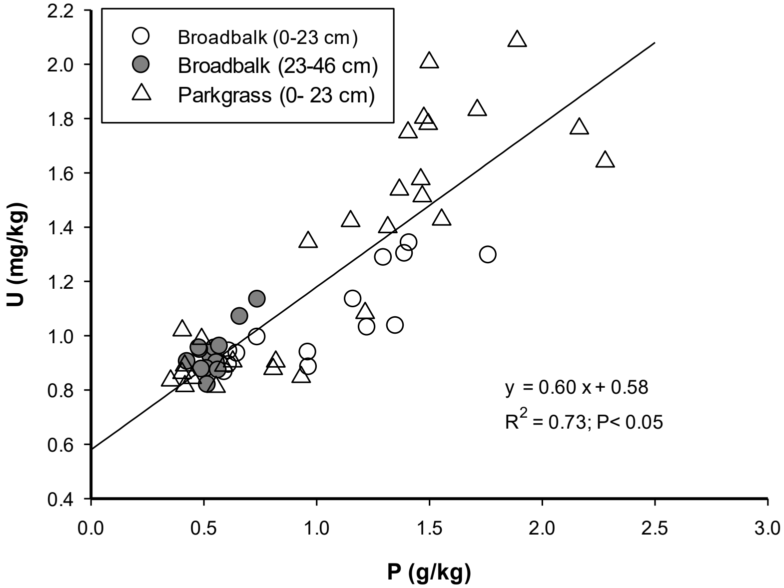

Figure C-3. Relationship between concentrations of P and U in Broadbalk and Park Grass Experiments.

5. Conclusions

The increasing trend in soil (0-23 cm) U concentrations on plots receiving P fertilizers on Broadbalk and Park Grass appear to be ongoing; increases were 7.8 µg U kg^{-1} yr^{-1} on Park Grass, and 3.4 µg kg^{-1} yr^{-1} on Broadbalk. Fertilizer derived U is most likely accumulated in the topsoil (0-23 cm) and in the acid extractable fraction of soil. No lime effects on U accumulation are observed in Park Grass. According to the observation from Rothamsted Experiment Station, it is estimated that the inputs are about 7 g U ha^{-1} yr^{-1} in the UK agricultural soils.

Appendix D

$\delta^{18}O_p$ in mineral phosphorus fertilizers

APPENDIX D

Table D-1. Uranium concentrations and $\delta^{18}O_p$ values in mineral P-fertilizers

Typ / Description	Manufacturer	U (mg kg^{-1})[a]	P (g kg^{-1})[b]	P_2O_5 %	$\delta^{18}O_p$ (‰VSMOW)	U/P_2O_5 (10^{-4})
Superphosphate, 18%	BASF	87.2	86.8	19.9	20.1	4.4
Superphosphate, 18%	BASF	81.9	87.6	20.1	20.9	4.1
PK-fertilizer, 0-16-16	BASF	60.4	72.5	16.6	19.6	3.6
NP-fertilizer, 20-20-0	BASF	82.9	85.0	19.5	21.4	4.3
NPK-fertilizer; 12-19-4	BASF	44.3	56.1	12.9	19.9	3.4
NPK-fertilizer	BASF	43.4	37.6	8.6	21.3	5.0
NPK-fertilizer	BASF	41.8	37.2	8.5	21.4	4.9
NPK-fertilizer	BASF	47.6	55.4	12.7	20.9	3.7
NPK-fertilizer	BASF	42.0	51.2	11.7	21.0	3.6
NPK-fertilizer, 15-15-15	BASF	31.6	64.2	14.7	18.5	2.1
NPK-fertilizer	BASF	36.1	35.7	8.2	21.7	4.4
NPK-fertilizer, 15-15-15	BASF	55.7	63.5	14.6	20.9	3.8
NPK-fertilizer, 24-8-8	BASF	27.5	34.2	7.8	20.4	3.5
NPK-fertilizer w/ Mg, 16-8-12-5, w/ B, Mn and Cu	BASF	28.0	33.9	7.8	23.5	3.6
NPK-fertilizer w/ Mg, 15-9-15-2	BASF	35.2	38.1	8.7	20.8	4.0
NPK-fertilizer w/ S, 13-13-21-2	BASF	50.4	55.1	12.6	21.1	4.0
NPK-fertilizer w/ Mg & S; 13-9-16-4-3	BASF	31.1	36.9	8.4	20.8	3.7
Rohphosphat normal (Pebble-Phosphat)	BASF	159.0	146.1	33.5	21.2	4.7
Partially digested rock phosphate	BASF	106.0	104.6	24.0	19.9	4.4
Mg-Novaphos 17-7	S.I. Düngephosphate	90.2	77.4	17.7	19.9	5.1
PK-organic fertilizer; 0-16-16	S.I. Düngephosphate	78.8	70.3	16.1	19.6	4.9
PK-organic fertilizer; 0-15-20	S.I. Düngephosphate	70.5	66.6	15.3	19.2	4.6
PK-fertilizer, 0-16-16	S.I. Düngephosphate	78.8	70.3	16.1	21.1	4.9
NP-fertilizer, 20-20-0	Ruhr-Stickstoff	33.7	88.7	20.3	16.4	1.7
NPK-fertilizer, 13-13-21	Ruhr-Stickstoff	12.5	55.1	12.6	12.7	1.0
NP-fertilizer, 11-52-0	Guano-Werke	187.0	229.0	52.5	20.8	3.6
NPK-fertilizer, 15-15-15	Guano-Werke	49.5	64.5	14.8	20.3	3.4
NPK-fertilizer, 10-15-20	Guano-Werke	55.0	67.7	15.5	20.6	3.5
NPK-fertilizer, 6-12-18	Guano-Werke	39.4	55.0	12.6	21.2	3.1
NP-fertilizer	Höchst	43.2	114.4	26.2	21.2	1.6
NPK-fertilizer, 13-13-21	Hochst	39.1	43.7	10.0	19.1	3.9

a and b: data of U and P concentrations in P fertilizers are from Sattouf (2007).

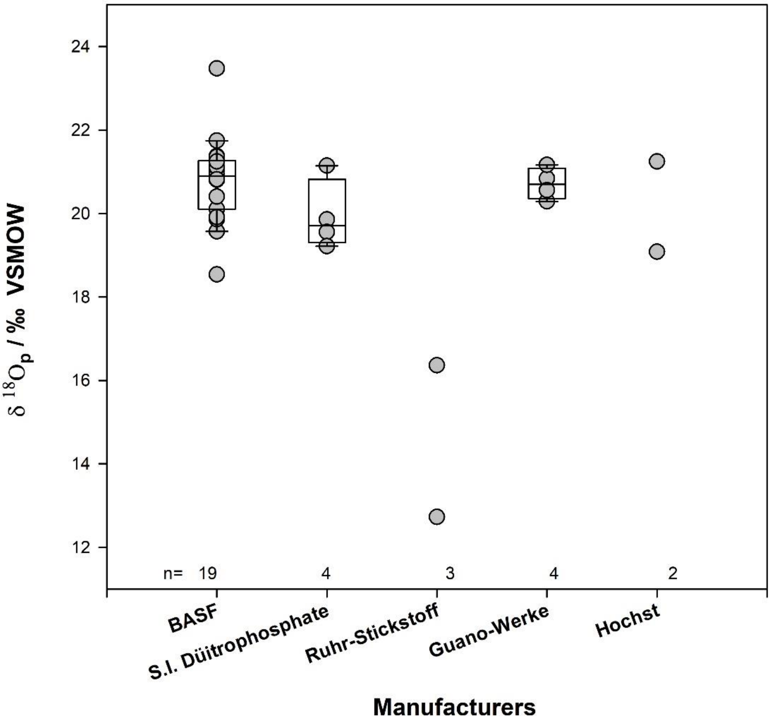

Figure D-1. $\delta^{18}O_p$ values in mineral P-fertilizers from four manufacturers.

APPENDIX D

References

REFERENCES

Agency for Toxic Substances and Disease Registry, U.S., (ATSDR), 2013. Toxicological Profile for Uranium. Department of Health and Human Services, Public Health Services, Atlanta, Georgia. http://www.atsdr.cdc.gov/toxprofiles/tp.asp?id=440&tid=77, accessed 24 Feb. 2020.

Altschuler, Z. S., 1958. Geochemistry of uranium in apatite and phosphorite. US Geological Survey. 314-D: 45–90.

Altschuler, Z. S., 1980. The geochemistry of trace elements in marine phosphorites: Part I. Characteristic abundances and enrichment. The Society of Economic Paleontologists and Mineralogist Special Publication, 29: 19–30.

Amelung, W., Antar, P., Kleeberg, I., Oelmann, Y., Luecke, A., Alt, F., Lewandowski, H., Pätzold, S. and Barej, J., 2015. The $\delta^{18}O$ signatures of HCl-extractable soil phosphates: methodological challenges and evidence of the cycling of biological P in arable soil. European Journal of Soil Science, 66 (6): 965-972.

Aubert, D., Probst, A. and Stille, P., 2004. Distribution and origin of major and trace elements (particularly REE, U and Th) into labile and residual phases in an acid soil profile (Vosges Mountains, France). Applied Geochemistry, 19(6): 899-916.

Avital, Y., Starinsky, A. and Kolodny, Y., 1983. Uranium geochemistry and fission-track mapping of phosphorites, Zefa field, Israel. Economic Geology, 78(1): 121-131.

Azouazi, M., Ouahidi, Y., Fakhi, S., Andres, Y., Abbe, J. C. and Benmansour, M., 2001. Natural radioactivity in phosphates, phosphogypsum and natural waters in Morocco. Journal of Environmental Radioactivity, 54(2):231-242.

Bachmaf, S., Planer-Friedrich, B. and Merkel, B. J., 2008. Effect of sulfate, carbonate, and phosphate on the uranium (VI) sorption behavior onto bentonite. Radiochimica Acta, 96: 359-366.

Baize, D., and van Oort, F., 2014. Potentially harmful elements in forest soils. In: Bini C. and Bech J. (Eds) PHEs, environment and human health. Springer, Dordrecht, pp. 151-198.

Banerjee, D., Khan, M., Srivastava, N. and Saigal, G., 1982. Precambrian phosphorites in the Bijawar rocks of Hirapur-Bassia areas, sagar district, madhya pradesh, India. Mineralium Deposita, 17, 349-362.

Baturin, G. and Kochenov, A., 2001. Uranium in phosphorites. Lithology and Mineral Resources, 36(4): 303-321.

REFERENCES

Baturin, G., Merkulova, K. and Chalov, P., 1972. Radiometric evidence for recent formation of phosphatic nodules in marine shelf sediments. Marine Geology, 13: 37-41.

Bauke, S. L., von Sperber, C., Tamburini, F., Gocke, M., Honermeier, B., Schweitzer, K., Baumecker, M., Don, A., Sandhage-Hofmann, A. and Amelung, W., 2018. Subsoil phosphorus is affected by fertilization regime in long-term agricultural experimental trials. European Journal of Soil Science, 69(1): 103-112.

Bell, K. G., 1963. Uranium in carbonate rocks. United States Geological Survey Professional Paper, 474A, AI-A29.

Bigalke, M., Schwab, L., Rehmus, A., Tondo, P. and Flisch, M., 2018. Uranium in agricultural soils and drinking water wells on the Swiss Plateau. Environment Pollution, 233: 943-951.

Bigalke, M., Ulrich, A., Rehmus, A. and Keller, A., 2017. Accumulation of cadmium and uranium in arable soils in Switzerland. Environmental Pollution, 221: 85-93.

Birch, G., Thomson, J., McArthur, J. and Burnett, W., 1983. Pleistocene phosphorites off the west coast of South Africa. Nature, 302: 601.

Blake, L. and Goulding, K. W. T., 2002. Effects of atmospheric deposition, soil pH and acidification on heavy metal contents in soils and vegetation of semi-natural ecosystems at Rothamsted xperimental Station, UK. Plant and Soil, 240(2):235-251.

Blake, R. E., Chang, S.J. and Lepland, A., 2010. Phosphate oxygen isotopic evidence for a temperate and biologically active Archaean ocean. Nature, 464(7291): 1029.

Brookfield, M., Hemmings, D. and Van Straaten, P., 2009. Paleoenvironments and origin of the sedimentary phosphorites of the Napo Formation (Late Cretaceous, Oriente Basin, Ecuador). Journal of South American Earth Sciences, 28(2): 180-192.

Burnett, W. C. and Veeh, H. H., 1977. Uranium-series disequilibrium studies in phosphorite nodules from the west coast of South America. Geochimica et Cosmochimica Acta, 41(6):755-764.

Canadian Council of Ministers of the Environment (CCME), 2007. Canadian soil quality guidelines for uranium: environmental and human health. Available online: https:// www.ccme.ca/files/Resources/supporting_scientific_documents/uranium_ssd_soil_1.2.pdf. Accessed 13 Dec. 2019.

REFERENCES

Cevik, U., Baltas, H., Tabak, A. and Damla, N., 2010. Radiological and chemical assessment of phosphate rocks in some countries. Journal of Hazardous Materials, 182(1-3): 531-535.

Chase, C. G. and Perry, E. C., 1972. The oceans: growth and oxygen isotope evolution. Science, 177(4053): 992-994.

Chernoff, C. B. and Orris, G. J., 2002. Data set of world phosphate mines, deposits, and occurrences: Part A. geologic data; Part B. location and mineral economic data. 2002-156.

Christensen, B. T., Thomsen, I. K., and Eriksen, J., 2019. The Askov long-term experiments: 1894-2019 – A unique research platform turns 125 years. DCA Report No. 151, Aarhus University – Danish Centre for Food and Agriculture, Tjele, Denmark.

Cook, P. J., 1972. Petrology and geochemistry of the phosphate deposits of northwest Queensland, Australia. Economic Geology, 67, 1193-1213.

Cook, P. J. and Shergold, J. H., 2005. Phosphate Deposits of the World: Volume 1: Proterozoic and Cambrian Phosphorites. Cambridge University Press.

Cook, P. J., 1984. Spatial and temporal controls on the formation of phosphate deposits-a review, Phosphate minerals. Springer, pp. 242-274.

Cook, P., O'Brien, G., Burnett, W. and Riggs. S., 1990. Neogene to Holocene phosphorites of Australia. In: Burnett, W.C. and Riggs, S.R. (Eds). Phosphate Deposits of the World, Cambridge University Press, Cambridge, pp. 98-115.

Cumberland, S. A., Douglas, G., Grice, K. and Moreau, J. W., 2016. Uranium mobility in organic matter-rich sediments: A review of geological and geochemical processes. Earth-Science Reviews, 159: 160-185.

Cuney, M., 2010. Evolution of uranium fractionation processes through time: driving the secular variation of uranium deposit types. Economic Geology, 105(3): 553-569.

Dall'Aglio M., 1971. Study of circulation of uranium in the supergene environment in the Italian alpine range. Geochimica et Cosmochimica Acta. 35: 47-59.

Dar, S. A., Khan, K. F., Khan, S. A., Mir, A. R., Wani, H. and Balaram, V., 2014. Uranium (U) concentration and its genetic significance in the phosphorites of the Paleoproterozoic Bijawar Group of the Lalitpur district, Uttar Pradesh, India. Arabian Journal of Geosciences, 7(6): 2237–2248.

de Ridder, M., de Jong, S., Polchar, J. and Lingemann, S., 2012. Risks and Opportunities in the Global Phosphate. The Hague Centre for Strategic Studies. ISBN/EAN: 978-94-91040-69-6.

Delijska, A., Blazheva, T., Petkova, L. and Dimov, L., 1988. Fusion with lithium borate as sample preparation for ICP and AAS analysis. Analytical and Bioanalytical Chemistry, 332: 362–365.

Dissanayake, C. B. and Chandrajith, R., 2009. Phosphate mineral fertilizers, trace metals and human health. Journal of the National Science Foundation of Sri Lanka, 37(3): 153-165.

Driessen, P., Deckers, J., Spaargaren, O. and Nachtergaele, F., 2000. Lecture notes on the major soils of the world. Food and Agriculture Organization (FAO).

Dutton, A., Wilkinson, B. H., Welker, J. M., Bowen, G. J. and Lohmann, K. C., 2005. Spatial distribution and seasonal variation in $^{18}O/^{16}O$ of modern precipitation and river water across the conterminous USA. An International Journal,19(20): 4121-4146.

Echevarria, G., Sheppard, M. I., and Morel, J., 2001. Effect of pH on the sorption of uranium in soils. Journal of Environmental Radioactivity, 53(2): 257-264.

Envrionmental Protection Agency (EPA), 1999. Understanding variation in partitioning coefficients, Kd, values: Volume II: Review of geochemistry and available Kd values for cadmium, caesium, chromium, lead, plutonium, radon, strontium, thorium, tritium and uranium. US-EPA, Office of Air and Radiation, Washington, USA. EPA 402-R-99-004B.

Eskilsson, C. S. and Björklund, E., 2000. Analytical-scale microwave-assisted extraction. Journal of Chromatography A, 902(1): 227-250.

European Food Safety Authority (EFSA), 2009. Scientific Opinion of the Panel on Contaminants in the Food Chain on a request from German Federal Institute for Risk Assessment (BfR) on uranium in foodstuff, in particular mineral water. European Food Safety Authority. The Food Safety Authority Journal,1018: 1-59. http://www.efsa.europa.eu/de/efsajournal/doc/1018.pdf, accessed 22 Feb. 2020.

European Parliament (EP), Council of the European Union (EU), 2019. Regulation (EU) 2019/1009 of the European Parliament and of the Council of 5 June 2019, laying down rules on the making available on the market of EU fertilizing products and amending regulations (EC) No 1069/2009 and (EC) No 1107/2009 and repealing regulation (EC) No 2003/2003. Available online: https://eur-lex.europa.eu/legalcontent/EN/TXT/PDF/?uri=CELEX:32019R1009&from=EN. Accessed 13 Dec. 2019.

Fayek, M., Horita, J. and Ripley, E. M., 2011. The oxygen isotopic composition of uranium minerals: A review. Ore Geology Reviews, 41(1):1-21.

Filgueiras, A. V., Lavilla, I. and Bendicho, C., 2002. Chemical sequential extraction for metal partitioning in environmental solid samples. Journal of Environmental Monitoring, 4(6): 823-857.

Föllmi, K., 1996. The phosphorus cycle, phosphogenesis and marine phosphate-rich deposits. Earth-Science Reviews, 40(1-2): 55-124.

Giammar, D., 2001. Geochemistry of uranium at mineral-water interfaces: rates of sorption-desorption and dissolution-precipitation reactions. California Institute of Technology.

Giblin, A. M., Batts, B. D. and Swaine, D. J., 1981. Laboratory simulation studies of uranium mobility in natural waters. Geochimica Cosmochimica Acta, 45: 699–709.

Goulding, K. W. T., Poulton, P. R., Webster, C. P. and Howe, M. T., 2000. Nitrate leaching from the Broadbalk Wheat Experiment, Rothamsted, UK, as influenced by fertilizer and manure inputs and the weather. Soil Use and Management, 16(4):244-250.

Gudmundsson, Th., Gudmundsson S. Th. and Thorvaldsson, G., 2014. Soil phosphorus fractionation in Icelandic long-term grassland field experiments. Iceland Agricultural Science, 27: 81-94.

Gudmundsson, Th., Þorvaldsson G. and Björnsson, H., 2011. Langtímaáhrif áburðar á jarðveg og uppskeru á Geitasandi ‘Long term effects of fertilisers on soils and yield at Geitasandur’, 35: 79.

Guillaumont, R. and Mompean, F. J., 2003. Update on the chemical thermodynamics of uranium, neptunium, plutonium, americium and technetium, Amsterdam, Elsevier, 5: 64-70.

Haneklaus, N., Sun, Y., Bol, R., Lottermoser, B. and Schnug, E., 2017. To extract, or not to extract uranium from phosphate rock, that is the Question. Environmental Science &Technology, 753-754.

He, G., and Zhou, Y., 2015. Geology of phosphate rock in china: distribution, rock type and metallogenic perspective. Global Environmental Research, 19, 91-96.

Helfenstein, J., Tamburini, F., von Sperber, C., Massey, M.S., Pistocchi, C., Chadwick, O. A., Vitousek, P.M., Kretzschmar, R. and Frossard, E., 2018. Combining spectroscopic and isotopic techniques gives a dynamic view of phosphorus cycling in soil. Nature communications, 9(1): 3226.

Hendricks, S. and Hill, W., 1950. The nature of bone and phosphate rock. Proceedings of the National Academy of Sciences, 36(12): 731-737.

Herring, J. S., 2013. Uranium and thorium resources. In: Tsoulfanidis, N. (Ed.), Nuclear Energy. Springer, New York, pp. 463–490.

Hodell, D. A., Mueller, P. A. and Garrido, J. R., 1991. Variations in the strontium isotopic composition of seawater during the Neogene. Geology, 19: 24-27.

Holland, H. D., 1984. The chemical evolution of the atmosphere and oceans. Princeton University Press.

Howard, P. and Hough, M., 1979. On the geochemistry and origin of the D Tree, Wonarah and Sherrin Creek phosphorite deposits of the Georgina Basin, northern Australia. Economic Geology, 74: 260-284.

Hren, M., Tice, M. and Chamberlain, C., 2009. Oxygen and hydrogen isotope evidence for a temperate climate 3.42 billion years ago. Nature, 462(7270): 205.

Hu, Z. and Gao, S., 2008. Upper crustal abundances of trace elements: a revision and update. Chemical Geology, 253: 205–221.

Huhle, B., Kummer, S. and Merkel, B., 2008. Mobility of uranium from phosphate fertilizers in sandy soils. Loads and Fate of fertilizer-derived uranium. Backhuys Publishers, Leiden, pp.978-90.

Imas, P. and Lati, J., 2005. Uranium in soils, fertilizers and crops. ICL Fertilizers Israel.

International Atomic Energy Agency (IAEA), 2003. Extent of environmental contamination by naturally occurring radioactive material and technological options for mitigation, Technical reports series, No. 419, Vienna.

IUSS Working Group WRB, 2015. World Reference Base for Soil Resources 2014, update 2015, International soil classification system for naming soils and creating legends for soil maps. World Soil Resources Reports No.106. FAO, Rome.

Jaffrés, J. B., Shields, G. A. and Wallmann, K., 2007. The oxygen isotope evolution of seawater: A critical review of a long-standing controversy and an improved geological water cycle model for the past 3.4 billion years. Earth-Science Reviews, 83(1-2): 83-122.

Jaisi, D. P. and Blake, R. E., 2014. Advances in using oxygen isotope ratios of phosphate to understand phosphorus cycling in the environment. Advances in Agronomy, 125:1-53.

Jallad, I. S., Abu Murry, O. S. and Sadaqah, R. M., 1989, Upper Cretaceous phosphorites of Jordan, In: Notholt, A. J. G, Sheldon R. P. and Davidson, D. F. (Eds.) Phosphate Deposit of the World, Vol. 2, Phosphate Rock Resources, Cambridge Univ. Press, pp. 344-351.

Jarvis, I., 1995. Phosphorite geochemistry: state-of-the-art and environmental concerns. Oceanographic Literature Review, 8: 639.

Jones, R. L., 1992. Uranium and phosphorus contents in Morrow plot soils over 82 years. Communications in Soil Science and Plant Analysis, 23(1-2): 67-73.

Kabata-Pendias A and Pendias H., 2001. Trace elements in soils and plants. Boca Raton, FL: CRC Press. pp. 214.

Kastner, M., Garrison, R., Kolodny, Y., Reimers, C. and Shemesh, A., 1990. Coupled changes of oxygen isotopes in PO_4^{3-} and CO_3^{2+} in apatite, with emphasis on the Monterey Formation, California. In: Riggs S.R., Burnett W.C. (Eds.), Phosphate Deposits of the World: Vol. 3, Genesis of Neogene to Modern Phosphorites, Cambridge Univ. Press, pp. 312-324

Keith, S., Faroon, O., Roney, N., Scinicariello, F., Wilbur, S., Ingerman, L., Llados, F., Plewak, D., Wohlers, D. and Diamond, G., 2013. Toxicological profile for uranium. Agency for Toxic Substances and Disease Registry (US), pp. 39-175.

Khater, A. E. M., Galmed, M. A., Nasr, M. M. and El-Taher, A., 2016. Uranium and rare earth elements in Hazm El-Jalamid phosphate, Saudi Arabia: concentrations and geochemical patterns comparison. Environmental Earth Sciences, 75:1261.

Knauth, L. P. and Lowe, D. R., 2003. High Archean climatic temperature inferred from oxygen isotope geochemistry of cherts in the 3.5 Ga Swaziland Supergroup, South Africa. Geological Society of America Bulletin, 115(5): 566-580.

Knauth, L. P. and Epstein, S., 1976. Hydrogen and oxygen isotope ratios in nodular and bedded cherts. Geochimica et Cosmochimica Acta, 40(9): 1095-1108.

Kolodny, Y. and Luz, B., 1992. Isotope signatures in phosphate deposits: Formation and diagenetic history, Isotopic signatures and sedimentary records. In: Clauer N., Chaudhuri S. (Eds.), Lecture Notes in Earth Sciences, Springer, pp. 69-121.

Kolodny, Y., and Kaplan, I. R., 1970. Uranium isotopes in sea-floor phosphorites. Geochimica et Cosmochimica Acta, 34(1):3-24.

Kolodny, Y., Luz, B. and Navon, O., 1983. Oxygen isotope variations in phosphate of biogenic apatites, I. Fish bone apatite-rechecking the rules of the game. Earth and Planetary Science Letters, 64: 398-404.

Kratz, S. and Schnug, E., 2006. Rock phosphates and P fertilizers as sources of U contamination in agricultural soils, In: Merkel B.J., Hasche-Berger A. (Eds), Uranium in the Environment. Springer, Berlin, pp. 57-67.

Kratz, S., Fleckenstein, J. and Schnug, E., 2004. Uran in P-haltigen Mineraldüngern (Uranium in mineral P fertilizers). Federal Agricultural Research Centre (FAL): Annual Report 2004, pp. 22-23. Available online: https://d-nb.info/1010831046/34. Accessed 19 June 2019.

Kratz, S., Knappe, F., Rogasik, J. and Schnug, E., 2008. Uranium balances in agroecosystems, In de Kok. L. J. and Schnug, E. (Eds.), Loads and Fate of Fertilizer-derived Uranium. Backhuys Publishers, Leiden, pp. 179-190.

Kratz, S., Schick, J. and Schnug, E., 2016. Trace elements in rock phosphates and P containing mineral and organo-mineral fertilizers sold in Germany. Science of the Total Environment, 542: 1013-1019.

Kress, A. and Veeh, H., 1980. Geochemistry and radiometric ages of phosphatic nodules from the continental margin of northern New South Wales, Australia. Marine Geology, 36: 143-157.

Kusakabe, M. and Matsubaya, O., 1986. Volatiles in Magmas, volcanic gases, and thermal waters. Bull. Volcanol. Soc. Japan Spec. Issue 30, 267-283 (in Japanese with English abstract).

Lamas, M., 2005. Factors affecting the availability of uranium in soils. Landbauforschung Völkenrode Sonderheft 278, Braunschweig.

Land, L. S. and Lynch, F. L.,1996. $\delta^{18}O$ values of mudrocks: more evidence for an ^{18}O-buffered ocean. Geochimica et Cosmochimica Acta, 60(17): 3347-3352.

Langmuir, D.,1978. Uranium solution-mineral equilibria at low temperatures with applications to sedimentary ore deposits. Geochimica et Cosmochimica Acta, 42(6): 547-569.

Lecuyer, C., Grandjean, P. and Sheppard, S. M., 1999. Oxygen isotope exchange between dissolved phosphate and water at temperatures ≤135 °C: inorganic versus biological fractionations. Geochimica et Cosmochimica Acta, 63(6): 855-862.

Levina, S. D., Smilkstyn, A. O. and Karpov, L. N., Radioactivity of Phosphorites, Litologiya fosforitonosnykh otlozhenii (Lithology of Phosphorite-Bearing Sediments), In: Sokolova, A.S. (Eds), Moscow, Nauka, 1976, pp. 148–155.

Liesch, T., Hinrichsen, S. and Goldscheider, N., 2015. Uranium in groundwater—fertilizers versus geogenic sources. Science of the Total Environment, 536: 981-995.

Longinelli, A. and Nuti, S., 1968. Oxygen-isotope ratios in phosphate from fossil marine organisms. Science, 160(3830): 879-882.

Longinelli, A. and Nuti, S., 1973. Revised phosphate-water isotopic temperature scale. Earth and Planetary Science Letters, 19(3): 373-376.

Lottermoser, B., 2009. Trace metal enrichment in sugarcane soils due to the long-term application of fertilisers, North Queensland, Australia: geochemical and Pb, Sr, and U isotopic compositions. Australian Journal of Soil Research, 47: 1-10.

Lucas, J. and Abbas, M., 1989. Uranium in natural phosphorites: the Syrian example. L'uranium dans les phosphorites naturelles: l'exemple syrien. Sciences Géologiques, bulletins et mémoires, 42(3): 223-236. In: Lucas, J., Cook, J. P and Prevot, L. (Eds.), Sciences Géologiques. Bulletin, pp. 223-236.

Macdonald, A. J., Poulton, P. R., Clark, I. M., Scott, T., Glendining, M. J., Perryman, S. A. M., Storkey, J., Bell, J., Shield, I., McMillan, V. and Hawkins, J., 2018. Guide to the Classicals and other Long-term experiments, Datasets and Sample Archive. Rothamsted Research, Harpenden, Herts (ISBN 978-1-9996750-0-4; www.rothamsted.ac.uk), pp. 1-57.

Makarov, E. A., 1963. Crystal chemistry of uranium minerals. In: Vinogradov, A. P. (Eds.), Basic Features of Uranium Behaviour. Moscow, AN SSSR, pp. 27-45 (in Russian).

McArthur, J., Sahami, A., Thirlwall, M., Hamilton, P. and Osborn, A., 1990. Dating phosphogenesis with strontium isotopes. Geochimica et Cosmochimica Acta, 54:1343-1351.

McDowell, R., 2012. The rate of accumulation of cadmium and uranium in a long-term grazed pasture: implications for soil quality. New Zealand Journal of Agricultural Research, 55(2): 133-146.

McKelvey, V. E., 1967. Phosphate deposits, U.S. Geological Survey Bulletin, 1252-D, pp. 1-22.

McManus, J., Berelson, W. M., Klinkhammer, G. P., Hammond, D. E. and Holm, C., 2005. Authigenic uranium: relationship to oxygen penetration depth and organic carbon rain. Geochimica et Cosmochimica Acta, 69(1): 95-108.

Menzel, R. G., 1968. Uranium, radium, and thorium content in phosphate rocks and their possible radiation hazard. Journal of Agricultural and Food Chemistry, 16(2): 231-234.

Morrison, S. J., Spangler, R. R. and Tripathi, V. S., 1995. Adsorption of uranium (VI) on amourphous ferric oxyhydroxide at high contrations of dissolved carbon (IV) and sulfur (VI). Journal of Contaminant Hydrology, 17: 333-346.

Muehlenbachs, K., 1998. The oxygen isotopic composition of the oceans, sediments and the seafloor. Chemical Geology, 145(3): 263-273.

National Council on Radiation Protection and Measurements (NCRP), 1984. Exposures from the uranium series with emphasis on radon and its daughter. Protection and Measurements. National Council on Radiation Protection and Measurements, Bethesda, MD. Report No. 77, 56-68.

National Research Council (NRC), 2012. Uranium occurrences, resources, and markets. Uranium mining in Virginia: scientific, technical, environmental, human health and safety, and regulatory aspects of uranium mining and processing in Virginia. Washington, DC: The National Academies Press.

Notholt, A. J. G., 1986. Phosphate Deposits of the World: Volume 3, Neogene to Modern Phosphorites, 156. Cambridge University Press.

Nziguheba, G., and Smolders, E., 2008. Inputs of trace elements in agricultural soils via phosphate fertilizers in European countries. Science of the Total Environment, 390(1): 53-57.

Obersteiner, M., Peñuelas, J., Ciais, P., Van Der Velde, M. and Janssens, I. A., 2013. The phosphorus trilemma. Nature Geoscience, 6(11): 897.

Papastefanou, C., Stoulos, S., Ioannidou, A. and Manolopoulou, M., 2006. The application of phosphogypsum in agriculture and the radiological impact. Journal of Environmental Radioactivity, 89(2):188-198.

Parker, H. 1984. Tennessee Valley Authority National Fertilizer Development Center progress 83 (No. TVA/OACD-84/4). Muscle Shoals, AL (USA). Office of Agricultural and Chemical Development.

Partin, C. A., Bekker, A., Planavsky, N. J., Scott, C. T., Gill, B. C., Li, C. and Love, G. D., 2013. Large-scale fluctuations in Precambrian atmospheric and oceanic oxygen levels from the record of U in shales. Earth and Planetary Science Letters, 369: 284-293.

Pätzold, S., Hejcman, M., Barej, J., Schellberg, J., 2013. Soil phosphorus fractions after seven decades of fertilizer application in the Rengen Grassland Experiment. Journal of Plant Nutrition and Soil Science, 176(6): 910-920.

Peterman, Z. E., 1979. Strontium isotope geochemistry of late Archean to late Cretaceous tonalites and trondhjemites. Developments in Petrology, 6: 133-147.

Petr, P., 2016. Phosphate Rocks, apatites and their synthetic analogues- synthesis, structure, properties and applications, IntechOpen, pp. 335.

Piper, D. Z. and Kolodny, Y., 1987. The stable isotopic composition of a phosphorite deposit: $\delta^{13}C$, $\delta^{34}S$, and $\delta^{18}O$. Deep Sea Research Part A. Oceanographic Research Papers, 34(5-6):897-911.

Pokryshkin, V. I., 1981. Regularities of the Localization of Precambrian and Phanerozoic Commercial-Grade Phosphorite Deposits in the World, Moscow: Nedra.

Pufahl, P. K. and Groat, L. A., 2017. Sedimentary and Igneous Phosphate Deposits: Formation and Exploration: An Invited Paper. Economic Geology, 112(3): 483-516.

Rafsanjani, M. H., Kratz, S., Fleckenstein, J. and Schnug, E., 2008. Solubility of uranium in fertilizers. Agricuture and Forestry Research, 58:231-234.

Rao, C. R. M., Sahuquillo, A. and Lopez Sanchez, J. F., 2008. A review of the different methods applied in environmental geochemistry for single and sequential extraction of trace elements in soils and related materials. Water, Air, and Soil Pollution,189(1-4): 291-333.

Rapin, F., Tessler, A., Campbell, P. G. C and Carignan, R., 1986. Potential artifacts in the determination of metal partitioning in sediments by a sequential extraction procedure, Environmental Science and Technology, 20(8): 836–840.

Regenspurg, S., Margot-Roquier, C., Harfouche, M., Froidevaux, P., Steinmann, P., Junier, P. and Bernier-Latmani, R., 2010. Speciation of naturally-accumulated uranium in an organic-rich soil of an alpine region (Switzerland). Geochimica et Cosmochimica Acta, 74(7): 2082-2098.

Riedel, T. and Kübeck, C., 2018. Uranium in groundwater-a synopsis based on a large hydrogeochemical dataset. Water Research, 129: 29-38.

Robert, F. and Chaussidon, M., 2006. A palaeotemperature curve for the Precambrian oceans based on silicon isotopes in cherts. Nature, 443(7114): 969.

Rogasik, J., Kratz, S., Funder, U., Panten, K., Barkusky, D., Baumecker, M., Gutser, R., Lausen, P., Scherer, H., Schmidt, L. and Schnug, E., 2008. Uranium in soils of German long-term fertilizer experiments, In: de Kok. L. J. and Schnug, E. (Eds.), Loads and Fate of Fertilizer-derived Uranium. Backhuys Publishers, Leiden, pp. 135-146.

Roth, N. and FitzGerald, R., 2015. Human and environmental impact of uranium derived from mineral phosphate fertilizers. Swiss Center for Applied Human Toxicology (SCAHT) report for Swiss Federal Office for Agriculture (BLW).

Rothbaum, H., McGaveston, D., Wall, T., Johnston, A. and Mattingly, G., 1979. Uranium accumulation in soils from long-continued applications of superphosphate. Journal of Soil Science, 30(1): 147-153.

Salmanzadeh, M., Schipper, L. A., Balks, M. R., Hartland, A., Mudge, P. L. and Littler, R., 2017. The effect of irrigation on cadmium, uranium, and phosphorus contents in agricultural soils. Agriculture, Ecosystems & Environment, 247:84-90.

Sastre, J., Sahuquillo, A., Vidal, M. and Rauret, G., 2002. Determination of Cd, Cu, Pb and Zn in environmental samples: microwave-assisted total digestion versus aqua regia and nitric acid extraction. Analytica Chimica Acta, 462(1): 59-72.

Sattouf, M., 2007. Identifying the origin of rock phosphates and phosphorous fertilizsers using isotope ratio techniques and heavy metal patterns. Landbauforschung Völkenrode Special Issue 311, Braunschweig.

Sattouf, M., Kratz, S., Diemer, K., Fleckenstein, J., Rienitz, D., Schiel, D. and Schnug, E., 2008. Significance of uranium and strontium isotope ratios for retracing the fate of uranium during the processing of phosphate fertilizers from rock phosphates. In: De Kok, L. J. and Schnug, E. (Eds). Loads and Fate of fertilizer-derived uranium. Backhuys Publishers, Leiden. pp: 978-90.

Sattouf, M., Kratz, S., Diemer, K., Rienitz, O., Fleckenstein, J., Schiel, D. and Schnug, E., 2007. Identifying the origin of rock phosphates and phosphorus fertilizers through high precision measurement of the strontium isotopes ^{87}Sr and ^{86}Sr. Landbauforschung Völkenrode, 57: 1-11.

Schellberg, J., Möseler, B. M., Kühbauch, W. and Rademacher, I. F., 1999. Long-term effects of fertilizer on soil nutrient concentration, yield, forage quality and floristic composition of a hay meadow in the Eifel mountains, Germany. Grass and Forage Science, 54(3): 195-207.

Schipper, L. A., Sparling, G. P., Fisk, L., Dodd, M., Power, I. and Littler, R. A., 2011. Rates of accumulation of cadmium and uranium in a New Zealand hill farm soil as a result of long-term use of phosphate fertilizer. Agriculture, Ecosystems & Environment, 144(1): 95-101.

Schnug, E. and Haneklaus, N., 2015. Uranium in phosphate fertilizers–review and outlook, In: Merkel B., Arab A. (Eds). Uranium-Past and Future Challenges. Springer, pp. 123-130.

Schnug, E. and Lottermoser, B. G., 2013. Fertilizer-derived uranium and its threat to human health. Environmental Science & Technology, 47, (6): 2433-2434.

Schnug, E., Haneklaus, S., Schnier, C. and Scholten, L., 1996. Issues of natural radioactivity in phosphates. Communications in Soil Science and Plant Analysis, 27(3-4): 829-841.

Shemesh, A., Kolodny, Y. and Luz, B., 1983. Oxygen isotope variations in phosphate of biogenic apatites, II. Phosphorite rocks. Earth and Planetary Science Letters, 64(3): 405-416.

Shemesh, A., Kolodny, Y. and Luz, B., 1988. Isotope geochemistry of oxygen and carbon in phosphate and carbonate of phosphorite francolite. Geochimica et Cosmochimica Acta, 52: 2565-2572.

Shepherd, T. J., Rankin, A. H. and Alderton, D. H., 1985. A practical guide to fluid inclusion studies. Blackie.

Sheppard, S. and Evenden, W., 1988. Critical compilation and review of plant/soil concentration ratios for uranium, thorium and lead. Journal of Environmental Radioactivity, 8(3): 255-285.

Silvertown, J., Poulton, P., Johnston, E., Edwards, G., Heard, M. and Biss, P. M., 2006. The Park Grass Experiment 1856-2006: its contribution to ecology. Journal of Ecology, 94(4):801-814.

Smidt G. A., Hassoun, R., Erdinger, L., Schäf, M., Knolle, F., Utermann, J., Duijnisveld, W. H., Birke, M. and Schnug, E., 2011. Uranium in German tap and groundwater – occurrence and origins. In: Merkel B., Schipek M. (Eds), The New Uranium Mining Boom. Springer, Berlin, pp. 807-820.

Smolders, E., 2017. Scientific aspects underlying the regulatory framework in the area of fertilisers–state of play and future reforms. European Union, IP/A/IMCO/2016-19-PE 595.354.

Sokolov, A., 1996. Evolution of the uranium potential of phosphorites. Geokhimiya, 1117-1119.

Stephens, N. P. and Carroll, A. R., 1999. Salinity stratification in the Permian Phosphoria sea; a proposed paleoceanographic model. Geology, 27(10): 899-902.

Stojanovic, M., Popic, J. M., Stevanovic, D., Martinovic, L., 2006. Phosphorus fertilizers as a source of uranium in Serbian soils. Agronomy for Sustainable Development, 26(3): 179-183.

Sun, Y., Amelung, W., Wu, B., Haneklaus, S., Maekawa, M., Lücke, A., Schnug, E. and Bol, R., 2019. 'Co-evolution' of uranium concentration and oxygen stable isotope in phosphate rocks. Applied Geochemistry, 104476.

Syers, J. K., Mackay, A. D., Brown, M. W. and Currie, L. D., 1986. Chemical and physical characteristics of phosphate rock materials of varying reactivity. Journal of the Science of Food and Agriculture, 37(11): 1057-1064.

Takeda, A., Tsukada, H., Takaku, Y., Hisamatsu, S. I. and Nanzyo, M., 2006. Accumulation of uranium derived from long-term fertilizer applications in a cultivated Andisol. Science of the Total Environment, 367(2-3): 924-931.

Tamburini, F., Bernasconi, S. M., Angert, A., Weiner, T. and Frossard, E. 2010. A method for the analysis of the δ^{18}O of inorganic phosphate extracted from soils with HCl. European Journal of Soil Science, 61(6): 1025-1032.

Tamburini, F., Pfahler, V., B nemann, E. K., Guelland, K., Bernasconi, S. M. and Frossard, E., 2012. Oxygen isotopes unravel the role of microorganisms in phosphate cycling in soils. Environmental Science & Technology, 46(11): 5956-5962.

Tang, C., Shindo, S. and Machida, I., 1998. Topographical effects on the distributions of rainfall and ^{18}O distributions: a case in Miyake Island, Japan. Hydrological processes, 12(4): 673-682.

Taylor, H. P., 1968. The oxygen isotope geochemistry of igneous rocks. Contributions to Mineralogy and Petrology, 19(1): 1-71.

Taylor, J. H. P. and Epstein, S., 1962. Relationship between ^{18}O/^{16}O ratios in coexisting minerals of igneous and metamorphic rocks: part 1: principles and experimental results. Geological Society of America Bulletin, 73(4): 461-480.

Taylor, M. and Kim, N., 2008. The fate of uranium contaminants of phosphate fertilizer. In: de Kok. L. J. and Schnug, E. (Eds.), Loads and Fate of Fertilizer-derived Uranium. Backhuys Publishers, Leiden, pp.147-155.

Taylor, M., Kratz, S., Schick, J., Schnug, E. and Smidt, G., 2014. Comparing trace element concentrations in inorganic and organic fertilizers (Conference Paper). New Zealand Soil Science Society conference “Soil science for future generations”, at Hamilton, New Zealand.

Taylor, M. D., 2007. Accumulation of uranium in soils from impurities in phosphate fertilizers. Landbauforschung Völkenrode, 57(2): 133.

Tessier, A., Campbell, P. G. and Bisson, M., 1979. Sequential extraction procedure for the speciation of particulate trace metals. Analytical Chemistry, 51(7): 844-851.

Tulsidas, H., Gabriel, S., Kiegiel, K., Haneklaus, N., 2019. Uranium resources in EU phosphate rock imports. Resources Policy, 61: 151-156.

Tunney, H., Stojanović, M., Mrdaković Popić, J., McGrath, D. and Zhang, C., 2009. Relationship of soil phosphorus with uranium in grassland mineral soils in Ireland using soils from a long-term phosphorus experiment and a National Soil Database. Journal of Plant Nutrition and Soil Science, 172(3): 346-352.

Turner, D. and Whitfield, M., 1979. Control of seawater composition. Nature, 281: 468.

U.S. Geological Survey (USGS), 2018, Mineral commodity summaries 2018. U.S. Geological Survey, pp.200.

Ulrich, A. E., Schnug, E., Prasser, H. M. and Frossard, E., 2014. Uranium endowments in phosphate rock. Science of Total Environment, 478: 226-234.

United States Environmental Protection Agency (USEPA), 1994. method 3051, microwave-assisted acid digestion of sediments, sludges, soils and oils, Washington DC.

United States Nuclear Regulatory Commission (USNRC), 1992. A Summary of NRC's Interim Radiological Cleanup Criteria and Current Dose Bases. U.S. Nuclear Regulatory Commission, Washington.

Utermann, J. and Fuchs, M., 2008, Uranium in German soils. In: De Kok, L. J. and Schnug, E. (Eds). Loads and Fate of fertilizer-derived uranium. Backhuys Publishers, Leiden. pp: 978-90.

Van Kauwenbergh S. J., 2010. World phosphate rock reserves and resources. Muscle Shoals, IFDC.

Van Kauwenbergh, S. J., 1997. Cadmium and other minor elements in world resources of phosphate rock. The International Fertilizer Society Proceedings 400. York, UK: The International Fertilizer Society.

Vandenhove, H., Van Hees, M., Wouters, K. and Wannijn, J., 2007. Can we predict uranium bioavailability based on soil parameters? Part 1: Effect of soil parameters on soil solution uranium concentration. Environmental Pollution, 145(2): 587-595.

Volkov, R., 1994. Geochemistry of uranium in Vendian-Cambrian phosphorites. Geokhimiya, 7: 1042-1051.

Wakefield, Z. T., 1980. Distribution of cadmium and selected heavy metals in phosphate fertilizer processing. National Fertilizer Development Center, Tennessee Valley Authority.

Watts, C. W., Clark, L. J., Poulton, P. R., Powlson, D. S. and Whitmore, A. P., 2006. The role of clay, organic carbon and long-term management on mouldboard plough draught measured on the Broadbalk wheat experiment at Rothamsted. Soil Use and Management, 22(4):334-341.

Webeck, E., Matsubae, K., Nakajima, K., Nansai, K. and Nagasaka, T., 2015. Phosphorus Flows in the Asian Region. Global Environmental Research, 15: 9-17.

Western Sahara Resource Watch (WSRW) Report, P for plunder, 2019. ISBN: 978-82-93425-27-4.

Wetterlind, J., Richer De Forges, A., Nicoullaud, B. and Arrouays, D., 2012. Changes in uranium and thorium contents in topsoil after long-term phosphorus fertilizer application. Soil Use and Management, 28(1): 101-107.

Windmann, H., 2019. A contribution to the risk assessment of uranium contamination in the food chain through phosphate containing fertilizers, feed and food additives. PhD thesis, Technical University of Braunschweig.

World Health Organization (WHO), 2011. Guidelines for Drinking-Water Quality, Fourth Edition. Geneva, pp. 430-431. http://whqlibdoc.who.int/publications/2011/9789241548151_eng.pdf, accessed 21-02-2020

Xing, B. and Yeneman, P., 1998. Microwave digestion for analysis of metals in soil. Communications in Soil Science and Plant Analysis, 29: 7-8.

Yamaguchi, N., Kawasaki, A. and Iiyama, I., 2009. Distribution of uranium in soil components of agricultural fields after long-term application of phosphate fertilizers. Science of the Total Environment, 407(4): 1383-1390.

Zanin, Y. N., Zamirailova, A., Fomin, A., Gilinskaya, L. and Kireev, A., 2000. Uranium of sedimentary apatite in catagenesis. Geochemistry International, 38: 452-458.

Zanin, Yu. N., Gilinskaya, L. G., Krasil'nikova, N. A., Krivoputskaya, L. M., Mirtov, Yu. V. and Stolpovskaya, V. N., 1985. Calcium phosphates in phosphates of different types. International Geology Review, 27(10): 1212-1229.

Zielinski, R. A., Orem, W. H., Simmons, K. R. and Bohlen, P. J., 2006. Fertilizer-derived uranium and sulfur in Rangeland soil and runoff: A case study in central Florida. Water, Air, and Soil Pollution, 176(1): 163-183.

Band / Volume 514
Crystallisation of Oxidic Gasifier Slags
J. P. Schupsky (2020), III, 127, XXII pp
ISBN: 978-3-95806-506-2

Band / Volume 515
Modeling and validation of chemical vapor deposition for tungsten fiber reinforced tungsten
L. Raumann (2020), X, 98, XXXVIII pp
ISBN: 978-3-95806-507-9

Band / Volume 516
Zinc Oxide / Nanocrystalline Silicon Contacts for Silicon Heterojunction Solar Cells
H. Li (2020), VIII, 135 pp
ISBN: 978-3-95806-508-6

Band / Volume 517
Iron isotope fractionation in arable soil and graminaceous crops
Y. Xing (2020), X, 111 pp
ISBN: 978-3-95806-509-3

Band / Volume 518
Geophysics-based soil mapping for improved modelling of spatial variability in crop growth and yield
C. Brogi (2020), xxi, 127 pp
ISBN: 978-3-95806-510-9

Band / Volume 519
Measuring and modelling spatiotemporal changes in hydrological response after partial deforestation
I. Wiekenkamp (2020), xxxvii, 276 pp
ISBN: 978-3-95806-512-3

Band / Volume 520
Characterization of Root System Architectures from Field Root Sampling Methods
S. Morandage (2020), xxii, 157 pp
ISBN: 978-3-95806-511-6

Band / Volume 521
Generation Lulls from the Future Potential of Wind and Solar Energy in Europe
D. S. Ryberg (2020), xxvii, 398 pp
ISBN: 978-3-95806-513-0

Band / Volume 522
Towards a Generalized Framework for the Analysis of Solar Cell Performance based on the Principle of Detailed Balance
B. J. Blank (2020), iv, 142 pp
ISBN: 978-3-95806-514-7

Band / Volume 523
A Robust Design of a Renewable European Energy System Encompassing a Hydrogen Infrastructure
D. G. Çağlayan (2020), xxii, 312 pp
ISBN: 978-3-95806-516-1

Band / Volume 524
Control and Optimization of a Lorentz Force Based Actuator System for External Flow
M. F. Seidler (2020), xii, 136 pp
ISBN: 978-3-95806-518-5

Band / Volume 525
ETV Online Tagung 2020
Industrielle Groß- und Hochtemperaturwärmepumpen im Energiesystem
D. Stolten, G. Markowz (Hrsg.) (2020), ca. 71 pp
ISBN: 978-3-95806-519-2

Band / Volume 526
Atmospheric Trace Gas Measurements Using Chemical Ionisation Time-of-Flight Mass Spectrometry
Y. Li (2020), xi, 110 pp
ISBN: 978-3-95806-520-8

Band / Volume 527
Uranium accumulation in agricultural soils as derived from long-term phosphorus fertilizer applications
Y. Sun (2020), XII, 136 pp
ISBN: 978-3-95806-521-5

Weitere ***Schriften des Verlags im Forschungszentrum Jülich*** unter
http://wwwzb1.fz-juelich.de/verlagextern1/index.asp

Energie & Umwelt / Energy & Environment
Band / Volume 527
ISBN 978-3-95806-521-5

Mitglied der Helmholtz-Gemeinschaft

JÜLICH
Forschungszentrum